P-14-26

System design of Dome plug

Experience of low-pH concrete mix B200

Material properties from laboratory tests and full-scale castings

Jonas Magnusson, Alexandre Mathern
NCC Engineering

April 2015

Svensk Kärnbränslehantering AB
Swedish Nuclear Fuel
and Waste Management Co

Box 250, SE-101 24 Stockholm
Phone +46 8 459 84 00

ISSN 1651-4416
SKB P-14-26
ID 1449354
April 2015

System design of Dome plug

Experience of low-pH concrete mix B200

Material properties from laboratory tests and full-scale castings

Jonas Magnusson, Alexandre Mathern
NCC Engineering

Keywords: Low-pH concrete, Self-compacting concrete, Deposition tunnel end plug, Material properties, Shrinkage, Creep, Bond between concrete and rock, Full-scale casting, B200, Dome Plug, KBP1004.

Summary

SKB is developing a special method for the final disposal of canisters for spent nuclear fuel in tunnels at a depth of about 470 meters, called KBS-3V. The plug reference design concept for closure of the deposition tunnels is based on a bentonite seal supported by a spherical concrete dome structure arching between recesses constructed in the rock walls.

The plug system is designed for a service life of 100 years. It aims at ensuring a watertight separation between the sealed deposition tunnels and the transport tunnels. The plug has to withstand the high pressure from the ground water and the swelling of the backfill clay until the transport tunnels are, in their turn, backfilled and the natural geohydrological conditions are restored.

According to the current design, the concrete plug is built with low-pH self-compacting concrete B200, a mix specially developed to fulfill the requirements specific to the repository concept, in particular to avoid possible negative effects from leachate from the concrete on the properties of the bentonite.

This report summarizes the results from tests on material properties of the low-pH concrete mix B200 conducted within the project KBP 1004 – System design of dome plugs for deposition tunnels. Within the project, a full-scale test of the plug system was conducted with an unreinforced concrete dome in the Äspö Hard Rock Laboratory under realistic conditions.

In total, three large scale castings were conducted within the framework of the project, namely: a concrete specimen (4×2×2 m), the concrete back-wall of the tunnel and finally the full-scale concrete dome (around 8 m in height) together with a concrete monolith (2×1.4×1.5 m). Properties of the fresh concrete were recorded and the mechanical properties of the hardened concrete were determined from tests on cubes, cylinders and cores at different ages.

Besides, tests were also conducted in laboratory to study the shrinkage properties of the low-pH concrete mix B200, the creep properties of the concrete under high sustained compressive stresses and the properties of the rock-concrete interface.

The shrinkage has been measured during approximately 3 years on concrete prisms under different curing conditions.

Creep tests were conducted on sealed concrete cylinders at three different stress levels, approximately 40%, 50% and 75% of the compressive strength. The specimens have been loaded at an age of approximately 3 months and measured over a period of more than 3 years.

The behaviour in shear and tension of the interface between the concrete plug and the wire sawn rock surface was also investigated at different times after casting. The mechanical testing was performed on specimens core-drilled from small scale rock-concrete blocks manufactured in laboratory.

In addition, mechanical properties of the hardened concrete material were investigated as part of the tests previously mentioned, namely: the compressive strength, the splitting tensile strength, the direct tensile strength, the modulus of elasticity and the fracture energy.

These tests aim at contributing to experience on the mechanical, functional and production related characteristics of the low-pH concrete mix B200. The results of these tests will help to improve numerical modelling of the structural behaviour of the concrete plug prior to and under loading in order to analyse the possible release from the rock during the hardening process of the concrete or through early cooling of the plug as well as the effects of the pressure on deformations, cracking and water tightness of the concrete plug.

Sammanfattning

SKB utvecklar en särskild metod för slutförvaring av kapslar för använt kärnbränsle i tunnlar på ett djup av cirka 470 meter, som kallas KBS-3V. Designkonceptet av pluggen för förslutning av deponeringstunnlar, bygger på ett tätskikt av bentonit och ett mothåll i form av en sfärisk kupolformad betongplugg. Betongpluggen vilar genom valvverkan mot fördjupningar som sågats i bergväggen.

Pluggsystemet konstrueras för en livslängd på 100 år. Syftet är att säkerställa en vattentät avgränsare mellan de förseglade deponeringstunnlarna och transporttunnlarna. Pluggen ska kunna motstå grundvattnets höga tryck samt svällningen i återfyllningsleran tills transporttunnlarna, i sin tur, återfylls och de naturliga geohydrologiska förhållandena återställs.

Enligt den nuvarande utformningen, uppförs betongpluggen med självkompakterande låg-pH betong B200, en betong som utvecklats för att uppfylla de speciella krav som gäller för slutförvaret. Dessa speciella krav inriktar sig särskilt på att undvika möjliga negativa effekter som lakvattnet från betongen kan ha på bentonitens funktion.

I denna rapport sammanfattas resultaten från tester på materialegenskaper av låg-pH betong B200 som genomfördes inom projektet KBP 1004 – Systemkonstruktion av valvplugg för deponeringstunnlarna. Inom projektet har ett fullskaligt demonstrationsförsök av pluggen utförts med en oarmerad betongkupol i Äspölaboratoriet under realistiska förhållanden.

Totalt har tre storskaliga försök gjorts inom ramen för projektet, nämligen: en provgjutning (4×2×2 m), motgjutningen av den bakre väggen i tunneln och slutligen den fullskaliga betongkupolen (cirka 8 meter i höjd) tillsammans med en betongmonolit (2×1,4×1,5 m). Egenskaper hos den färska betongen registrerades och de mekaniska egenskaperna hos den härdade betongen bestämdes från prover på kuber, cylindrar och kärnor vid olika åldrar.

Dessutom genomfördes provningar också i laboratorium för att studera krympningsegenskaper av låg-pH betong B200, krypegenskaperna hos betongen under höga långvariga tryckspänningar och egenskaperna av gränsskiktet mellan berget och betongen.

Krympningen har mätts under cirka 3 år på betongprismor under olika härdningsförhållanden.

Krypförsöken genomfördes på förseglade betongcylindrar vid tre olika spänningsnivåer, cirka 40 %, 50 % och 75 % av tryckhållfastheten. Proverna belastades cirka 3 månader efter gjutning och mätningarna pågick i mer än 3 år.

Beteendet i skjuvning och drag av gränsskiktet mellan betongpluggen och den wire-sågade bergytan undersökts också vid olika tidpunkter efter gjutning. De mekaniska testerna utfördes på kärnborrade cylindrar från småskaliga block bestående av bergblock som motgjutits med betong i laboratoriet.

Dessutom har mekaniska egenskaper hos det härdade betongmaterialet undersökts inom de tester som nämnts tidigare, dvs tryckhållfasthet, spräckhållfasthet, ren draghållfasthet, elasticitetsmodul och brottenergi.

Syftet med dessa prover är att bidra till erfarenheten om de mekaniska, funktionsmässiga och produktionsrelaterade aspekterna hos låg pH-betong B200. Med resultaten av dessa prover kan numerisk modellering av betongpluggens strukturella beteende förbättras innan och under belastning, för att analysera möjligheten för pluggen att lossna från berget under betongens härdningsprocess eller genom tidig kylning av pluggen, samt effekterna av trycket på deformationer, sprickor och vattentäthet av betongpluggen.

Contents

Notations

Roman upper case letters

E_0	Secant modulus calculated between 0.5 MPa and 0.45·fc at 90 days after casting.
E_{0m}	Mean value of secant modulus calculated between 0.5 MPa and 0.45·f_c at 90 days after casting.
E_c	Modulus of elasticity for concrete.
$E_{c,core}$	Modulus of elasticity of concrete from test on a drilled core.
E_c^*	Secant modulus evaluated between 0.5 MPa and $\sigma_{cm}(t_0)$.
$E_{ci}(t_0)$	Instantaneous modulus of elasticity at the time of loading t_0.
$E_{cim}(t_0)$	Mean value of instantaneous modulus of elasticity at the time of loading t_0.
E_{cm}	Mean value of modulus of elasticity of concrete.
$E_{cm,core}$	Mean value of modulus of elasticity of concrete from tests on drilled cores.
G_F	Fracture energy of concrete.
G_{Fm}	Mean value of fracture energy of concrete.
K	Elastic stiffness of concrete.
L	Length.
R^2	Coefficient of determination.

Roman lower case letters

a	Notation used to indicate a failure mode at the interface.
b	Notation used to indicate a failure mode mainly at the interface.
c	Notation used to indicate a failure mode with an inclined failure plane crossing the interface.
l_g	Gauge length.
$f_{7\ days}$	Concrete strength at 7 days.
$f_{28\ days}$	Concrete strength at 28 days.
$f_{90\ days}$	Concrete strength at 90 days.
f_c	Compressive strength of concrete.
$f_{c,core}$	Compressive strength of concrete of a core test.
$f_{c,cube}$	Compressive strength of concrete from a cube test.
$f_{c,cyl}$	Compressive strength of concrete from a cylinder test.
$f_{ci,cube}$	Any individual test results of compressive strength of concrete from cube tests for the test series considered.
f_{cm}	Mean value of compressive strength of concrete.
$f_{ck,cube}$	Characteristic cube compressive strength of concrete.
$f_{cm}(t)$	Mean value of compressive strength of concrete at an age of t days.
$f_{cm,28\ days}$	Mean value of compressive cylinder strength of concrete at 28 days.
$f_{cm,core}$	Mean value of compressive strength of concrete from cube tests.
$f_{cm,cube}$	Mean value of compressive strength of concrete from cube tests.
$f_{cm,cyl}$	Mean value of compressive strength of concrete from cylinder tests.
f_t	Direct tensile strength of concrete.
$f_{t,core}$	Direct tensile strength of concrete from core test.
f_{tm}	Mean value of tensile strength of concrete.
$f_{tm,core}$	Mean value of direct tensile strength of concrete from a core test.
$f_{t,sp}$	Tensile splitting strength of concrete.
$f_{t,sp,core}$	Tensile splitting strength of concrete of a drilling core.
$f_{t,sp,cube}$	Tensile splitting strength of concrete from a cube test.
$f_{tm,sp}$	Mean value of tensile splitting strength of concrete.

$f_{tm,sp,core}$	Mean value of tensile splitting strength of concrete from core tests.
$f_{tm,sp,cube}$	Mean value of tensile splitting strength of concrete from cube tests.
h	Height.
n_A	Fitting parameter.
s	Shear cycle on intact interface; coefficient depending on the type of cement.
$s\#$	Shear cycle on broken interface.
t	Time being considered; age of the concrete.
t_0	Age of the concrete at time of loading.
t_A	Fitting parameter.
t_s	Fitting parameter.
w	Crack opening.
x	Function argument.
y	Function value.

Greek letters

$Ø$	Diameter.
β_{cc}	Coefficient depending on the age of the concrete t.
δ	Displacement.
δ_e	Elastic deformation.
ε_c	Total strain of concrete specimen.
$\varepsilon_c(t)$	Total strain of concrete specimen at time t.
$\varepsilon_{c,control}(t)$	Total strain of concrete control specimen at time t.
$\varepsilon_{cc}(t,t_0)$	Creep strain at time t of concrete specimen loaded at an age t_0.
$\varepsilon_{ci}(t_0)$	Average instantaneous strain directly after loading at t_0.
$\varepsilon_{c\sigma}(t,t_0)$	Total stress-induced strain at time t in concrete loaded at an age t_0.
η	Ratio representing the deviation from a linear elastic response.
μ	Mean value; friction coefficient of the broken interface.
ρ	Density.
σ	Standard deviation; stress.
σ_c	Compressive stress in the concrete.
$\sigma_c(\varepsilon_c)$	Compressive stress in the concrete associated to ε_c.
$\sigma_c(t_0)$	Applied stress at the time of loading (creep inducing stress).
$\sigma_{cm}(t_0)$	Mean value of applied stress at the time of loading (creep inducing stress).
$\varphi(t,t_0)$	Creep coefficient at time t of a concrete loaded at an age t_0.

Other acronyms and abbreviations

ASTM	American Society for Testing and Materials (Standards organization).
BASF	Chemical company.
B200	Low-pH concrete recipe used in the project.
CBI	Swedish Cement and Concrete Research Institute.
CEN	European Committee for Standardization.
CV	Coefficient of Variation.
C.lab	Central laboratory – business unit within Thomas Concrete Group.
DOMPLU	Full-scale experiment of a dome plug at Äspö HRL.
EN	European standard.
fib	International Federation for Structural Concrete.
HRL	Hard Rock Laboratory at Äspö.
KBP 1004	Project on system design of dome plugs for deposition tunnels (Systemkonstruktion av valvplugg för deponeringstunnlarna).

KBS	Nuclear fuel safety (Kärnbränslesäkerhet).
KBS-3	Technology for disposal of high-level radioactive waste developed by SKB.
KBS-3V	Design alternative of the KBS-3 method based on vertical emplacement of the canisters with the spent nuclear fuel.
LTU	Luleå University of Technology.
RH	Relative humidity.
SCC	Self-Compacting Concrete.
SIS	Swedish Standards Institute.
SKB	Swedish Nuclear Fuel and Waste Management Company (Svensk Kärnbränslehantering AB).
Swerock	Supplier of ready-mixed concrete, gravel and crushed rock.
TR	Test Run.

1 Introduction

1.1 Background

SKB is developing a special method for the final disposal of spent nuclear fuel in tunnels at a depth of about 470 meters. This method called KBS-3V is based on three protective barriers: the copper of the canisters in which the fuel is encapsulated, a bentonite clay buffer around the canisters and the rock.

The outer sealing structure at the end of the deposition tunnels is designed as a concrete plug with a flat pressurised side towards the backfilled deposition tunnel and a spherical front side arching between recesses wire-sawn in the rock walls of the tunnel. The concrete plug is designed for a service life of 100 years. It aims at ensuring a watertight separation between the sealed deposition tunnels and the transport tunnels, which can withstand the high pressure from the ground water and the swelling of the backfill clay until the transport tunnels are, in their turn, backfilled and the natural geohydrological conditions are restored.

The structure will endure a high pressure from swelling forces in the backfill clay, at present by introduction of a specially designed backfill transition zone assumed to be confined to approximately 2 MPa. However, due to the uncertainty a backfill swelling design pressure of 4 MPa has been adopted, which also shall be combined with the ground water pressure of about 5 MPa.

The bentonite buffer rings around the deposited canister are sensitive to erosion, which leads to that only a small leakage through the concrete plug is allowed. However, the final value for the maximum allowed leakage passing a plug is not yet established, but acceptable leakage values as low as 0.0025 l/min have been discussed. Awaiting the final design value to be determined the measuring range for the measuring equipment developed for the plug structure has tentatively been selected at 0.0025–0.05 l/min (i.e. approximately 4–70 l/day).

SKB's current reference design for the concrete plug is cast with low-pH self-compacting concrete B200. This concrete mix was developed by Vogt et al. (2009) to fulfil the requirements specific to the repository concept, in particular to avoid possible negative effects from leachate from the concrete on the swelling properties of the bentonite.

The project KBP 1004 – System design of dome plugs for deposition tunnels, was initiated as part of the development of the KBS-3V disposal technology. It comprises a full-scale demonstration test with an unreinforced concrete dome plug (DOMPLU), conducted under realistic conditions in the Äspö Hard Rock Laboratory (Dahlström et al. 2009, Malm 2012).

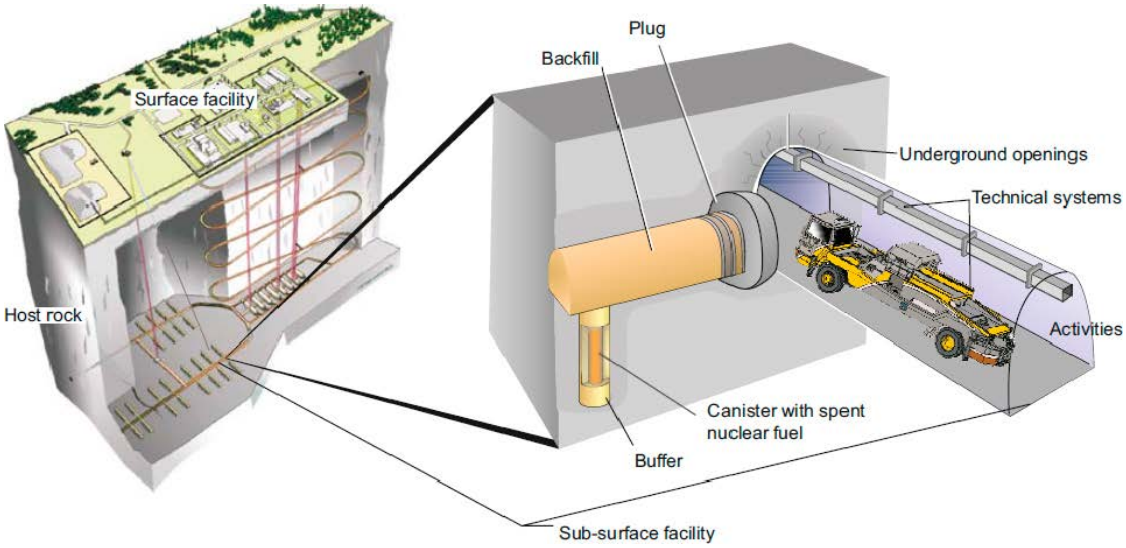

Figure 1-1. *Principle layout of the KBS-3V system during the operational phase (SKB 2010).*

The main advantages of being able to perform the concrete plug without reinforcement are to avoid damage caused by corrosion of the reinforcement and to prevent cracking in the plug due to restraint from the reinforcement to shrinkage of the concrete. In addition, building the concrete plug unreinforced leads to time and cost savings during installation.

1.2 Aim and scope

A series of large-scale castings and laboratory tests were conducted within the KBP 1004 project. These tests aimed at investigating further the mechanical, functional and production related aspects of the low-pH concrete mix B200 and at gaining experience prior and through the casting of the dome plug.

Three large-scale castings were conducted at the Äspö Hard Rock Laboratory within the framework of this project, namely: a concrete specimen (4×2×2 m), the concrete back-wall of the tunnel and finally the full-scale concrete dome (more than 8 m in height) together with a concrete monolith (2×1.4×1.5 m). Several test series were also conducted in laboratory condition.

This report summarizes the results from the tests conducted on the low-pH concrete mix B200 within the KBP 1004 project. The results of these tests can be divided into four categories:

- hardened concrete properties,
- shrinkage,
- creep,
- and interaction between concrete and rock.

Some of the mechanical properties of the hardened concrete material were studied both in conjunction with large-scale castings and in conjunction with laboratory studies of creep and interaction between concrete and rock. The properties studied are for instance: compressive strength, splitting tensile strength, direct tensile strength, modulus of elasticity and fracture energy. Hardened concrete properties are primarily tested in order to categorize and describe the concrete. However, some properties (e.g. direct tensile strength, modulus of elasticity and fracture energy) were especially studied in order to contribute to improve numerical modelling of the structural behaviour of the concrete plug. These large-scale castings provided also information on the properties of the fresh concrete.

Shrinkage properties and creep properties of the concrete under high stress level were studied in laboratory. These results will contribute to improve numerical modelling of the structural behaviour of the concrete plug prior to and under loading, in order to analyse among others the effects of the pressure on deformations, cracking and water tightness of the concrete plug.

The mechanical properties at the interface between the concrete plug and the wire sawn rock surface were also investigated at different times after casting. These properties can be used to improve modelling of the rock-concrete interface to determine for instance if the concrete plug will release from the rock during the hardening process of the concrete or through early cooling of the plug.

The main purpose of the report is to document the results from these tests. Major analyses of the test results are outside the scope of the report.

2 Low-pH concrete mix B200

The low-pH concrete mix B200, developed by Vogt et al. (2009) is studied in this report. This concrete mix was the one selected for the full-scale test of an end plug for deposition tunnels as part of the development of the KBS-3V disposal technology. The composition and mixing order of the concrete mixes used in the different tests were in accordance with the specifications reported by Vogt et al. (2009) as described in Table 2-1 to Table 2-3, unless otherwise stated.

Table 2-1. Composition of concrete mix B200.

Material	Manufacturer	Amount [kg/m^3]
Anläggningscement Degerhamn CEM I 42.5 MH/SR/LA	Cementa	120
Silica fume (SiO_2)	Elkem, Fesil	80
Water		165
Limestone filler Limus 25 ($CaCO_3$)	Nordkalk	369
Sand 0–8 mm (natural, from the Äspö area)		1,037
Gravel 8–16 mm (natural or crushed)		558
Glenium 51	BASF	6.38
Total		**2,335**

Table 2-2. Water ratios for concrete mix B200.

Water/cement	1.375
Water/binder	0.825
Water/powder	0.290

Table 2-3. Mixing order of B200.

Sequence	Activity
1	Aggregates and silica fume
2	Mixing
3	Cement and limestone filler
4	Mixing
5	Water and superplasticizer
6	Final mixing

The coarse aggregate (8–16 mm) used in this project was crushed granite from local producers. The fine aggregate (0–8 mm), which is considered to have more influence on the properties of the concrete, was natural sand taken from the same source in the Äspö area as in the development of the concrete mix.

Under the development of the concrete recipe, silica was added as fume (Vogt et al. 2009). This was also the case for the test series conducted in laboratory in this study (see test series 1–3 in Table 2-4). However, when it comes to the large-scale castings, silica was added as a slurry instead (test series 4-6 in Table 2-4) as it offers better dispersion properties and is easier and safer to handle. The mixing order used for B200 when silica was added as a slurry is described in Table 2-5.

Table 2-4. Overview of the test series.

Test series	Casting conditions	Concrete manufacturer	Aim and material properties studied
1 – Shrinkage	Laboratory	CBI Stockholm C.lab Göteborg	Shrinkage of concrete specimens under different curing conditions: at 50% relative humidity, sealed; and in water.
2 – Creep	Laboratory	CBI Borås	Creep properties under high sustained stress levels, equivalent to 40%, 50% and 75% of the compressive strength during 3 years. Properties of the concrete material in compression: *i.e. strength development over time, effect of different storage conditions and stress-strain relation in compression.*
3 – Bond concrete/rock	Laboratory	CBI Borås	Mechanical properties of the interface between the concrete plug and the wire sawn rock surface: *i.e. tensile bond strength and tensile softening behaviour of the interface, shear strength and residual shear strength of the broken interface.* Mechanical properties of the concrete material: *i.e. compressive strength, splitting tensile strength, direct tensile strength and fracture energy.*
4 – Concrete specimen	Field (large- scale)	Swerock	Compressive strength of concrete by tests on cubes cast at the concrete plant and on site.
5 – Concrete back-wall	Field (large-scale)	Swerock	Compressive strength of concrete by tests on cubes cast at the concrete plant and on site.
6 – Dome plug and concrete monolith	Field (full-scale)	Swerock	Mechanical properties of the concrete material: – tests on cubes cast at the concrete plant and on site after 7 days, 28 days and 90 days: *i.e. compressive strength and the tensile splitting strength.* – tests on cores drilled from the concrete monolith (horizontally or vertically) at different ages from 28 days to one year. *i.e. compressive strength, tensile splitting strength and modulus of elasticity.*

Table 2-5. Mixing order of B200 when silica is added as a slurry.

Sequence	Activity
1	Silica slurry and water
2	Cement, aggregates and sand
3	Mixing 30 s
4	Limestone filler
5	Mixing 60 s
6	Superplasticizer
7	Final mixing 180–240 s until the consistency becomes stable

3 Experience of low-pH concrete mix B200 – hardened concrete properties

3.1 Results from large-scale castings

Three full-scale castings were conducted at the Äspö Hard Rock Laboratory within the framework of this project, namely: a concrete specimen (4×2×2 m), the concrete back-wall of the tunnel and finally the concrete dome together with a concrete monolith (2×1.4×1.5 m).

The concrete used for the large-scale castings was produced at Swerock's concrete plant in Kalmar. The mixing order described in Table 2-5 was applied as silica was added as a slurry.

Standard tests were conducted on cubes cast at the large-scale castings. All cubes were cured in water until immediately before testing according to SIS (2009d). Compressive strength, splitting tensile strength and density were determined according to SIS (2009a, b, e).

3.1.1 Casting of the concrete specimen

A first trial of large-scale casting was performed at the Äspö Hard Rock Laboratory on February 23, 2012, as a concrete specimen with a square section of 2×2 m and a length of 4 m was cast. Three loads of concrete were used for the casting of the specimen.

The concrete was produced at Swerock's concrete plant in Kalmar. Silica was added as a slurry instead of as dry powder as it was the case for the tests related to the development of concrete mix B200. Therefore the mixing order was changed and was according to Table 2-5.

Concrete cubes of dimensions 150×150×150 mm were cast both at the concrete plant and on-site at the Äspö Hard Rock Laboratory and cured in water. The compressive and tensile splitting strengths were determined after 28 days and 90 days on cubes cast at the concrete plant, see Table 3-1. The compressive strength was also determined after 28 days on cubes cast on-site, see Table 3-2. Each of the three concrete loads was made of two separated batches. At the concrete plant, four cubes were produced for each batch (two for the compressive strength and two for the tensile splitting strength), while on-site, three cubes were produced for each load (one at the beginning, one at the middle and one at the end of the load). Mean values are given in Table 3-1 and Table 3-2 while detailed results can be found in Appendix A.

Table 3-1. Summary of results from compression and tensile splitting strength tests after 28 days and 90 days of cubes cast at the concrete plant, given as mean values and standard deviations in brackets.

Age [Days]	$f_{cm,cube}$ [MPa]	Density [kg/m^3]	$f_{tm,sp,cube}$ [MPa]	Density [kg/m^3]
28	68.0 (13.9)	2,358 (35)	5.8 (0.7)	2,383 (43)
90	86.5 (13.1)	2,345 (39)	6.4 (0.4)	2,362 (29)
$f_{90\ days}$ / $f_{28\ days}$	1.27		1.10	

Table 3-2. Summary of results from compression and tensile splitting strength tests after 28 days of cubes cast on site at the Äspö Hard Rock Laboratory, given as mean values and standard deviations in brackets.

Age [Days]	$f_{cm,cube}$ [MPa]	Density [kg/m^3]
28	60.7 (10.1)	2,326 (22)

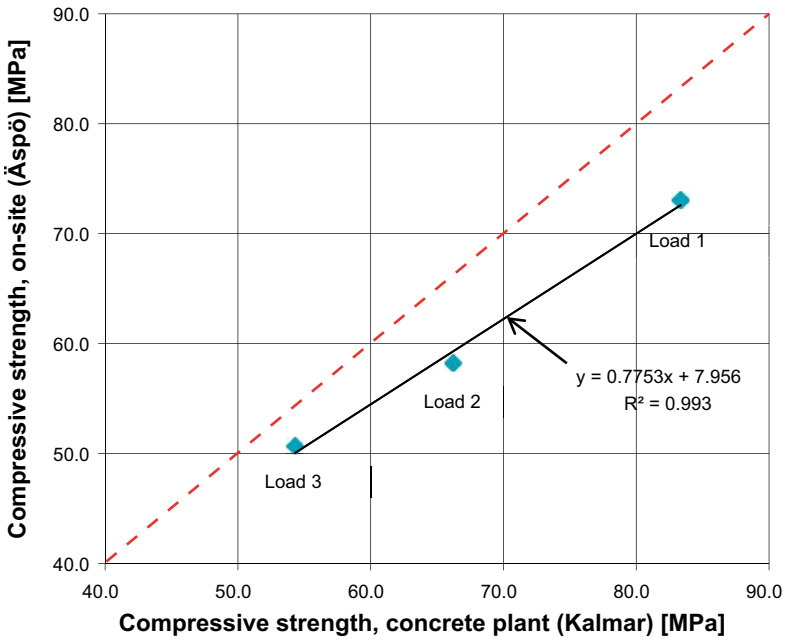

Figure 3-1. *Comparison of compressive strength after 28 days for cubes cast at the concrete plant and on-site at the Äspö Hard Rock Laboratory (average values for each concrete load).*

3.1.2 Casting of the concrete back-wall

A second trial of large-scale casting was performed at the Äspö Hard Rock Laboratory on June 20, 2012, as the back-wall of the tunnel was cast, see Figure 3-2. Three loads of concrete were used for the casting of the wall, which had a thickness of around 0.8 m.

The concrete was produced at Swerock's concrete plant in Kalmar. Silica was also added as a slurry and the concrete mixed according to the order presented in Table 2-5.

The compressive strength of concrete was determined after 28 days by testing three cubes of concrete cast at the concrete plant, one from each lorry load, and one cube cast on site from the third load. The cubes of dimensions 150×150×150 mm were cured in water until testing according to standards. The average result for the 3 cubes from the concrete plant and the result from the cube cast on site are given in Table 3-3. Detailed results are available in Appendix A.

Figure 3-2. *Concrete back-wall during the removal of the formwork.*

Table 3-3. Summary of results from compression tests after 28 days of cubes cast at the concrete plant (given as mean value and standard deviation in brackets) and of cube cast on site at the Äspö Hard Rock Laboratory.

	Kalmar – Concrete plant		Äspö Hard Rock Laboratory	
Age [Days]	$f_{cm,cube}$ [MPa]	Density [kg/m^3]	$f_{cm,cube}$ [MPa]	Density [kg/m^3]
28	40.5 (8.4)	2,347 (42)	29.5	2,390

3.1.3 Casting of the dome plug

The concrete dome plug was cast at the Äspö Hard Rock Laboratory on March 13, 2013. It has a maximum height (or diameter) of 8.1 m and a thickness at mid-height of approximately 1.8 m, with a flat pressurised side towards the backfilled deposition tunnel and a spherical front side arching between recesses wire-sawn in the rock walls of the tunnel for a total volume of approximately 93 m^3, as illustrated in Figure 3-3 and Figure 3-4.

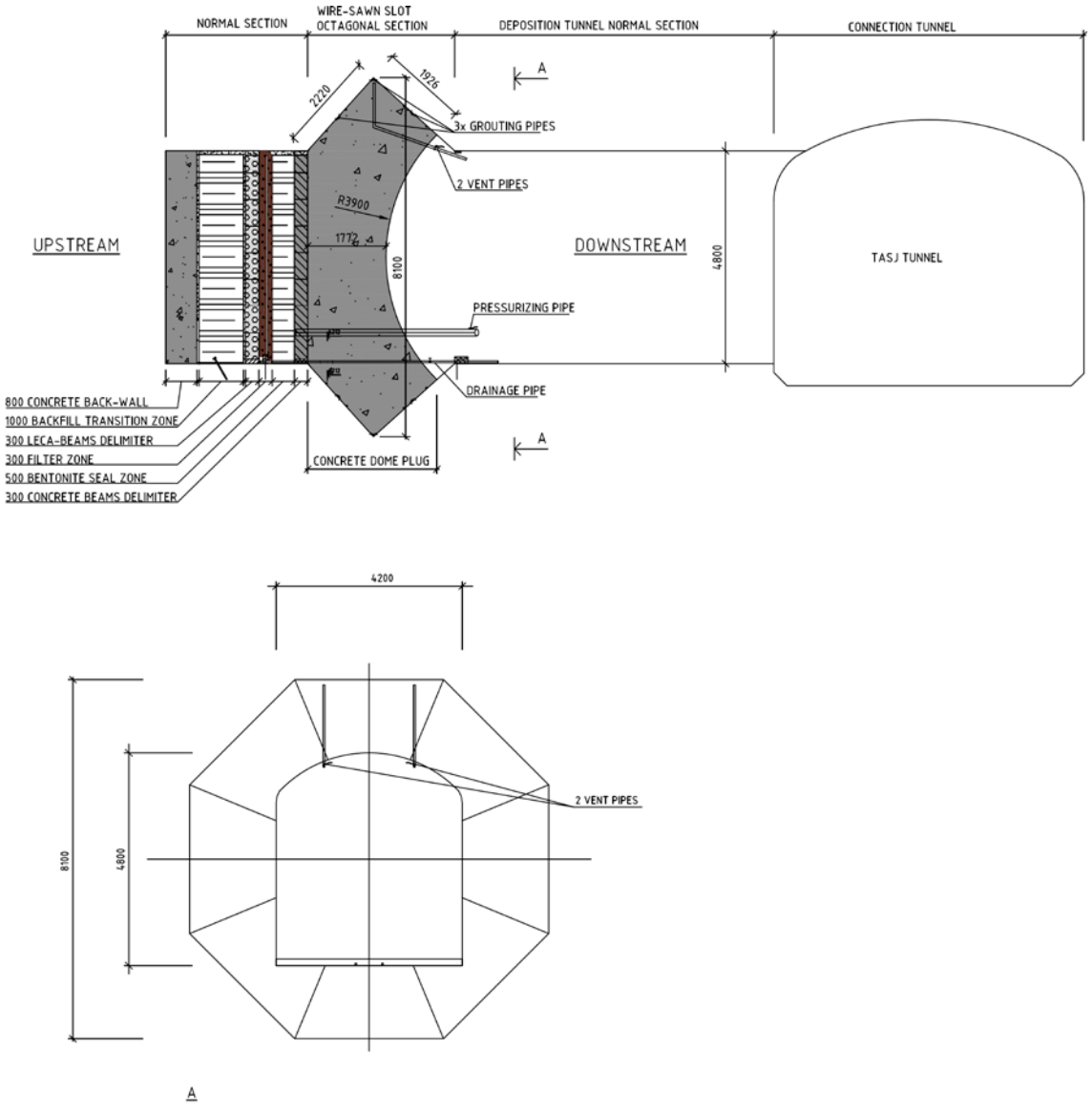

Figure 3-3. *Layout of the concrete dome plug and the backfill.*

Figure 3-4. *View of the form without the stiffeners before casting (left) and of the concrete dome plug after removal of the form (right).*

The low-pH SCC used was produced at a plant located in Kalmar, approximately 100 km from the site. Therefore, the concrete arrived on site in the tunnel at a depth of 470 meters around 2 hours after mixing. As for the castings of the concrete specimen and the concrete back-wall, silica was added as a slurry and the mixing was performed according to Table 2-5.

The casting of the dome plug required 13 lorry loads of concrete and lasted approximately 10 hours. The air content of the fresh concrete was between 5.8% and 9.0% with an average of 7.2%, which is high for concrete without air entraining agents. The intended air content was about 2%. A possible explanation for this difference could be a contamination of the superplasticizer used.

Cubes were cast from every two lorry loads to determine strength properties of the concrete at different ages: 6 cubes at the concrete plant in Kalmar and 6 cubes on site at the Äspö Hard Rock Laboratory. The same lorry loads were tested at both places, namely the ones with odd numbers.

The compressive strength and the tensile splitting strength were determined after 7 days, 28 days and 90 days on the cubes cast at the concrete plant and on site. Mean values are given in Table 3-4. The presented values are mean values and standard deviations based on tests on 7 cubes, one per lorry load tested. The results obtained at different ages are then compared in Table 3-5. Detailed results are given in Appendix A.

Table 3-4. Summary of results from compression and tensile splitting strength tests at different ages of cubes cast at the concrete plant and on site, given as mean values and standard deviations in brackets.

Property	Unit	Specimen	Origin	Age [days]		
				7	28	90
$f_{cm,cube}$	[MPa]	cube 150×150×150	Concrete plant	17.7 (1.3)	40.3 (2.0)	55.9 (3.0)
$f_{tm,sp,cube}$	[MPa]	cube 150×150×150	Concrete plant	2.15 (0.1)	4.13 (0.1)	5.09 (0.3)
$f_{cm,cube}$	[MPa]	cube 150×150×150	Äspö HRL	19.6 (0.9)	42.5 (2.0)	58.0 (3.5)
$f_{tm,sp,cube}$	[MPa]	cube 150×150×150	Äspö HRL	2.26 (0.1)	4.33 (0.2)	5.56 (0.2)

Table 3-5. Change of the average compression and tensile splitting strengths between different ages for cubes cast at the concrete plant and on site.

	Kalmar – Concrete plant		Äspö Hard Rock Laboratory	
	$f_{cm,cube}$	$f_{tm,sp,cube}$	$f_{cm,cube}$	$f_{tm,sp,cube}$
$f_{7\ days}$ / $f_{28\ days}$	0.44	0.52	0.46	0.52
$f_{28\ days}$ / $f_{28\ days}$	1.00	1.00	1.00	1.00
$f_{90\ days}$ / $f_{28\ days}$	1.39	1.23	1.36	1.28

From Figure 3-5 to Figure 3-8, the results from tests on cubes cast at the concrete plant are compared to the results from cubes cast on site. In Figure 3-5 and Figure 3-6, the compressive strength results and tensile splitting strength results are compared for each lorry load tested. The strength development and the scatter for all test results are shown in Figure 3-7 and Figure 3-8 respectively for the compressive strength results and the tensile splitting strength results.

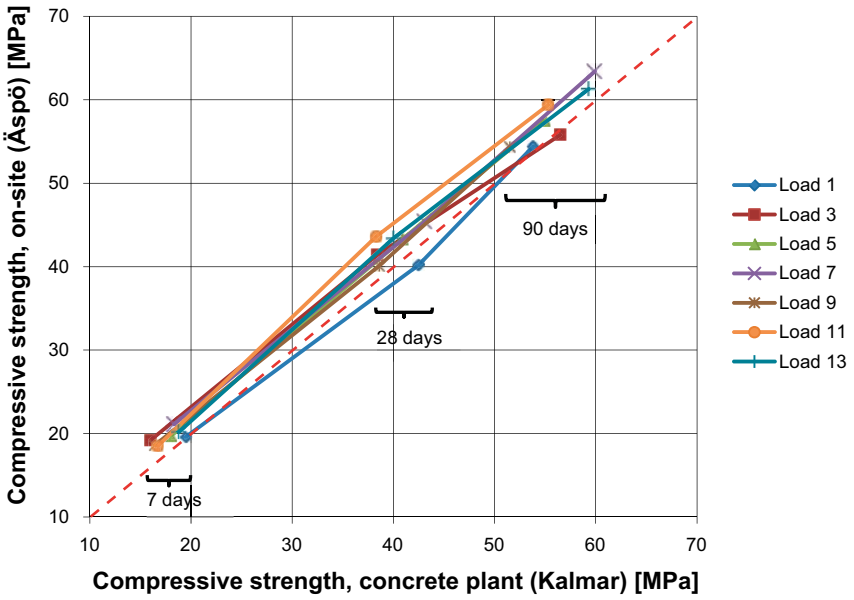

Figure 3-5. *Development of the compressive strength with time for the different lorry loads tested. Comparison between the results obtained on cubes cast at the concrete plant and on cubes cast on-site at the Äspö Hard Rock Laboratory.*

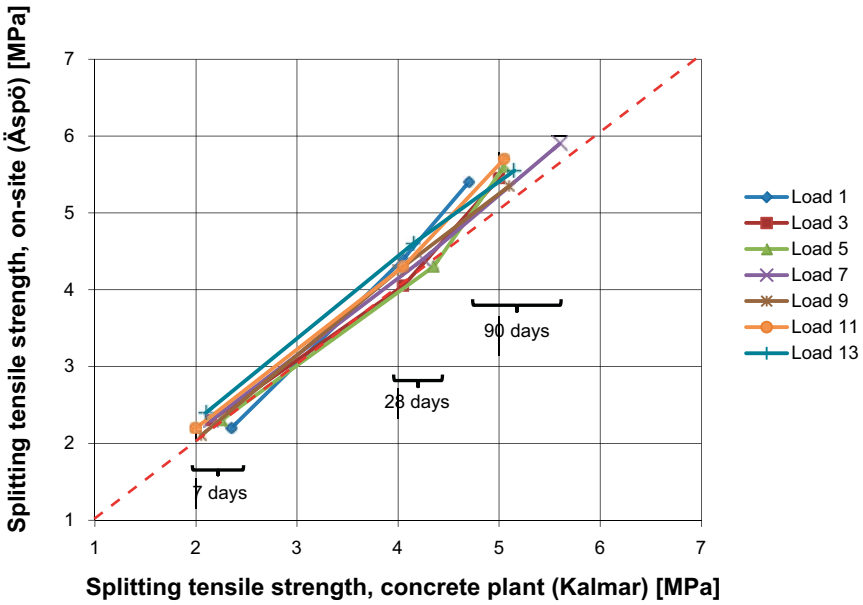

Figure 3-6. *Development of the tensile splitting strength with time for the different lorry loads tested. Comparison between the results obtained on cubes cast at the concrete plant and on cubes cast on-site at the Äspö Hard Rock Laboratory.*

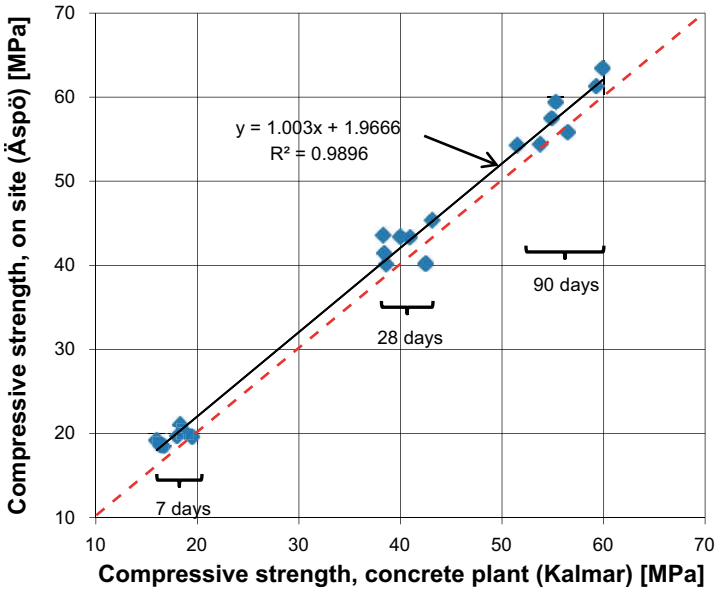

Figure 3-7. Development of the compressive strength with time, linear regression and coefficient of determination R^2 for all the results. Comparison between the results obtained on cubes cast at the concrete plant and on cubes cast on-site at the Äspö Hard Rock Laboratory.

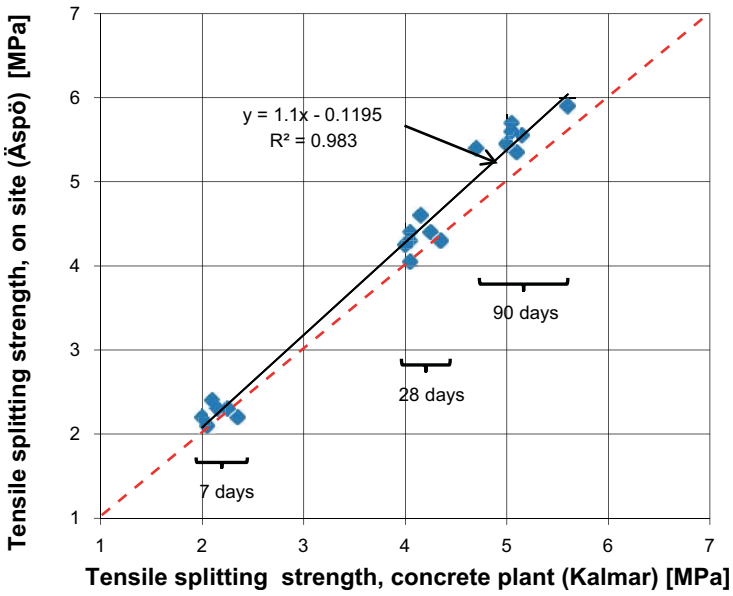

Figure 3-8. Development of the tensile splitting strength with time, linear regression and coefficient of determination R^2 for all the results. Comparison between the results obtained on cubes cast at the concrete plant and on cubes cast on-site at the Äspö Hard Rock Laboratory.

3.1.4 Results from tests on cores drilled from the concrete monolith

A concrete monolith of dimensions 2×1.4×1.5 m was cast right after the dome plug in the immediate vicinity of the plug see Figure 3-9. The concrete monolith was cast with the 14th concrete load under the same conditions as described in Section 3.1.3 for casting of the dome plug.

Horizontal and vertical concrete cores with a diameter of 100 mm and a length of approximately 1,000 mm were drilled from the monolith 7 days before their planned testing time, as indicated in Figure 3-10 and Figure 3-11. The cores were covered with plastic film directly after extraction and sent to the laboratory for testing. Three test specimens of either 100 mm or 200 mm in length were taken from each core and the specimens were then stored in water at 20°C until testing. The

extraction, manufacturing and testing of the test specimens was performed according to SIS (2009a, b, c). Tests were conducted at different ages to determine the compressive strength of both short and long cylinders in both horizontal and vertical direction, the tensile splitting strength of short horizontal cylinders and the modulus of elasticity of both horizontal and vertical long cylinders, see Figure 3-10, Figure 3-11 and Table 3-6 for the location of tested specimens in the monolith.

Table 3-6. Numbering of cores drilled from the concrete monolith.

Property	Cylinder type	Drilling direction	Age [days]						
			28	90	135	182	377	730	1,095
$f_{c,core}$	Short	Horizontal	11	21	31	41	51	61	71
$f_{c,core}$	Short	Vertical	A1	B1	C1				
$f_{c,core}$	Long	Horizontal	13	23	33				
$f_{c,core}$	Long	Vertical	A2	B2	C2				
$f_{t,sp,core}$	Short	Horizontal	12	22	32	42	52	62	72
$E_{c,core}$	Long	Horizontal		24	34				
$E_{c,core}$	Long	Vertical		B3	C3				

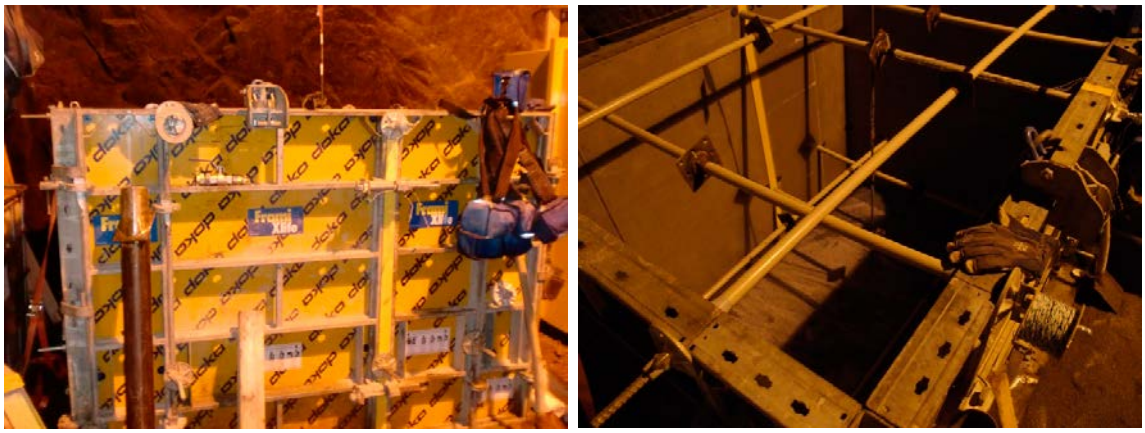

Figure 3-9. *Views of the form of the concrete monolith before casting.*

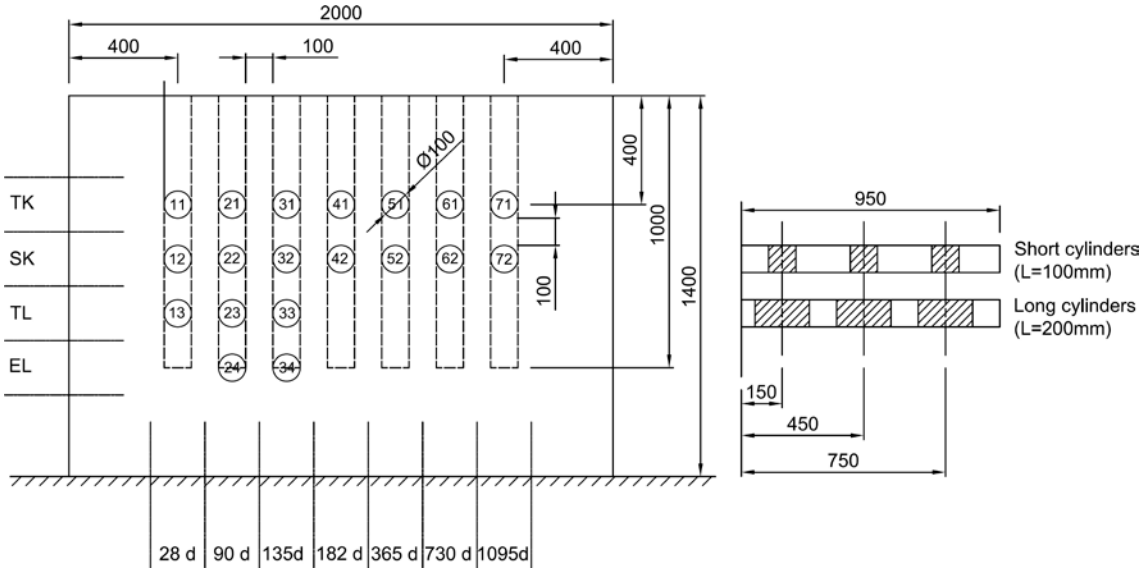

Figure 3-10. *Plan for drilling of horizontal cores from the concrete monolith (left) and extraction of test specimens from the cores (right).*

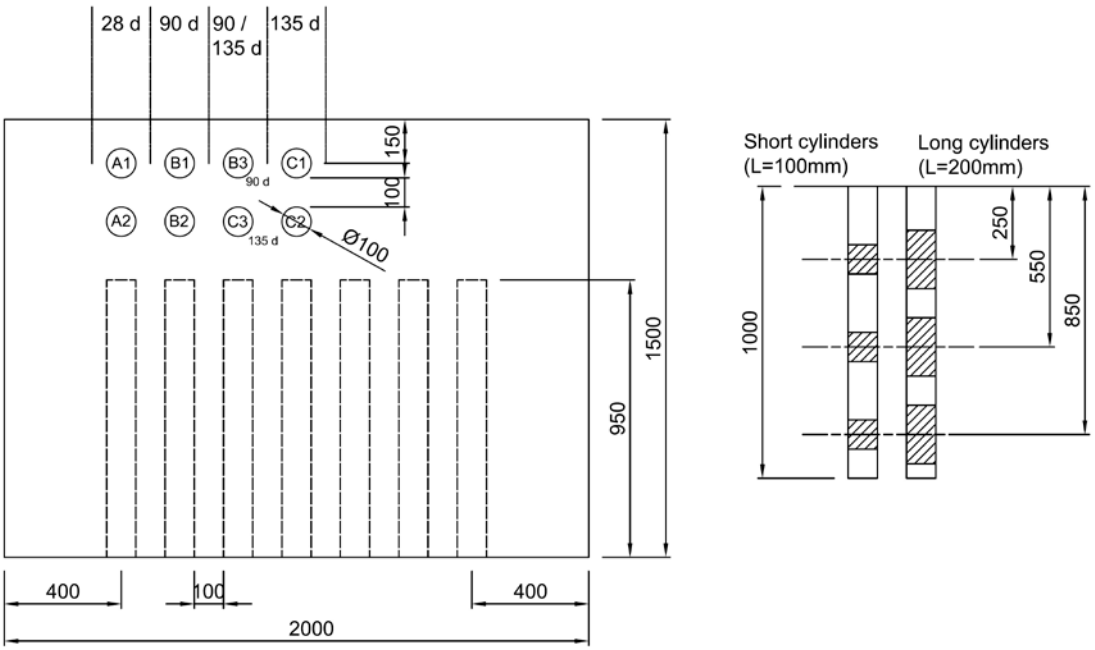

Figure 3-11. *Plan for drilling of vertical cores from the concrete monolith (left) and extraction of test specimens from the cores (right).*

The results of the tests on cores are given in Table 3-7. The presented results are mean values and standard deviations based on tests on 3 cores. Detailed results are available in Appendix A.

According to SIS (2007), the strength value obtained by compression tests on cores having equal length and diameter of 100 mm is equivalent to the one of 150 mm cubes cured under the same conditions, which is confirmed by Bartlett and MacGregor (2003) and True (2003). In Table 3-8, the mean values of compressive strength and tensile splitting strength obtained from tests on 100 mm cores drilled from the concrete monolith are compared to the results obtained from tests on cubes from concrete loads used to cast the dome plug (see Section 3.1.3). The core results are compared to the overall cube results as no cubes were tested from the lorry load used to cast the concrete monolith due to a change on site in the order of casting between the dome plug and the concrete monolith.

3.1.5 Comparison and discussion of the results

Overall, the results for the compressive strength obtained at the concrete plant and on-site are very close to each other, indicating that the transport does not seem to have an influence on the compressive strength of the concrete. However, results from tests on cubes from the back-wall casting, and to a lesser extent also from the specimen casting, have shown a lower compressive strength on-site than at the concrete plant.

Table 3-7. Summary of results from tests on cores drilled from the concrete monolith, given as mean values of three tests and standard deviations in brackets.

Property	Unit	Specimen	Age [days]				
			28	90	135	182	377
$f_{cm,core}$	[MPa]	core Ø100×100 (horizontal)	40.2 (1.4)	62.6 (1.9)	64.0 (3.1)	68.9 (2.7)	73.8 (0.9)
$f_{cm,core}$	[MPa]	core Ø100×100 (vertical)	40.5 (0.8)	62.0[1)] (1.0)	–	–	74.6 (1.6)
$f_{cm,core}$	[MPa]	core Ø100×200 (horizontal)	39.8 (3.1)	58.7 (4.3)	–	–	67.3 (6.1)
$f_{cm,core}$	[MPa]	core Ø100×200 (vertical)	41.7 (1.3)	61.9 (1.4)	–	–	73.2 (2.8)
$f_{tm,sp,core}$	[MPa]	core Ø100×100 (horizontal)	4.20 (0.15)	5.23 (0.12)	5.23 (0.15)	5.97 (0.15)	6.28 (0.10)
$E_{cm,core}$	[MPa]	core Ø100×200 (horizontal)	–	29.8 (2.4)	–	–	30.8 (2.0)
$E_{cm,core}$	[MPa]	core Ø100×200 (vertical)	–	30.2 (0.6)	–	–	31.6 (1.5)

[1)] From 4 tests.

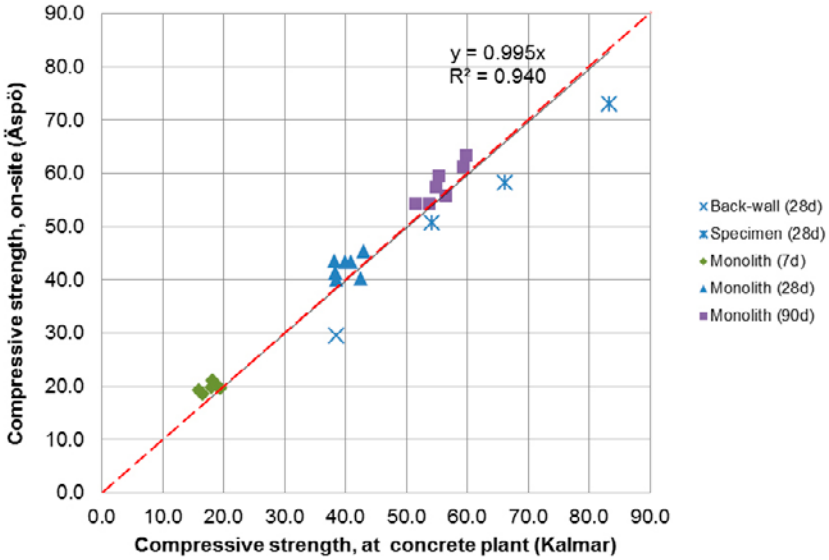

Figure 3-12. *Comparison of compressive strength for cubes cast at the concrete plant and on-site at the Äspö Hard Rock Laboratory (average values for each concrete load when more than one cube tested per load) and trend line considering all the test series.*

Table 3-8. Comparison between compressive and tensile splitting strength results between tests on cubes and on cores drilled from the concrete monolith both cast at the Äspö Hard Rock Laboratory.

Property	Unit	Specimen	Age [days]	
			28	90
$f_{cm,cube}$	[MPa]	cube 150×150×150 (Äspö)	42.5	58.0
$f_{cm,core}$	[MPa]	core Ø100×100 (horizontal)	40.2	62.6
$f_{cm,core}$	[MPa]	core Ø100×100 (vertical)	40.5	62.0
$f_{cm,core}/f_{cm,cube}$	[–]	horizontal core / cube	0.95	1.08
$f_{cm,core}/f_{cm,cube}$	[–]	vertical core / cube	0.95	1.07
$f_{tm,sp,cube}$	[MPa]	cube 150×150×150 (Äspö)	4.33	5.56
$f_{tm,sp,core}$	[MPa]	core Ø100×100 (horizontal)	4.20	5.23
$f_{tm,sp,core}/f_{tm,sp,cube}$	[–]	horizontal core / cube	0.97	0.94

3.2 Results from laboratory tests

The concrete mixes used in laboratory tests were produced locally following the mixing order detailed in Table 2-3 as silica was added as fume in these mixes.

3.2.1 Results from tests conducted in parallel to creep tests

In parallel to the creep tests described in Chapter 5, concrete cubes and cylinders were tested to evaluate the mechanical behaviour of the concrete material in compression. The test results were used to establish stress levels in the creep tests, strength development over time, effects of different storage conditions and stress-strain relation in compression.

The tests were performed in two separate test runs; the first was cast on May 25, 2011; and the second on December 19, 2011. The final concrete mixes for the two test runs were very similar and differ only marginally from the reference composition for B200 as indicated in Table 2-1. The exact composition of each concrete mix is described in detail in Flansbjer and Magnusson (2014a). The concrete had a slump flow value of approximately 680 mm and 690 mm in the first and second run, respectively.

The compressive strength (f_{cm}) tests were conducted according to SIS (2009a). In both the test runs the compressive strength was determined using cubes 150×150×150 mm ($f_{cm,cube}$) and cylinders Ø150×300 mm ($f_{cm,cyl}$). In the first test run small cylinders Ø100×200 mm were also tested according to the same method. The modulus of elasticity (E_0, E_c) was evaluated from compression tests on cylinders Ø150×300 mm according to SIS (2005b). The specimens were stored in water at a temperature of approximately 20°C up to the time of testing.

In addition concrete cylinders of two different sizes, $h = 2 \cdot Ø$ and $h = 3 \cdot Ø$, were manufactured and stored in sealed plastic pipes in the same way as the creep specimens, see Section 5.1. At the time of testing the plastic pipes were removed and the ends of cylinders were cut and face-ground to the final length.

The compressive strength parameters were evaluated at a concrete age of approximately 90 days. In the first test run the cube strength was also evaluated at the actual time for the start of the creep tests at an age of 110 days. To study the concrete strength development during the time for the creep tests, the cube strength has been determined every twelve months from the start of the first and the second creep test run, respectively.

A summary of the concrete properties for the first test run can be found in Table 3-9 and for the second test run in Table 3-10. Detailed results are given in Appendix A and more information on these tests can be found in Flansbjer and Magnusson (2014a).

From Table 3-9 and Table 3-10 it can be noted that there is an unexpected small difference between the cube strength and cylinder strength in both test runs. The ratio $f_{cm,cube} / f_{cm,cyl}$ for standard specimens is 1.03 and 1.06 for the first and second test run, respectively. However, both the cube strength and the cylinder strength were significantly lower after 87–90 days in the second test run compared with the first test run, despite that the same concrete recipe was used. The reason for this discrepancy in strength values has not been found. The reduction was not as pronounced for the cylinders stored in the sealed plastic pipes. It was also not observed for the cubes tested after 450–470 days, for which the compressive strength was on the contrary slightly higher in average in the second test run. This trend was confirmed by results after 820 days, which indicated an increase in the strength of the cubes of the second test run and a stagnation of the ones of the first test run, as illustrated in Figure 3-13.

Table 3-9. Summary of concrete properties in the first test run, given as mean values and standard deviations in brackets

Property	Unit	Specimen dim. [mm]	Curing condition	Age [days] 90	110 [2]	450	820	1,185
$f_{cm,cube}$	[MPa]	150×150×150	water	76.7 (1.4)	75.4 (1.1)	85.9 (2.0)	85.1 (1.5)	87.2 (1.3)
$f_{cm,cyl}$	[MPa]	Ø150×300	water	74.6 (0.5)	–	–	–	–
E_{0m}	[GPa]	Ø150×300	water	33.2 (0.6)	–	–	–	–
E_{cm}	[GPa]	Ø150×300	water	33.5 (0.6)	–	–	–	–
$f_{cm,cyl}$	[MPa]	Ø100×200	water	75.3 (0.2)	–	–	–	–
$f_{cm,cyl}$	[MPa]	Ø100×200	sealed pipe [1]	75.0 (0.5)	–	–	–	–
$f_{cm,cyl}$	[MPa]	Ø100×300	sealed pipe [1]	70.5 (2.3)	–	–	–	–

[1] Manufactured and stored in sealed plastic pipes in the same way as the creep test specimens.

[2] Concrete age at the start of the creep tests.

Table 3-10. Summary of concrete properties in the second test run, given as mean values and standard deviations in brackets.

Property	Unit	Specimen dim. [mm]	Curing condition	Age [days] 87	470	820
$f_{cm,cube}$	[MPa]	150×150×150	water	67.8 (2.1)	86.6 (2.7)	91.1 (0.8)
$f_{cm,cyl}$	[MPa]	Ø150×300	water	64.0 (0.2)	–	–
$f_{cm,cyl}$	[MPa]	Ø90×180	sealed pipe [1]	71.3 (0.8)	–	–
$f_{cm,cyl}$	[MPa]	Ø90×270	sealed pipe [1]	68.7 (1.3)	–	–

[1] Manufactured and stored in sealed plastic pipes in the same way as the creep test specimens.

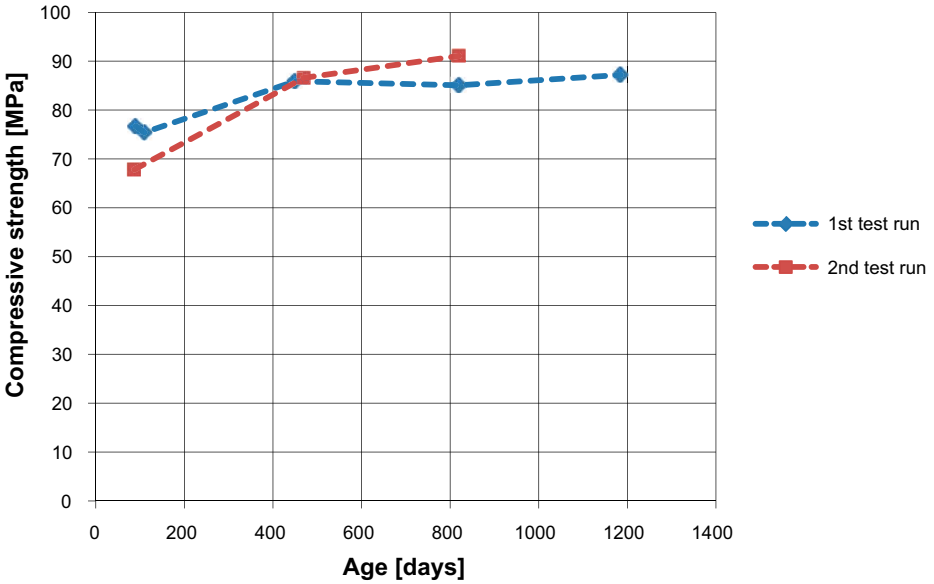

Figure 3-13. *Development of compressive strength determined on cubes of dimensions 150×150×150 mm from the first and the second test runs (average values from 3 or 5 tests).*

Comparing the results for the small cylinders (Ø100×200 mm) in the first test run, the different curing conditions for the cylinders stored in water and those stored in sealed plastic pipes do not seem to have any significant influence on the compressive strength, see Table 3-9.

The small concrete cylinders (Ø100×200 mm and Ø90×180 mm) stored in sealed plastic pipes were used to determine the compressive stress-strain relations, see Appendix A. In the second test run the stress-strain relations were also determined for the slender cylinders (Ø90×270 mm) to examine if the higher slenderness, corresponding to the creep tests specimens, affected the response. The strain was measured as the mean value of three inductive displacement transducers with a gauge length of 100 mm. The elastic modulus E_0 was calculated as the secant modulus between 0.5 MPa and $0.45 \cdot f_c$. The compressive stress $\sigma_c(\varepsilon_c)$ is compared with a linear response $E_0\varepsilon_c$ using a ratio η defined as:

$$\eta = \left| \frac{E_0 \varepsilon_c}{\sigma_c(\varepsilon_c)} \right| - 1 \qquad (3\text{-}1)$$

In Table 3-11 the linear elastic response $E_0\varepsilon_c$ and the resulting ratio $E_0\varepsilon_c / f_c$ is given for η equal to 0.01; 0.02 and 0.05; representing a deviation from linearity by 1%, 2% and 5%, respectively. The mean values of the compressive strength $f_{cm,cyl}$ and the elastic modulus E_{0m} at 90 days after casting are also given.

There was no major difference in the behaviour between the slender (Ø90×270 mm) and shorter specimen (Ø90×180 mm). The modulus of elasticity was approximately the same and the elastic region was even a little bit larger for the slender specimens, see Table 3-11. However, as in the first test run, the slender specimens show slightly lower compressive strength at 90 days.

Table 3-11. Evaluation of linearity from the stress-strain relations.

Specimen dimensions [mm]	Test run	$f_{cm,cyl}$ [MPa]	E_{0m} [GPa]	Mean value $E_0\varepsilon_c$ [MPa] η=0.01	η=0.02	η=0.05	Mean value $E_0\varepsilon_c / f_{cyl}$ [%] η=0.01	η=0.02	η=0.05
Ø100×200	1	75.0	33.5	42.0	46.7	56.3	56	62	75
Ø90×180	2	71.3	34.0	33.0	36.5	43.3	46	51	61
Ø90×270	2	68.7	34.1	37.5	40.4	47.0	55	59	68

3.2.2 Results from tests conducted in parallel to tests on rock-concrete interface

The following mechanical properties of the concrete material were evaluated in parallel to the tests on bond between concrete and rock; compressive strength (f_{cm}), splitting tensile strength ($f_{tm,sp}$), direct tensile strength (f_{tm}) and fracture energy (G_{Fm}). Tests were conducted on concrete cubes, cylinders and cores drilled from two blocks of plain concrete cast on March 30, 2011 (see Figure 3-14). The block was similar in dimensions to the rock-concrete blocks used to determine the interface properties, as described in Chapter 6. A summary of the concrete properties can be found in Table 3-12. Detailed results are given in Appendix A and more information on these tests can be found in Flansbjer and Magnusson (2014b).

The compressive strength was determined using cubes 150×150×150 mm ($f_{cm,cube}$) and cylinders Ø150×300 mm ($f_{cm,cyl}$) according to SIS (2009a). The specimens were stored in water at temperature of approximately 20°C.

The compressive strength and the splitting tensile strength were determined at different ages using cored specimens Ø100×100 mm according to SIS (2009c, b) respectively. All cored specimens were taken from the plain concrete blocks. The specimens were drilled and prepared the day before testing. The development of the compressive strength and the tensile splitting strength is shown in Figure 3-15.

Table 3-12. Summary of concrete properties, given as mean values and standard deviations in brackets.

Property	Unit	Specimen	Age [days]		
			12	29	90
$f_{cm,cube}$	[MPa]	cube 150×150×150	–	–	81.9 (2.2)
$f_{cm,cyl}$	[MPa]	cylinder Ø150×300	–	–	78.0 (0.6)
$f_{cm,core}$	[MPa]	core Ø100×100	33.7 (0.5)	55.1 (0.9)	82.2 (1.2)
$f_{tm,sp,core}$	[MPa]	core Ø100×100	3.3 (0.2)	4.3 (0.3)	5.5 (0.4)
$f_{tm,core}$ [1)]	[MPa]	core Ø65×100	–	–	3.2 (0.4)
$f_{tm,core}$ [2)]	[MPa]	core Ø100×100	–	–	3.6 (0.2)
G_{Fm}	[N/m]	core Ø100×100	–	–	121 (15)

[1)] Obtained from core specimens Ø65×100 mm with hinged end conditions.

[2)] Obtained from notched core specimens Ø100×100 mm with fixed end conditions.

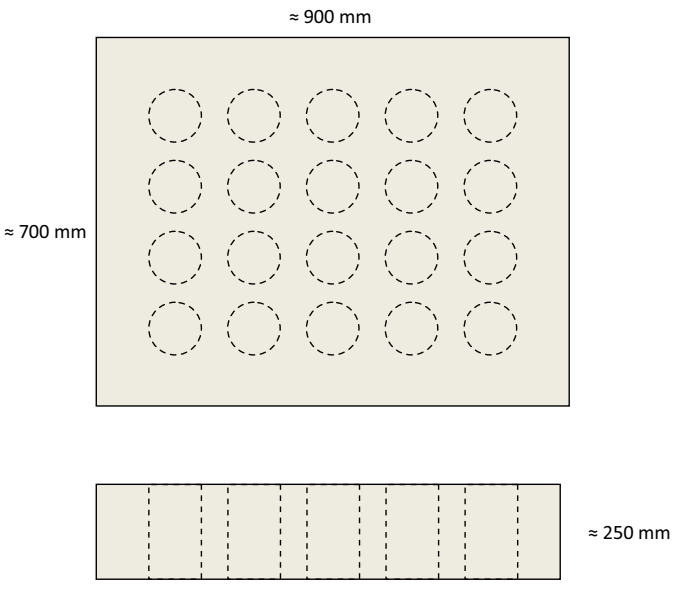

Figure 3-14. *Sketch of block used for direct tensile tests and material tests.*

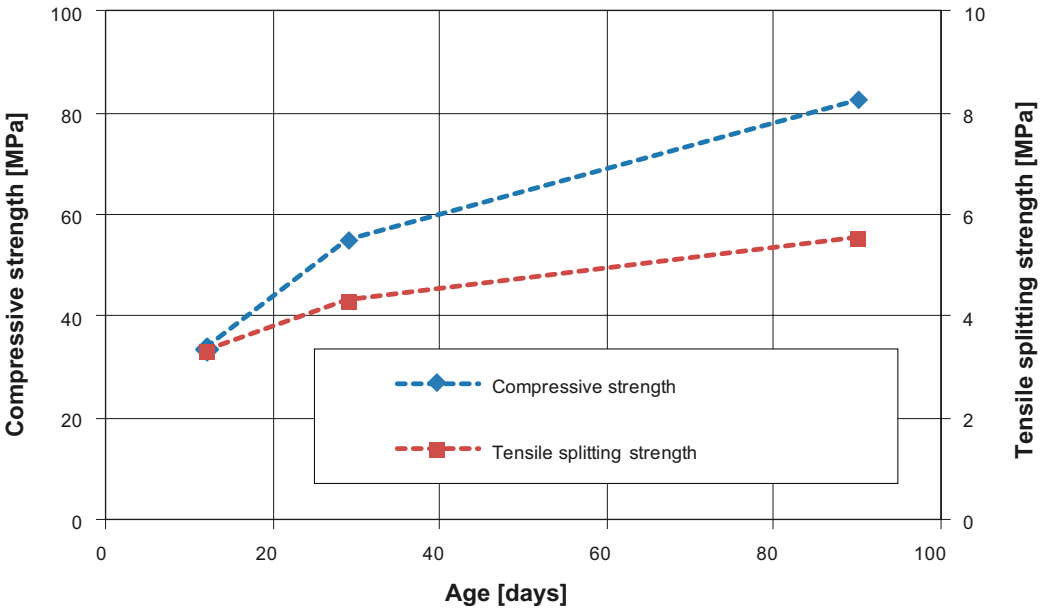

Figure 3-15. *Development of compressive strength and tensile splitting strength, both determined from core specimens Ø100×100 mm.*

The material characteristics in tension were evaluated by using two different methods. In the first method, the tensile strength was determined using cored specimens Ø65×100 mm according to CBI-method no. 6, which is based on SIS (2005a). In this method the loading platens are free to rotate by the use of hinged connections. In the second method, the tensile strength and the softening behaviour of the concrete were evaluated from direct tensile tests, performed on notched core specimens Ø100×100 mm with fixed end conditions. The tensile stress-crack opening relations are shown in Figure 3-16. The fracture energy was calculated from the area under the stress-crack opening curve; see Table 3-12.

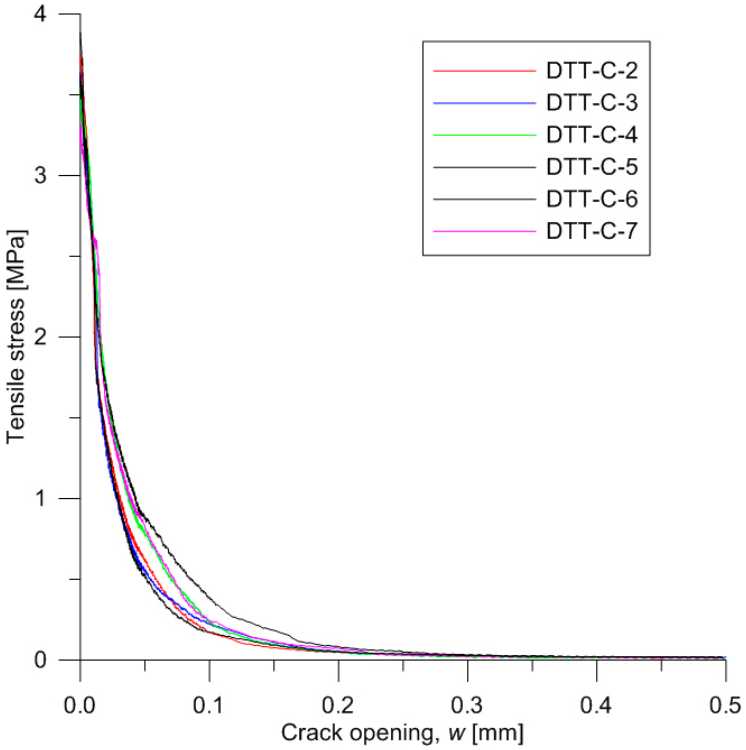

Figure 3-16. *Tensile stress vs. crack opening from direct tensile tests on notched concrete specimens (DTT-C-#).*

3.3 Discussion of the results

3.3.1 Reproducibility of concrete mix B200

It is of importance that concrete mix B200 can be reproduced at other laboratories and at concrete plants. Therefore, results obtained in this study, within the KBP 1004 project, are compared to results reported in Vogt et al. (2009). The comparison is made with compressive and splitting tensile strength results for cubes of dimensions 150×150×150 mm, which were cured in water until testing. The water cured 150 mm cube is used since it is the standard specimen according to SIS (2001). The comparison is primarily based on mean values since the degree of scatter of the results is not reported in Vogt et al. (2009).

In Table 3-13, a comparison is made between compressive strength results at 90 days from tests on cubes cast at different laboratory. The results obtained in the KBP 1004 project are compared to the results reported in Vogt et al. (2009) from the development of concrete mix B200. The results from Vogt et al. (2009) are from two laboratories. It should be noted that in Vogt et al. (2009) the results are recalculated from 100 mm cubes to 150 mm cubes.

The available information (mean values, standard deviations or lowest value) suggests a rather expected variation inside each test series, see Table 3-13. However, the results obtained in the different test series suggest a significant variation between the test series. Considering only the mean values of the five test series gives a fictitious mean value of 75.2 MPa and a fictitious standard deviation of 5.3 MPa for concrete mix B200; i.e. a much larger variation between the test series than inside each test series. That the scatter between test series is larger than within each test series is as expected; the question is how large this scatter may be. The available data concerning density offer no explanation to the variations between tests series. When considering only the results from the thirteen cubes tested at 90 days within the KBP 1004 project, the mean value becomes 76.6 MPa and the standard deviation becomes 5.6 MPa. This gives a coefficient of variation of 7.3%, which is somewhat higher than expected but not alarmingly high.

Table 3-13. Comparison between mean compressive strength results at 90 days from tests on cubes cast at different laboratory and results from the development of concrete mix B200.

Test series	Origin	$f_{cm,cube}$ [1] [MPa]	Remarks
R-09-07 (Vogt et al. 2009)	LTU[2, 3]	77.1	Reference results for B200. Obtained from curve fitting.
	CBI Sthlm[2, 4]	72.6[5]	Original tests series. (Lowest value 71.6 MPa)
Creep tests – first test run	CBI Borås[6]	76.7 (1.4)	Density 2,360 (14.1) kg/m^3 [8]
Creep tests – second test run	CBI Borås[6]	67.8[7] (2.1)	Density 2,370 (0.0) kg/m^3 [8]
Bond tests	CBI Borås[6]	81.9 (2.2)	Density 2,374 (5.5) kg/m^3 [8]

[1] When information concerning the standard deviation is available it is given in brackets.

[2] Based on 100 mm cubes castings in laboratory conditions and recalculated to 150 mm cubes. No information concerning standard deviation or density available.

[3] Cubes cast and tested at LTU.

[4] Cubes cast and tested at CBI's laboratory in Stockholm.

[5] Tested at 91 days.

[6] Cubes cast and tested at CBI's laboratory in Borås.

[7] Tested at 87 days.

[8] Mean value and standard deviation in brackets.

Concrete mix B200 is in Vogt et al. (2009) classified as a C54/66, using the terminology of SIS (2005c). The characteristic cube strength, $f_{ck,cube,}$ is then 66 MPa.

An indicative way of evaluating the scatter of compressive strength results obtained in the KBP 1004 project could be to use the conformity criteria defined in SIS (2001). Accordingly, the two following criteria should be satisfied:

$$f_{cm,cube} \geq f_{ck,cube} + 1.48 \cdot \sigma \quad (3\text{-}2)$$

$$f_{ci,cube} \geq f_{ck,cube} - 4 \quad (3\text{-}3)$$

It should be noted that the use of these criteria in this case is very approximate because it does not concern a continuous production at a concrete plant and the number of results used (3) is lower than 15. Nevertheless, if applying these criteria to each test series described in Table 3-13, it can be interesting to observe that the second test run of the creep tests just fails to meet the requirement concerning the mean compressive strength. On the other hand when considering the results from the thirteen cubes tested at 90 days in the KBP 1004 project, the requirement for the strength class C54/66 are met.

In Table 3-14, a comparison is made between compressive strength results from tests on cubes cast at different large-scale castings in the KBP 1004 project, and results reported in Vogt et al. (2009). The results from Vogt et al. (2009) comprise both results from cubes cast at different laboratories and cubes cast at a large-scale casting. The results in Vogt et al. (2009) are recalculated from 100 mm cubes to 150 mm cubes. It should also be mentioned that under the development of the concrete recipe, silica was added as fume (Vogt et al. 2009); however, when it comes to the three large-scale castings carried out within the KBP 1004 project, silica was added as a slurry.

In all tests reported in Vogt et al. (2009) relatively similar results were achieved; which suggested that no major changes were needed to use concrete mix B200 at large-scale castings.

The first two large-scale castings carried out within the KBP 1004 project were the ones of the concrete specimen and the concrete back-wall. These castings should be considered as test castings before the full-scale casting of the dome plug. The compressive strength results obtained from these tests differ considerably from each other. The results from the back-wall casting were low; while the results from the concrete specimen casting were surprisingly high. The results also present a large scatter within each test series.

The compressive strength results from the casting of the dome plug show a much lower scatter. However the compressive strength is lower in average than what was expected. The difference compared to previous results (Vogt et al. 2009) can almost certainly be explained by the high air content. According to Ljungkrantz et al. (1997), for each percent of air above the intended air content, the compressive strength decreases by 5%. There are indications that the high air content is related to problems with the use of the superplasticizer.

Table 3-14. Comparison between mean compressive strength results from tests on cubes cast during different large-scale castings and results from tests on cubes cast during the development of concrete mix B200.

Test series	Origin	$f_{cm,cube}$ [1] Age [days]		Remarks
		28	90	
R-09-07 (Vogt et al. 2009)	LTU[2, 3]	53	77	Reference results for B200. Obtained from curve fitting.
	CBI Sthlm[2, 4]	43.4	72.6[5]	Original tests series. (Lowest value 42.5 / 71.6 MPa)
	Kungsör[6]	48.5	–	First field test.
Concrete specimen	Concrete plant[7]	68.0 (13.9)	86.5 (13.1)	Large scatter in the results.
	Äspö HRL[8]	60.7 (10.1)	–	Large scatter in the results.
Back-wall	Concrete plant[7]	40.5 (8.4)	–	Large scatter in the results.
	Äspö HRL[8]	29.5	–	Only one result.
Dome plug	Concrete plant[7]	40.3 (2.0)	55.9 (3.0)	High air content[9]
	Äspö HRL[8]	42.5 (2.0)	58.0 (3.5)	High air content[9]

[1] When information concerning the standard deviation is available it is given in brackets.

[2] Based on 100 mm cubes castings in laboratory conditions and recalculated to 150 mm cubes.

[3] Cubes cast and tested at LTU.

[4] Cubes cast and tested at CBI's laboratory in Stockholm.

[5] Tested at 91 days.

[6] First field test for the concrete mix B200, cast at a mobile concrete producer in Kungsör.

[7] Cubes cast at Swerock's concrete plant in Kalmar.

[8] Cubes cast at Äspö HRL.

[9] High air content, an average of 7.2% compared to an intended air content of about 2%.

In Table 3-15, a comparison is made between tensile splitting strength results obtained in this study from tests on cubes cast at different large-scale castings, and results reported in Vogt et al. (2009). The tensile splitting strength results from the casting of the dome plug show a much better agreement with previous results (Vogt et al. 2009) than the results from the compressive strength.

Table 3-15. Comparison between mean tensile splitting strength results from tests on cubes cast during different large-scale castings and results from tests on cubes cast during the development of concrete mix B200.

Test series	Origin	$f_{tm,sp,cube}$ [1] Age [days]		Remarks
		28	90	
R-09-07 (Vogt et al. 2009)	CBI Stockholm[2]	4.2	5.7[4]	Original tests series
	Kungsör[3]	4.1	–	First field test
Concrete specimen	Concrete plant[5]	5.8 (0.7)	6.4 (0.4)	
	Äspö HRL[6]	–	–	
Dome plug	Concrete plant[5]	4.1 (0.1)	5.1 (0.3)	High air content[7]
	Äspö HRL[6]	4.3 (0.2)	5.6 (0.2)	High air content[7]

[1] When information concerning the standard deviation is available it is given in brackets.

[2] Cubes cast and tested at CBI's laboratory in Stockholm.

[3] First field test, cast at a mobile concrete producer in Kungsör.

[4] Tested at 91 days.

[5] Cubes cast at Swerock's concrete plant in Kalmar.

[6] Cubes cast at Äspö HRL.

[7] High air content, an average of 7.2% compared to an intended air content of about 2%.

3.3.2 Fracture energy

The softening behaviour of the concrete was evaluated from direct tensile tests, performed on notched core specimens Ø100×100 mm with fixed end conditions 90 days after casting. The mean fracture energy obtained from 6 tests was 121 N/m.

The fracture energy measured in this study cannot be compared to previous results as it has not been measured previously for the concrete mix B200. The value of the fracture energy was chosen to 100 N/m in the numerical analyses reported in Malm (2012).

3.3.3 Development of strength with time

The compressive strength measured on concrete cores drilled from the monolith at different times after casting is compared to the strength results from cores from the tests on the rock-concrete interface in Figure 3-17.

The compressive strength results obtained on cores drilled from the concrete monolith are more than 25% lower after 28 days and more than 30% lower after 90 days than the ones obtained from cores drilled from the concrete blocks cast for the tests on bond between concrete and rock. The tensile splitting strength results obtained on cores in these two test series show a better agreement as illustrated in Figure 3-18.

In Figure 3-19, compressive strength results obtained on cubes from the dome plug casting are also compared to results from previous tests (Vogt et al. 2009).

The compressive strength results obtained on cubes drilled from the concrete monolith are also significantly lower than the results from previous tests (Vogt et al. 2009) after 90 days. The tensile splitting strength results obtained in these two test series are again in much better agreement as shown in Figure 3-20.

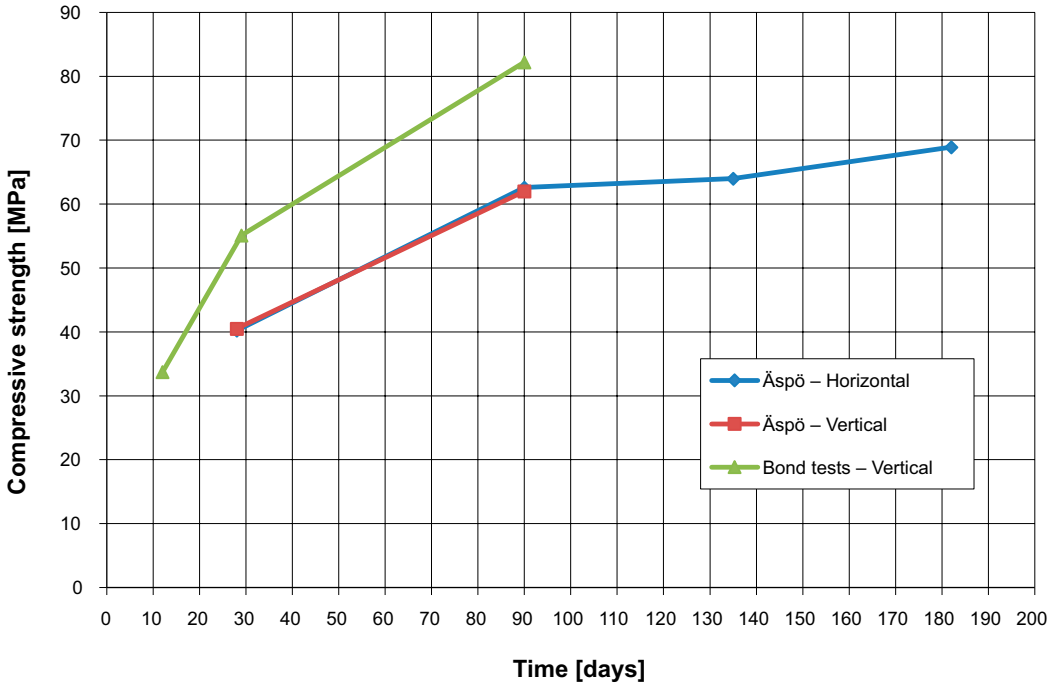

Figure 3-17. *Average compressive strength results obtained from tests on Ø100×100 mm cores, strength development with time and comparison between results obtained from cores drilled from the monolith (horizontally and vertically) and from concrete blocks in tests on rock-concrete interface.*

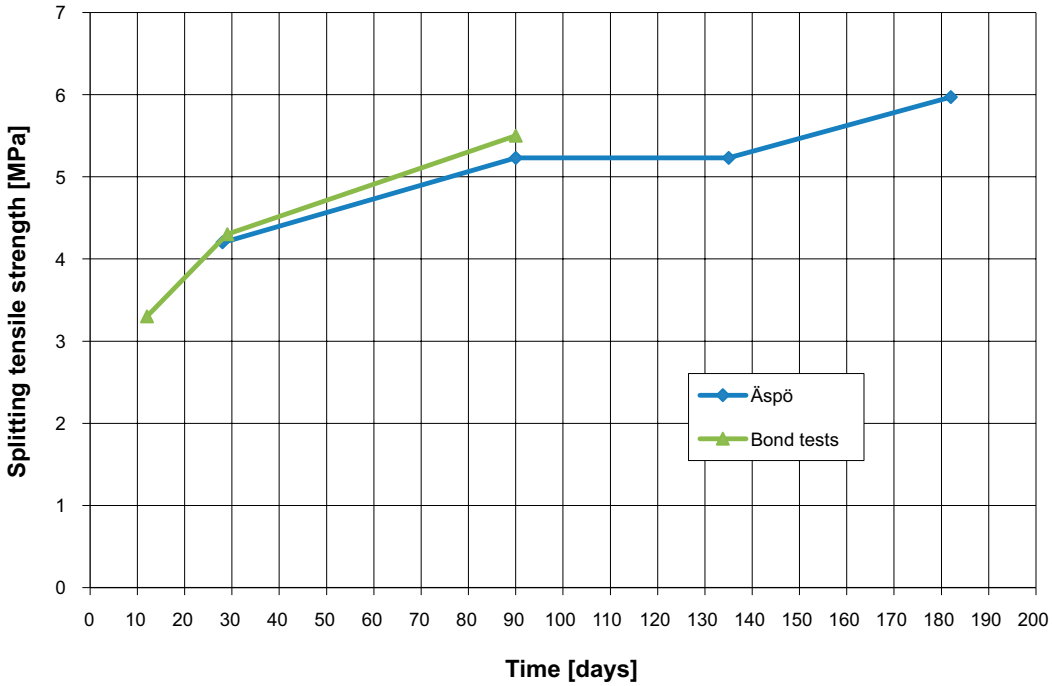

Figure 3-18. *Average splitting tensile strength results obtained from tests on Ø100×100 mm cores, strength development with time and comparison between results obtained from cores drilled from the monolith and from concrete blocks in tests on rock-concrete interface.*

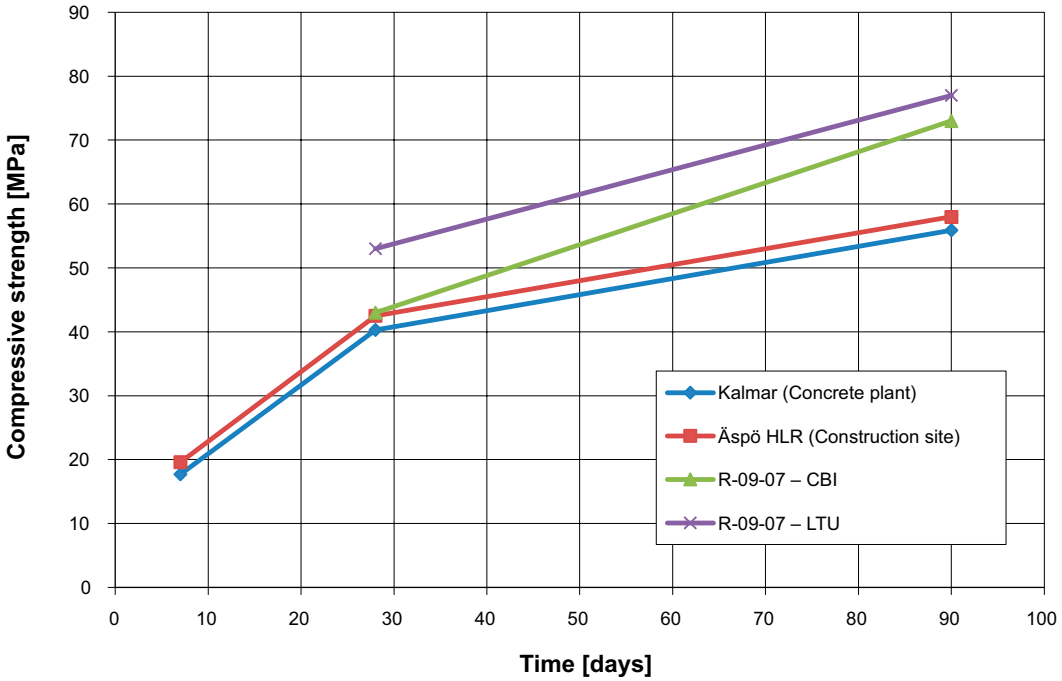

Figure 3-19. *Average compressive strength results obtained from tests on cubes, strength development with time and comparison between results obtained from the casting of the dome plug (from cubes cast at the concrete plant and on-site) and previous results from two different test series (Vogt et al. 2009) marked "R-09-07 – CBI" and "R-09-07 – LTU" depending on where the tests were conducted.*

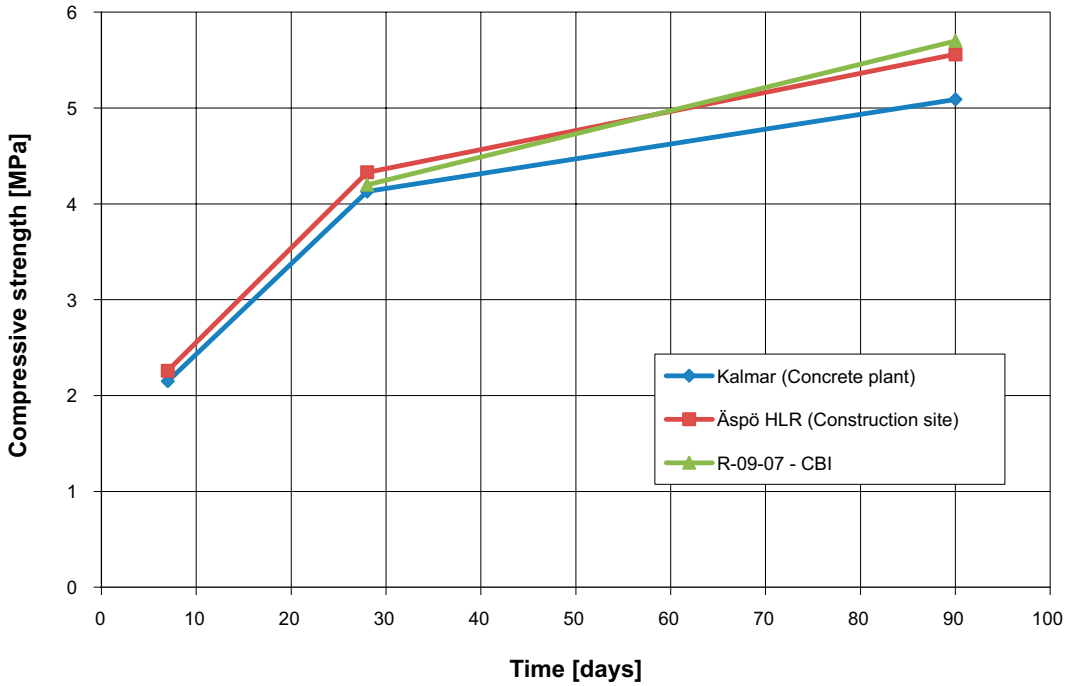

Figure 3-20. *Average splitting tensile strength results obtained from tests on cubes, strength development with time and comparison between results obtained from the casting of the dome plug (from cubes cast at the concrete plant and on-site) and previous results (Vogt et al. 2009) marked "R-09-07 – CBI":*

According to Eurocode 2 (SIS 2005c), the compressive strength of concrete at different ages can be estimated from expressions (3-2) and (3-3).

$$f_{cm}(t) = \beta_{cc}(t) \cdot f_{cm} \tag{3-4}$$

with:

$$\beta_{cc}(t) = exp\left[s\left(1-\sqrt{\frac{28}{t}}\right)\right] \tag{3-5}$$

Table 3-16. Parameters for development of the compressive strength with time according to Eurocode 2 model (SIS 2005c).

	$f_{cm,28\ days}$ [MPa]	s [–]	Correlation coefficient R^2 [–]
Cubes – plant	40.257	0.770	0.982
Cubes – site	42.486	0.731	0.979
Cores – monolith	40:317	0.869	0.903
All plug/monolith	41.055	0.840	0.967

Table 3-17. Parameters for development of the compressive strength with time reported in R-09-07 (Vogt et al. 2009).

	$f_{cm,28\ days}$ [MPa]	s [–]	t_s [h]	t_A [h]	n_A [–]
R-09-07	51.833	0.7647	3.2615	4.8922	3

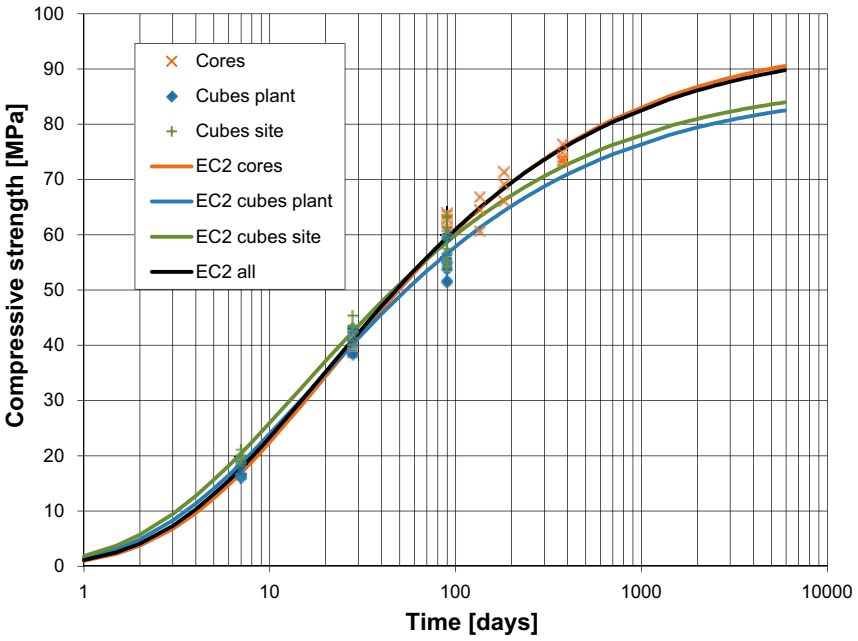

Figure 3-21. *Development of the compressive strength with time. Experimental data from the casting of the dome plug and the concrete monolith (compressive strength of 150 mm cubes cast at the concrete plant and on site and of 100 mm cores drilled from the concrete monolith) and best fit curves according to the strength development model of Eurocode 2 (SIS 2005c).*

4 Experience of low-pH concrete mix B200 – shrinkage

4.1 Overview of test series

Tests have been carried out to measure the shrinkage of the low-pH concrete B200 during approximately 3 years. The measurements were conducted on prisms of dimensions 100×100×400 mm with embedded stainless steel gauge studs at each end. Three tests series with different curing conditions were considered: (A) specimens kept in 50% relative humidity at 20°C; (B) sealed specimens; and (C) for specimens stored in water at 20°C. Butyl tape was used to seal the sealed specimens, as well as the ends with embedded stainless steel studs of the specimens kept in 50% relative humidity. The specimens were demoulded 24 hours after casting and their reference length determined as the specimen length (measured after they have been placed in their respective curing conditions) minus the length of one gauge stud (400–18=382 mm). The measurements were conducted in accordance with SIS (2000), except for the curing conditions of series (B) and (C). The tests were performed in parallel in two laboratories: CBI and C.lab. In each laboratory 15 specimens were tested, 5 for each test series. Summarized test data are discussed below while detailed results are provided in Appendix B.

4.2 Results from tests carried out at CBI

The results of the shrinkage measurements are presented in Figure 4-1 (specimens stored in 50% relative humidity), in Figure 4-2 (sealed specimens) and in Figure 4-3 (specimens stored in water).

The shrinkage drop around 90 days, for specimens stored in 50% relative humidity, in Figure 4-1, is due to the fact that the moisture level was higher around that time due to a problem with the humidity control in the room. Therefore, a straight line between the previous measurement point and the next one would probably be closer to the truth.

According to CBI's recommendation, the average shrinkage calculated for the specimens kept in water in Figure 4-3 do not include the results for Specimen 5, which are widely diverging from the results of the four other specimens. This is very likely due to the fact that for this specimen the gauge studs were glued to the ends with plastic paddings, which may have swelled when placed in water.

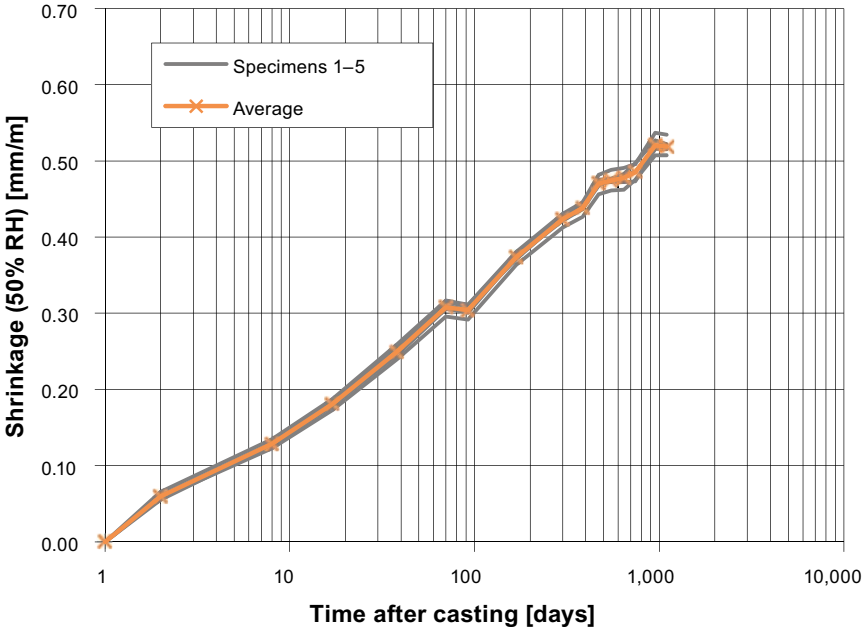

Figure 4-1. *Shrinkage for specimens stored in 50% relative humidity. Results from tests conducted at CBI.*

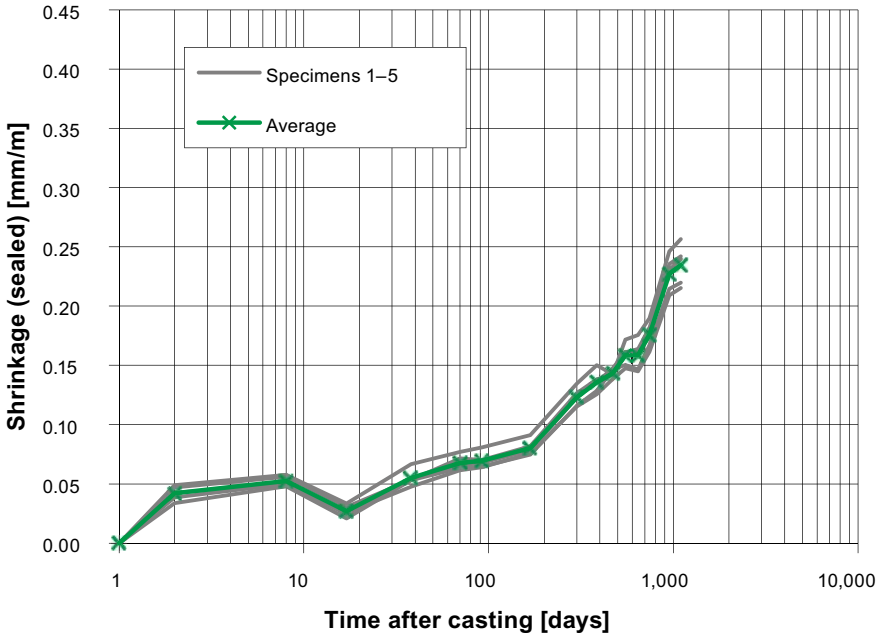

Figure 4-2. *Shrinkage for sealed specimens. Results from tests conducted at CBI.*

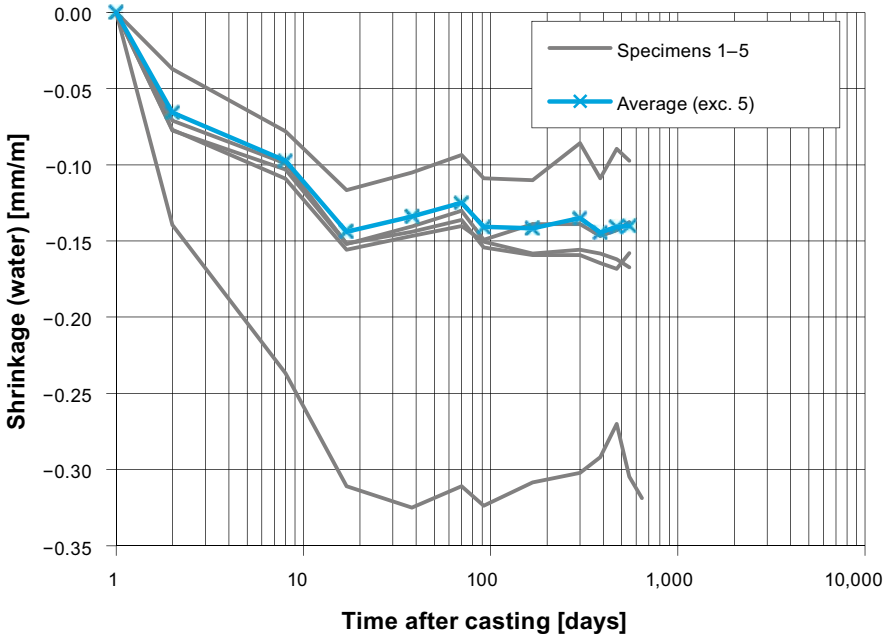

Figure 4-3. *Shrinkage for specimens stored in water. Results from tests conducted at CBI (the very divergent results measured for Specimen 5 are not taken into account to calculate the average).*

4.3 Results from tests carried out at C.lab

The results of the shrinkage measurements are presented in Figure 4-4 (specimens stored in 50% relative humidity), in Figure 4-5 (sealed specimens) and in Figure 4-6 (specimens stored in water).

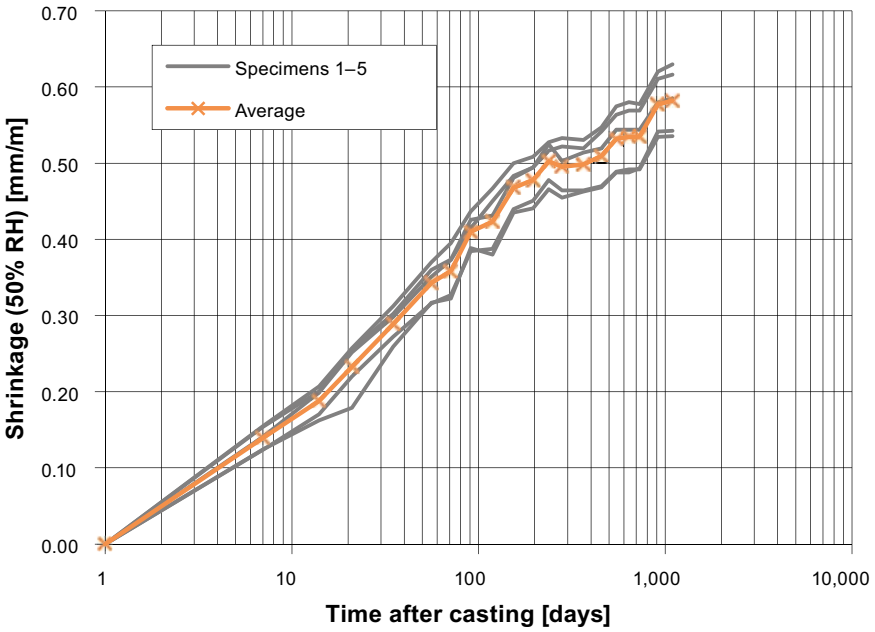

Figure 4-4. Shrinkage for specimens stored in 50% relative humidity. Results from tests conducted at C.lab.

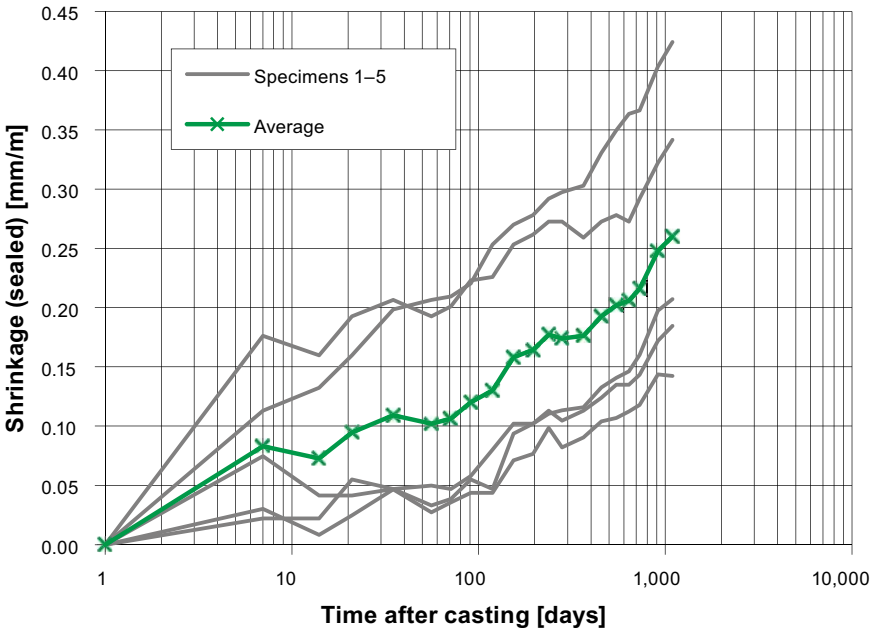

Figure 4-5. Shrinkage for sealed specimens. Results from tests conducted at C.lab.

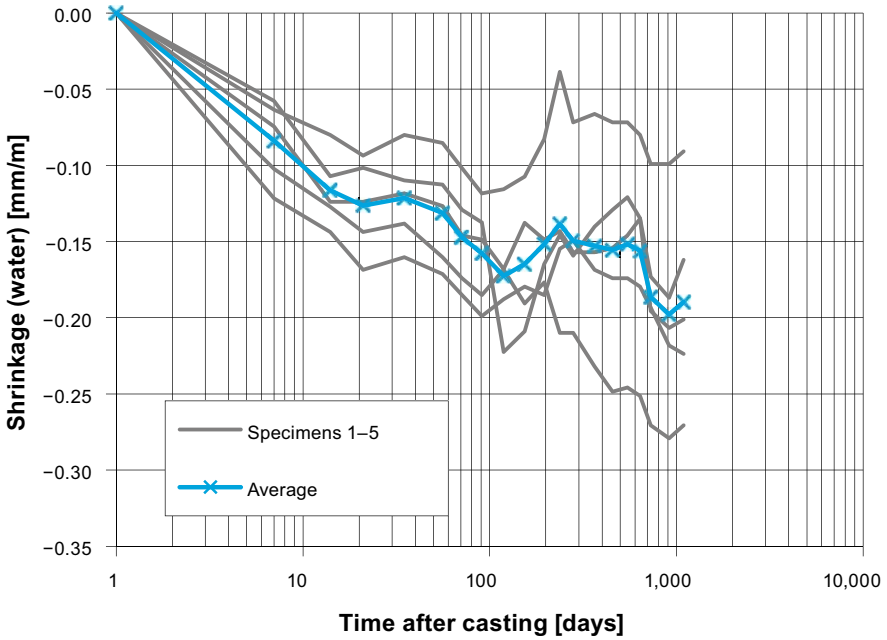

Figure 4-6. Shrinkage for specimens stored in water. Results from tests conducted at C.lab.

4.4 Results from previous tests conducted at CBI

Similar measurements of the shrinkage of concrete B200 on prisms were previously conducted at CBI (Vogt et al. 2009). The results of these tests are presented in Figure 4-7 (specimens stored in 50% relative humidity) and in Figure 4-8 (sealed specimens).

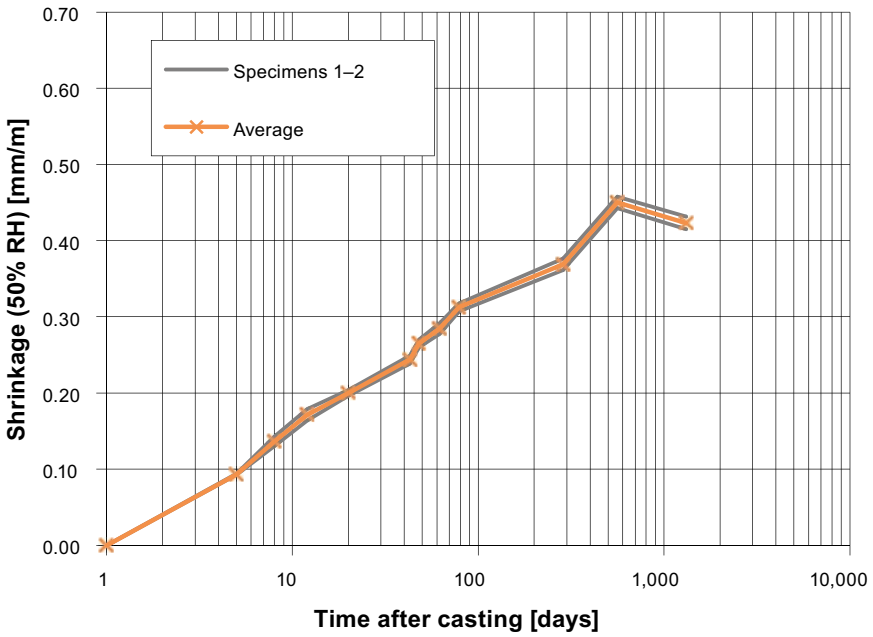

Figure 4-7. Shrinkage of specimens stored in 50% relative humidity. Results from previous tests conducted at CBI (Vogt et al. 2009).

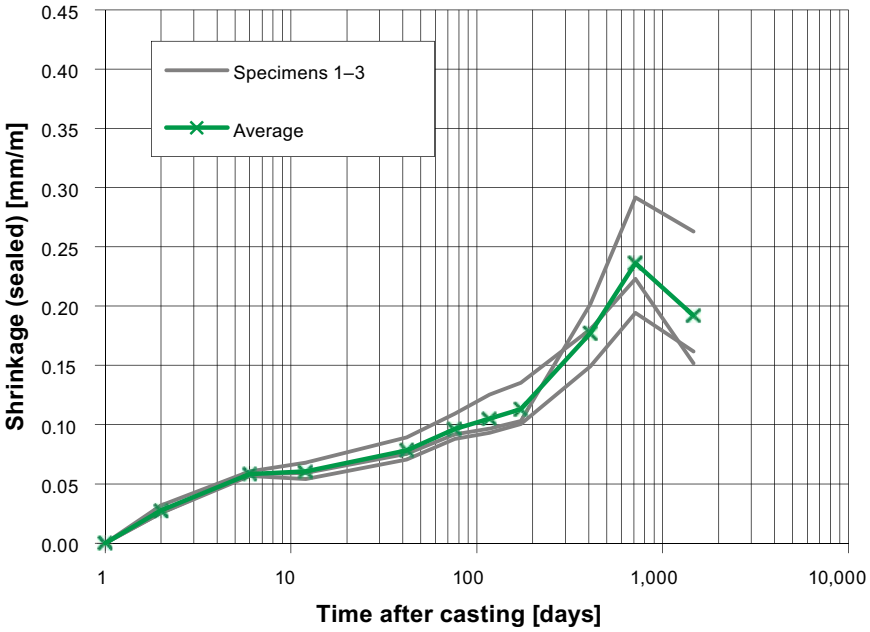

Figure 4-8. *Shrinkage of sealed specimens. Results from previous tests conducted at CBI (Vogt et al. 2009).*

4.5 Discussion of the results

Shrinkage measurements were conducted in this study on prisms of dimensions 100×100×400 mm during approximately 3 years. Three different curing conditions were considered: specimens kept in 50% relative humidity at 20°C; sealed specimens and specimens stored in water at 20°C.

The average results for all different storage conditions of the shrinkage measurements conducted at CBI and C.lab are compared with previous results (Vogt et al. 2009) in Figure 4-9. The average weight losses for each of these test series are presented in Figure 4-10.

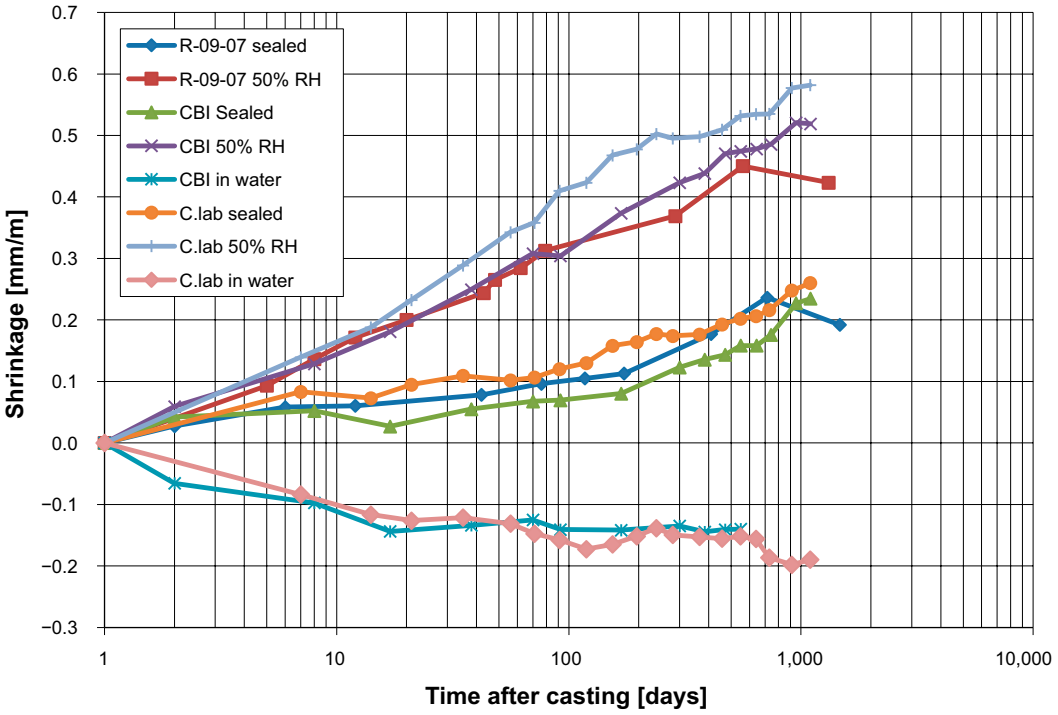

Figure 4-9. *Average shrinkage results for the different curing conditions for specimens tested at C.lab and at CBI and previous results from Vogt et al. (2009).*

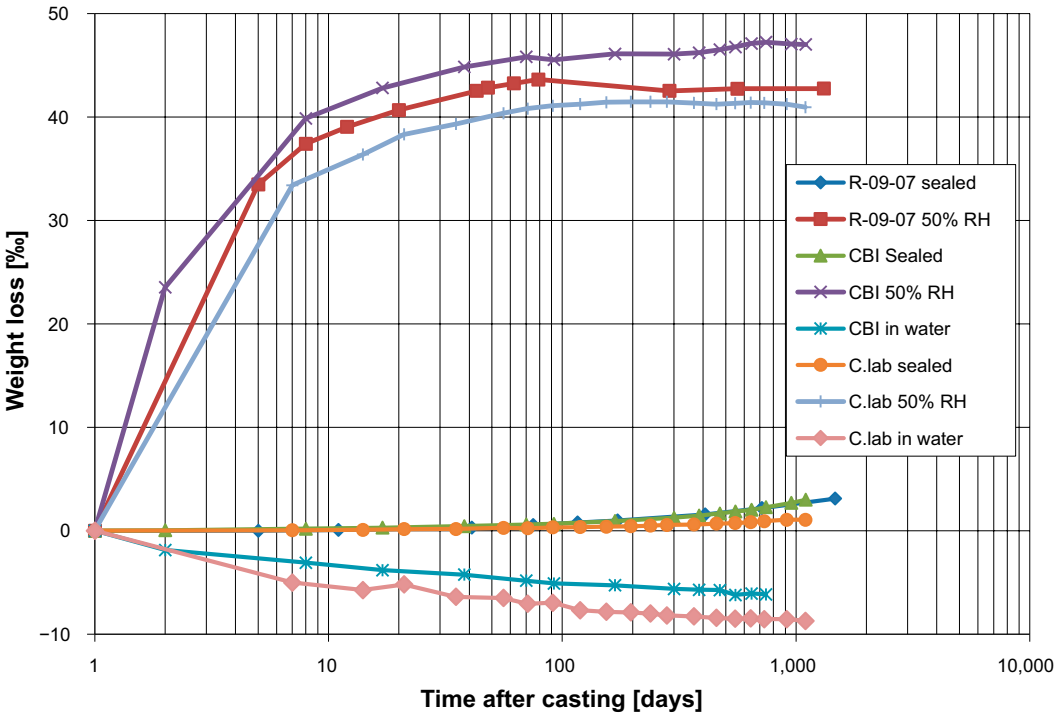

Figure 4-10. *Average weight loss for specimens tested at C.lab and at CBI and previous results from Vogt et al. (2009) for the different curing conditions.*

It can be noted that the results from the previous shrinkage measurements conducted at CBI (Vogt et al. 2009) for sealed specimens and specimens stored at 50% relative humidity are very similar to the results measured at CBI and C.lab. for similar curing conditions in the current KBP 1004 project.

Shrinkage results obtained in this study at two different laboratories are very similar to previous results reported in R-09-07 (Vogt et al. 2009) for sealed specimens and for specimens stored at 50%.

5 Experience of low-pH concrete mix B200 – creep

5.1 Overview of test series

The high pressure endured by the concrete plug during its service life results in high long-term stresses on the concrete. The aim of these tests is therefore to determine the creep properties of the low-pH concrete B200 in compression under high sustained stress levels. These results will contribute to improve numerical modelling of the structural behaviour of the concrete plug under sustained loading. In particular, it is important to analyse the effects of the pressure from the ground water and the swelling of the backfill clay on deformations, cracking and water tightness of the concrete plug.

In this study, the creep properties of the concrete B200 in compression were determined by tests on sealed concrete cylinders subjected to sustained longitudinal compressive load in mechanical rigs, as illustrated in Figure 5-1. The specimens were loaded at three different stress levels, approximately 40%, 50% and 75% of the compressive strength at the age of loading of approximately three months. The tests started in 2011 and are planned to last for three years, until the end of 2014.

The test method is based on ASTM (2010) and ISO (2009). The creep of the concrete is obtained by determining the total deformation of the loaded specimens and subtracting the shrinkage of the unloaded control specimens stored in the same environmental conditions.

The test programme is summarised in Table 5-1. The creep tests were performed in two test runs; two stress levels in the first test run (TR 1a and TR 1b) and one stress level in the second test run (TR 2). Five creep specimens were loaded for each stress level and for each test run five control specimens were remained unloaded.

The compressive strength and stress levels to be applied $\sigma_c(t_0)$ to the creep specimens were determined shortly before loading by compressive tests on concrete cubes and cylinders cast simultaneously with the casting of the creep specimens, as described in Section 3.2.1. However, since the strength obtained at 110 days in the first test run was somehow lower than the strength at 90 days and within the standard deviation, it was decided to use the strength values at 90 days to determine the stress levels to be used in the creep tests.

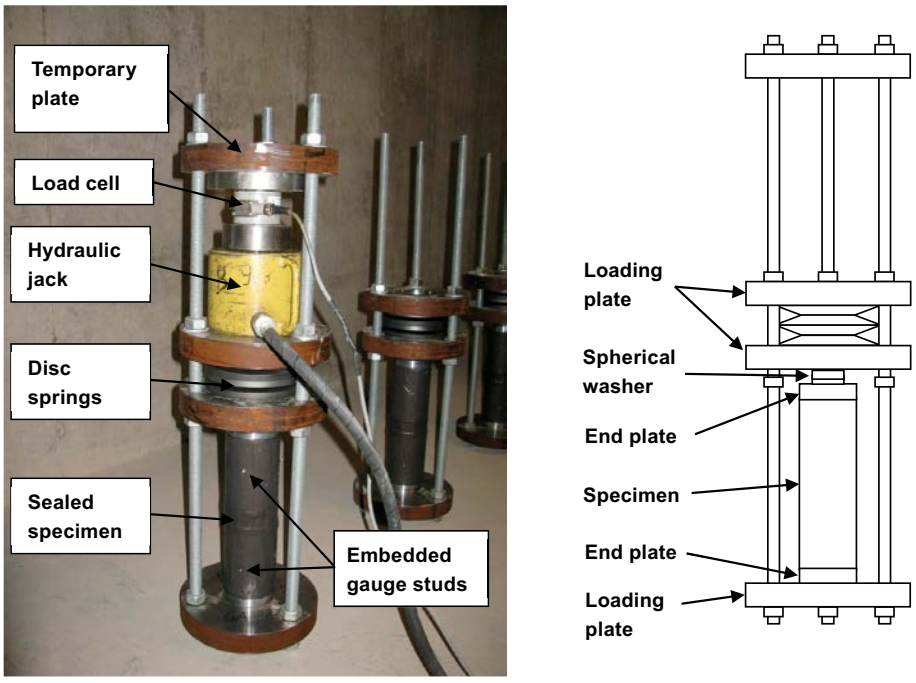

Figure 5-1. *Loading of a sealed creep test specimen in a mechanical creep rig (left) and schematic presentation of the rig (right).*

Table 5-1. Summary of creep test programme.

Test run	Dimensions [mm]	Age at time of loading t_0 [days]	Applied stress $\sigma_{cm}(t_0)$ [1] [MPa]	$\sigma_{cm}(t_0) / f_{cm,cyl}$ [2] [%]	$\sigma_{cm}(t_0) / f_{cm}$ [3] [%]	$E_{cim}(t_0)$ [GPa]
TR 1a	Ø100×300	110	30.0 (0.2)	40.2 (0.3)	42.6 (0.3)	32.9 (0.5)
TR 1b	Ø100×300	111	38.5 (0.5)	51.6 (0.6)	54.6 (0.7)	32.7 (0.8)
TR 2	Ø90×270	91	49.4 (0.6)	77.3 (0.9)	72.0 (0.9)	28.9 (1.0)

[1] $\sigma_{cm}(t_0)$ is the average value of the applied stress $\sigma_c(t_0)$ of the specimens in the test group.

[2] $f_{cm,cyl}$ is the average compressive strength from standard cylinders Ø150×300 mm.

[3] f_{cm} is the average compressive strength from sealed cylinders Ø100×300 mm and Ø90×270 mm for first and second test run, respectively.

The results from tests on compressive characteristics of the concrete material were also used to establish strength development over time, effects of different storage conditions and stress-strain relation in compression, as described in Section 3.2.1.

For a more comprehensive description of the method and detailed results see Flansbjer and Magnusson (2014a).

The specimens were placed and aligned in the mechanical rigs to ensure centric loading. Prior to loading the reference values of the specimen strains and spring deformation were measured. The predetermined stress was applied and the strains and the spring deformation were measured directly after. In addition, the strain values of the control specimens were measured immediately after the loaded specimens.

The subsequent strain measurements were done after approximately 2 hours and 6 hours, then daily for 1 week, weekly until the end of 1 month, monthly to the end of 1 year, and thereafter once every third month. Before each measurement occasion the load level was first determined by measuring the spring deformation, and adjusted if it varied more than ±2% from the correct load value. The strains of the control specimens were measured on the same schedule as the loaded specimens.

5.2 Results of creep tests

The total strain of the loaded creep specimens $\varepsilon_c(t)$ and the control specimens $\varepsilon_{c,control}(t)$ was calculated as the average value of the strain measurements at the three lines spaced uniformly around the periphery of the specimen. The total strain-time relations can be found in Flansbjer and Magnusson (2014a). The instantaneous elastic modulus $E_{ci}(t_0)$ of the creep specimens is calculated as the applied stress divided by the average strain $\varepsilon_{ci}(t_0)$ immediately after loading as:

$$E_{ci}(t_0) = \frac{\sigma_c(t_0)}{\varepsilon_{ci}(t_0)} \tag{5-1}$$

The mean value of the instantaneous elastic modulus $E_{cim}(t_0)$ of the specimens at each stress level is given in Table 5-1. In the first test run, the elastic modulus determined from the creep tests is in the same order of magnitude as those determined by material tests presented in Table 3-9 and Table 3-11. This is expected since the applied stress levels are within the assumed elastic range, see Table 3-11. However, in the second test run the instantaneous elastic modulus from the creep test is lower than that from the material tests given in Table 3-11. Here, the applied stress level is not in the assumed elastic range and a response corresponding to the elastic modulus from the material tests cannot be expected. A secant modulus E_c^* evaluated between 0.5 MPa and $\sigma_{cm}(t_0)$ = 49.4 MPa gives a better agreement to the instantaneous elastic modulus in the creep tests, see Appendix A. In addition some creep strains may have occurred before the measurement of strains, after loading had started.

The total stress-induced strain $\varepsilon_{c\sigma}(t, t_0)$ is calculated as the difference between the average strain values of the loaded specimens and the control specimens as:

$$\varepsilon_{c\sigma}(t, t_0) = \varepsilon_c(t) - \varepsilon_{c,control}(t) \tag{5-2}$$

The total stress-induced strain divided by the applied stress is given in Figure 5-2 to Figure 5-4. The creep strain $\varepsilon_{cc}(t, t_0)$ is calculated as the total stress-induced strain minus the strain immediately after loading as:

$$\varepsilon_{cc}(t,t_0) = \varepsilon_{c\sigma}(t,t_0) - \varepsilon_{ci}(t_0) = \varepsilon_c(t) - \varepsilon_{c,control}(t) - \varepsilon_{ci}(t_0) \quad (5\text{-}3)$$

The creep coefficient $\varphi(t, t_0)$ is expressed as the ratio between the creep strain and the initial strain immediately after loading:

$$\varphi(t,t_0) = \frac{\varepsilon_{cc}(t,t_0)}{\varepsilon_{ci}(t_0)} \quad (5\text{-}4)$$

The developments of the creep coefficients are presented in Figure 5-5 to Figure 5-7.

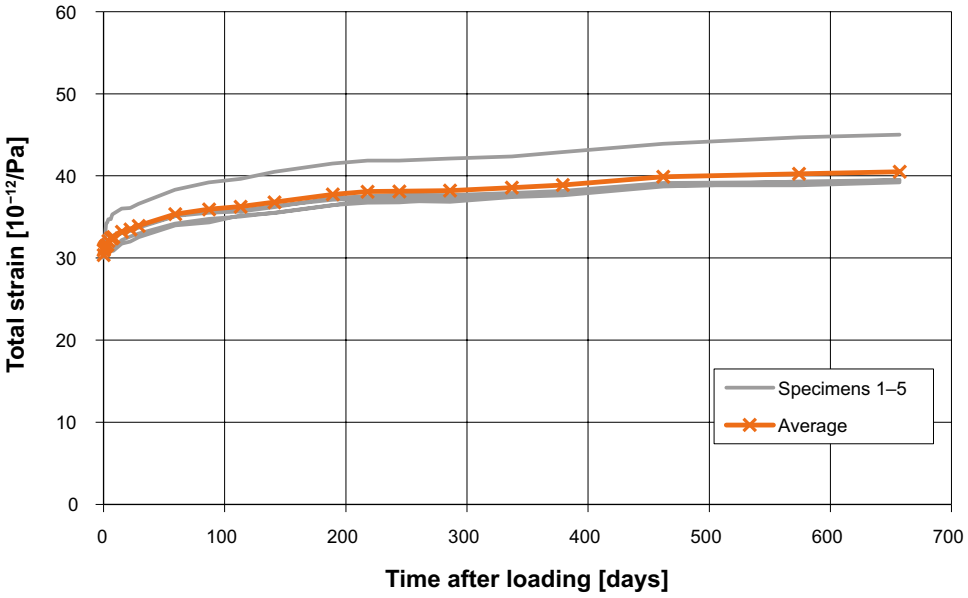

Figure 5-2. *Total stress-induced strain versus time after loading for the creep specimens in TR 1a; applied stress $\sigma_{cm}(t_0)$ = 30.0 MPa.*

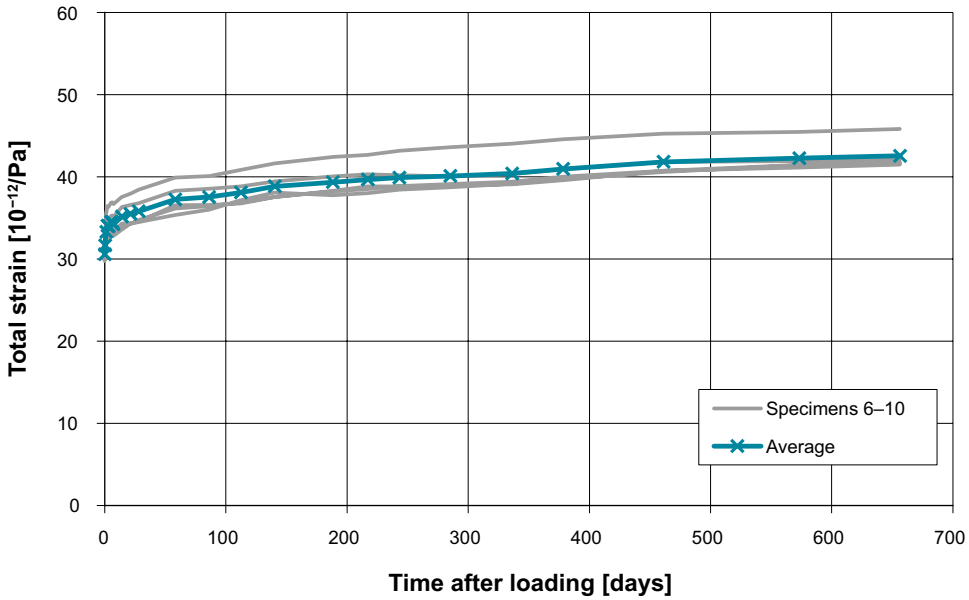

Figure 5-3. *Total stress-induced strain versus time after loading for the creep specimens in TR 1b; applied stress $\sigma_{cm}(t_0)$ = 38.5 MPa.*

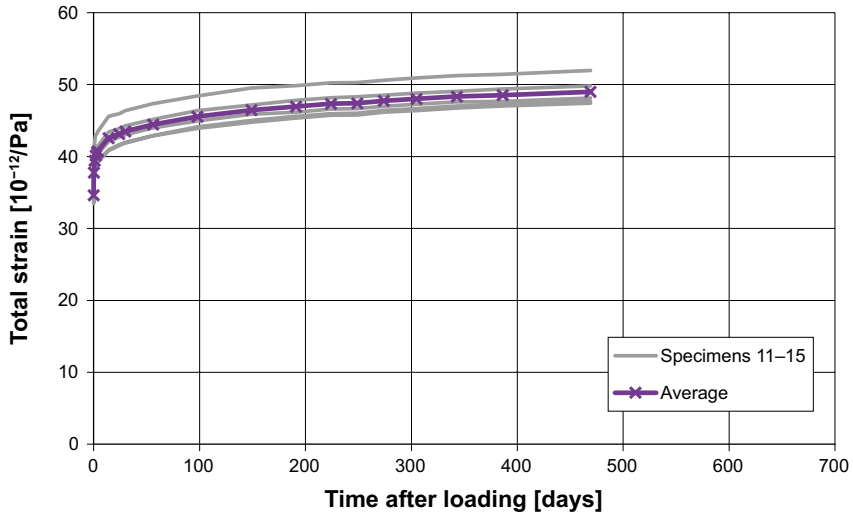

Figure 5-4. *Total stress-induced strain versus time after loading for the creep specimens in TR 2; applied stress $\sigma_{cm}(t_0)$ = 49.4 MPa.*

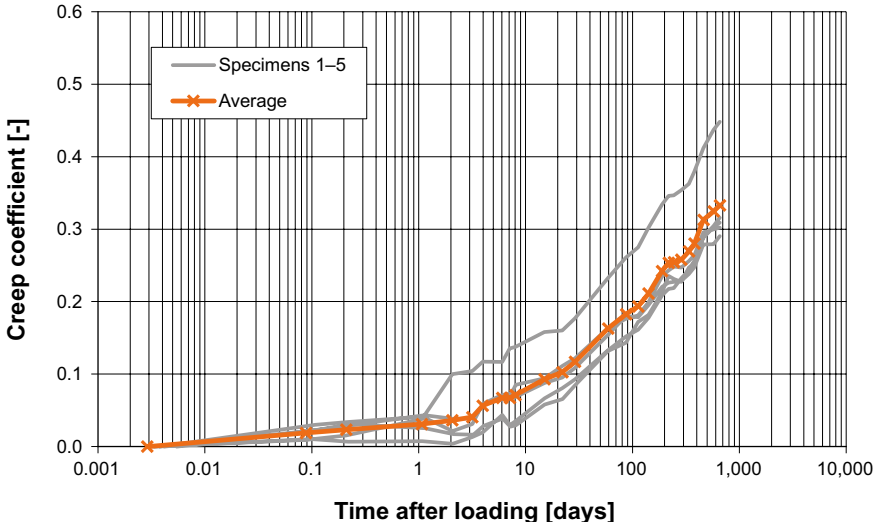

Figure 5-5. *Creep coefficient versus time after loading for the creep specimens in TR 1a; applied stress $\sigma_{cm}(t_0)$ = 30.0 MPa.*

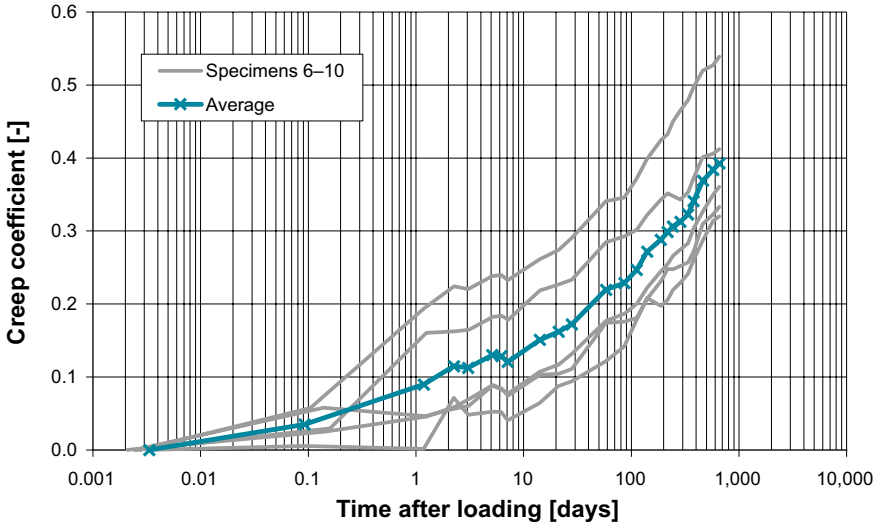

Figure 5-6. *Creep coefficient versus time after loading for the creep specimens in TR 1b; applied stress $\sigma_{cm}(t_0)$ = 38.5 MPa.*

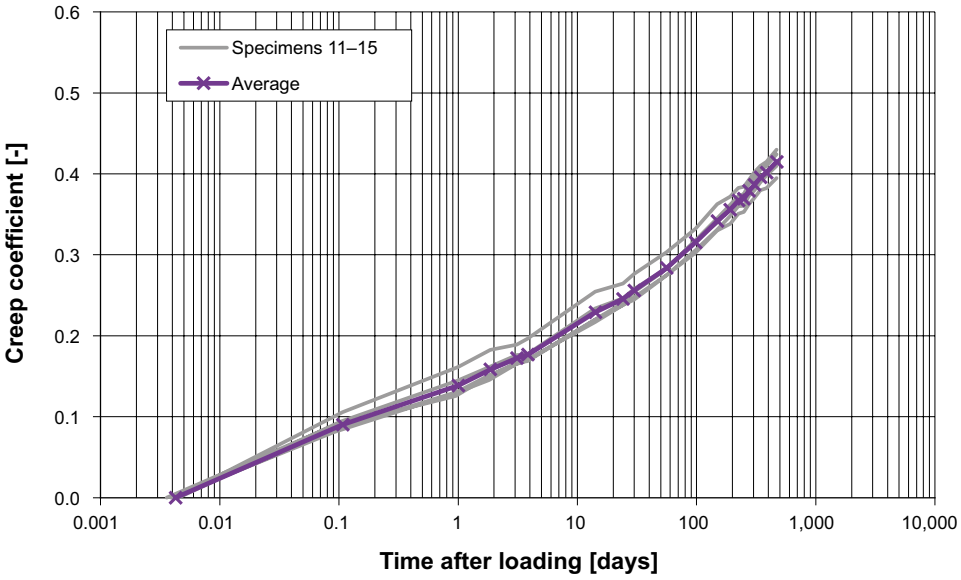

Figure 5-7. *Creep coefficient versus time after loading for the creep specimens in TR 2 applied stress $\sigma_{cm}(t_0)$ = 49.4 MPa.*

5.3 Discussion of the results

Figure 5-8 presents the mean value of the creep coefficient for each stress level. It can be seen that the higher the stress level is, the higher the creep coefficient is. In particular, the creep coefficient is increasing faster during the first days after loading for higher levels of sustained stresses. From 3 days after loading onwards, the rate of increase of the creep coefficient appears to be relatively similar for all the stress levels.

Previous tests were conducted at LTU on sealed concrete specimens loaded in hydraulic rigs at the age of 29 days and in mechanical rigs at the ages of 99 days and 385 days, as reported in R-09-07 (Vogt et al. 2009). The concrete specimens studied were cylinders of dimensions Ø100×100 mm.

In Figure 5-9, the creep coefficient measurements at different stress levels conducted in this study within the KBP 1004 project are compared to the previous results obtained for specimens loaded at 99 days by Vogt et al. (2009) at approximately 20% of their strength under short term loading.

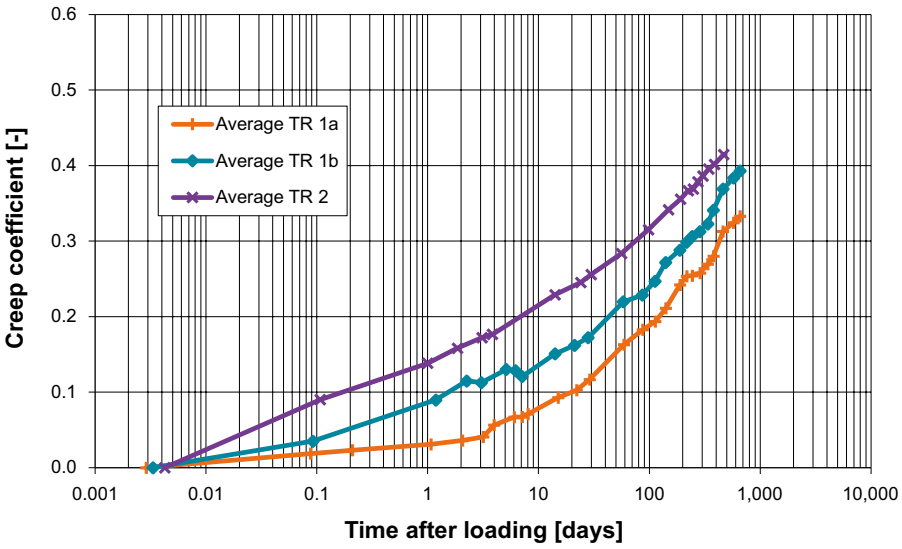

Figure 5-8. *Mean value of the creep coefficient versus time for TR 1a ($\sigma_{cm}(t_0)$ = 30.0 MPa), TR 1b ($\sigma_{cm}(t_0)$ = 38.5 MPa) and TR 2 ($\sigma_{cm}(t_0)$ = 49.4 MPa).*

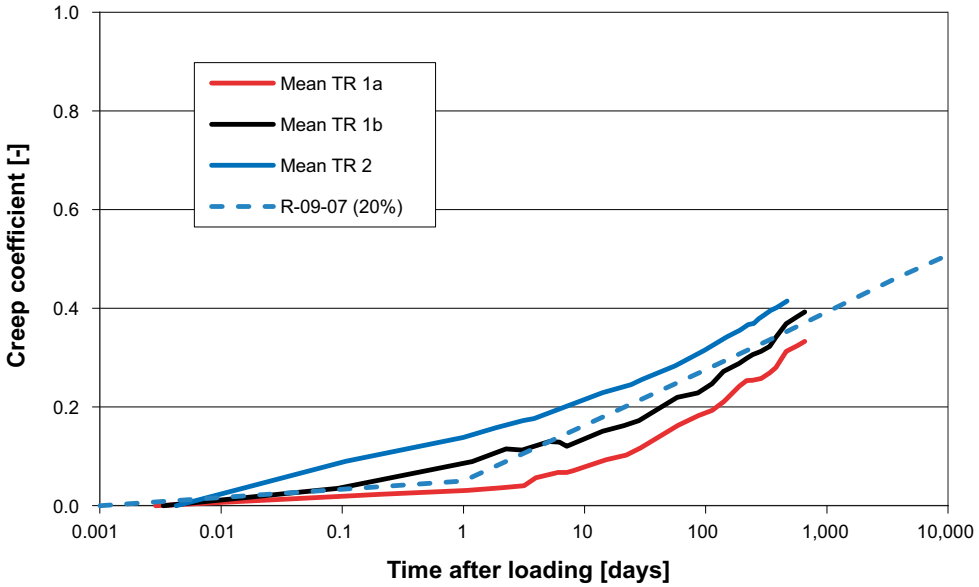

Figure 5-9. *Comparison of the mean value of the creep coefficient versus time for TR 1a (stress level of 40% of f_{cm}), TR 1b (50%) and TR 2 (75%) and of the trend curve for the creep coefficient from Vogt et al. (2009) marked "R-09-07 (20%)".*

As can be seen in Figure 5-9, results from Vogt et al. (2009) at 20% of the short term loading strength are similar to the results obtained in this study for a higher stress level of 50%. This may be due to the measurement methods used and to the different dimensions of the specimens studied for instance. Nevertheless, the rate of increase of the creep coefficient over time is similar in both studies.

According to FIB (2009), the ratio between the strength under sustained loading and the 28-day strength under short term loading is approximately 80% for concrete loaded at 28 days and 86% for concrete loaded at 90 days. Other studies conducted on high-performance concrete have highlighted that concrete can fail between 70% and 75% of its short term compressive strength when subjected to sustained stresses at an age of 56 days (Iravani and MacGregor 1994). This is because the compressive strength of concrete decreases with time under high sustained compressive stresses. However, one must also keep in mind the development of strength with time due to maturation of concrete, which acts as a counteracting effect.

Results obtained in this study within the KBP 1004 project show no indication that the stress levels applied as sustained loading will lead to failure in the concrete. It is however recommended to continue the creep measurements over a longer period of time.

6 Experience of low-pH concrete mix B200 – bond between concrete and rock

6.1 Overview of the test series

In this study, the mechanical properties of the interface between the low-pH concrete B200 and the wire-sawn rock surface were investigated. The aim was to improve the understanding of the interaction between the concrete surface of the plug and the surrounding rock surface. Modelling of the rock-concrete interface can for instance be used to determine if the plug will release from the rock during the hardening of the concrete or through cooling of the concrete plug.

The mechanical testing of the rock-concrete interface was conducted on cylinders, which were core-drilled from rock-concrete blocks. The blocks were manufactured in the laboratory by casting concrete against the wire sawn surfaces of rock panels from the Äspö Hard Rock Laboratory whose dimensions were approximately 800×700×150 mm. In total, five rock-concrete blocks were manufactured. In four blocks, the concrete was cast on top of a horizontal rock surface (denoted 1a, 1d, 2a and 2b). The fifth block was obtained by casting concrete against the vertical rock surfaces of the rock panel with two sawn surfaces (denoted 2a and 2b). In addition, two blocks of plain concrete were cast for preparation of material test specimens (see Section 3.2.2). After casting, the free concrete surfaces were covered with a moist micro-fiber fabric and a plastic foil. The day after casting the blocks were enclosed by the plastic foil, sealed with splicing tape and stored at a temperature of approximately 20°C.

The characteristics of the wire sawn rock surfaces were documented with optical 3D-scanning as shown in Figure 6-1, see Flansbjer and Magnusson (2014b) for more details.

The tensile bond strength has been determined by pull-off tests on cores drilled through the rock-concrete interface. The tensile softening behaviour of the interface was evaluated from direct tensile tests on rock-concrete cylinders. The shear strength of the interface and the residual shear strength of the broken interface were determined by shear load tests on cylinders at different constant normal stress levels.

Tests were also conducted to determine the mechanical properties of the concrete material, see Section 3.2.2. The following properties were evaluated: the compressive strength, the splitting tensile strength, the direct tensile strength and the fracture energy.

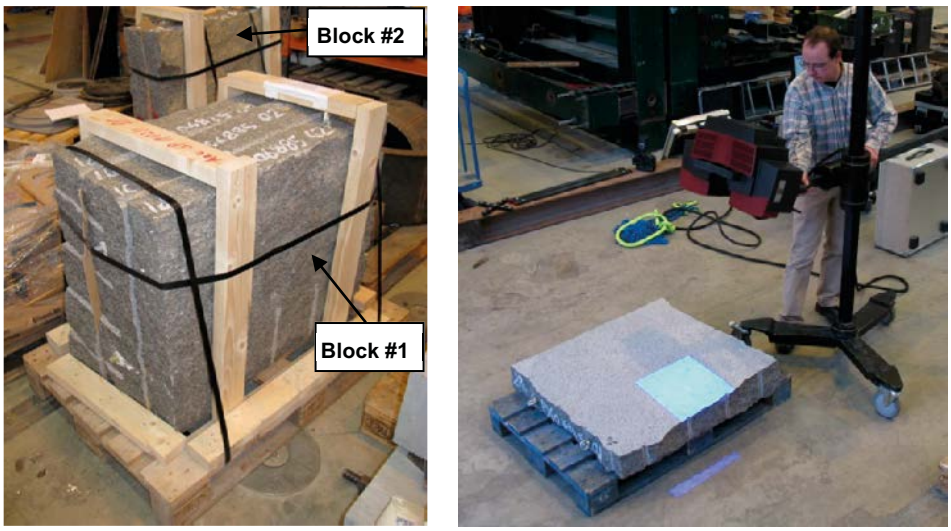

Figure 6-1. *Rock panels delivered from Äspö laboratory (left) and 3D-scanning of a wire sawn rock panel surface (right).*

6.2 Tensile bond strength

6.2.1 Results from pull-off tests

The tensile bond strength at the rock-concrete interface was determined at three different ages by pull-off tests using a circular loading plate bonded to the surface of Ø50 mm cores drilled through the concrete and approximately 3–4 mm into the rock, see Figure 6-2. The tests were performed on one interface where the concrete was cast on top of a horizontal rock surface (horizontal interface 1a) and one where the concrete was cast against a vertical rock surfaces (vertical interface 1c). A summary of the pull-off test results can be found in Table 6-1 and more detailed information in Flansbjer and Magnusson (2014b).

The peak tensile stress includes all tests where the failure occurred at the interface or in the concrete, whereas the tensile bond strength is restricted to the results where the failure occurred at the interface. No results were obtained at the age of 12 days for the vertical interface 1a, since the interface failed already when the cores where drilled through the interface. The development of the peak tensile stress is shown in Figure 6-3. The peak tensile stress was chosen due to a better statistical basis; however, there is a good correlation between the peak tensile stress and the bond strength. There is a significant difference in bond strength between the vertical interface and the horizontal interface. For the specimens taken from the vertical interface 1c the majority of the failures occurred at the interface, while for the specimens taken from the horizontal interface 1a the majority of the failures occurred in the concrete. The lower bond strength together with the interface failures suggest that the bond is weaker when the concrete is cast against a vertical rock surface.

Table 6-1. Summary of results from the tensile bond strength tests, given as mean values (standard deviations are given in brackets).

Property	Age [days]	Peak tensile stress [MPa]	Tensile bond strength [MPa]
Vertical interface 1c	12	– [1)]	– [1)]
	30	2.66 (*0.55*)	2.51 (*0.51*)
	91	3.00 (*0.48*)	2.90 (*0.42*)
Horizontal interface 1a	12	1.45 (*0.04*)	1.48 (–) [2)]
	33	3.31 (*0.29*)	3.37 (*0.14*)
	91	4.25 (*0.23*)	4.38 (*0.28*)

[1)] Interface failure at drilling – no results.

[2)] Only one result.

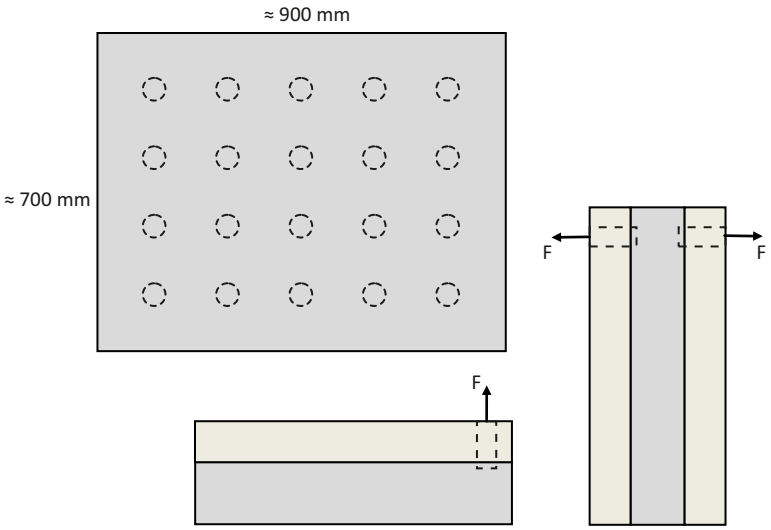

Figure 6-2. *Sketch of blocks used for simple bond tests (vertical and horizontal tests).*

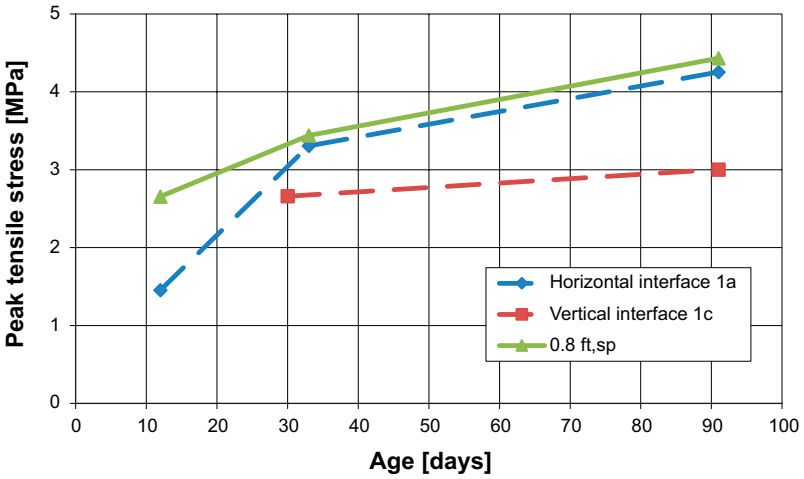

Figure 6-3. *Development of peak tensile stress at the rock-concrete interface and tensile strength of the concrete (assumed as 80% of the splitting tensile strength).*

6.2.2 Results from direct tensile tests

The tensile bond strength, together with the tensile softening behaviour of the concrete material and the rock-concrete interface, were also evaluated at an age of approximately 90 days from direct tensile tests, performed on cylinders with fixed end conditions following the recommendations given in RILEM (2001, 2007). The crack propagation at the rock-concrete interface was also registered in a detailed way by the use of optical full-field deformation measurements.

Cylinders with a diameter of 100 mm were core-drilled from the concrete blocks and the rock-concrete block 2a, where the concrete was cast on top of a horizontal rock surface. The cores were cut to a length slightly more than 100 mm, after which the top and bottom edges were face-ground down to approximately 100 mm. Around the mid-section of the concrete cylinders a 10 mm deep and 5 mm wide notch was cut (see Figure 6-5).

The tests were carried out in a servo-hydraulic machine using a moment stiff loading device in order to suppress rotations of the holders that could lead to bending failure. Specimens were glued to the lower loading platen using a "glue device" in order to ensure that the cylinder was centered and perpendicular to the face of the loading platen.

The tests were displacement controlled. The displacement was measured locally over the notch or joint with three inductive displacement transducers with a gauge length, l_g, of 31 mm and the mean value was used for the displacement control.

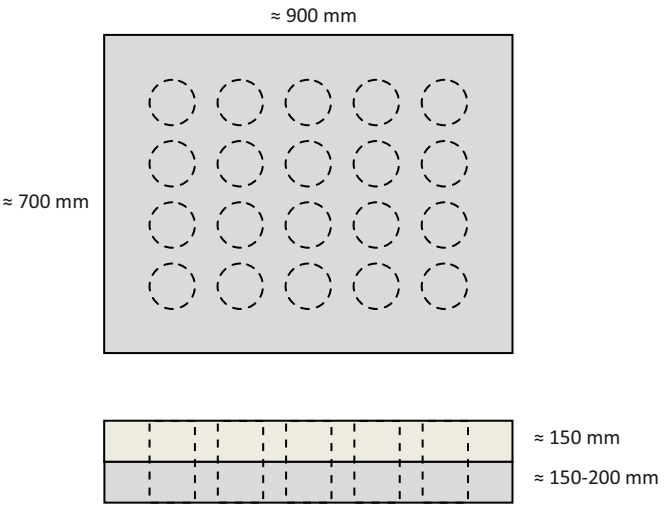

Figure 6-4. *Sketch of block used for direct tensile tests.*

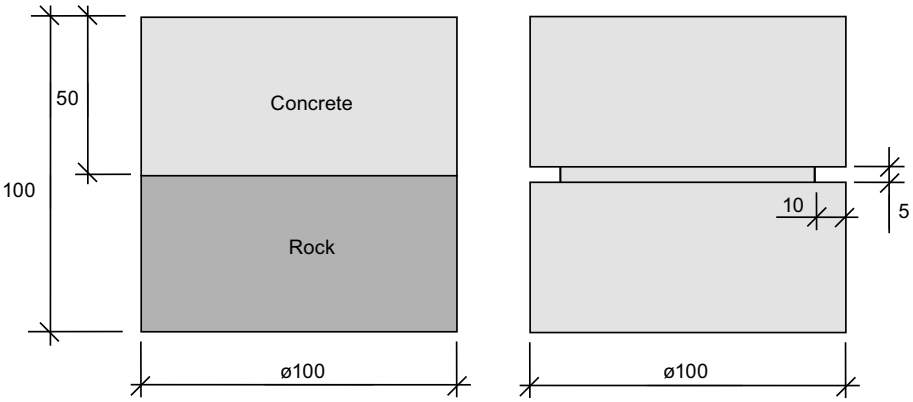

Figure 6-5. *Geometry of tensile test specimens.*

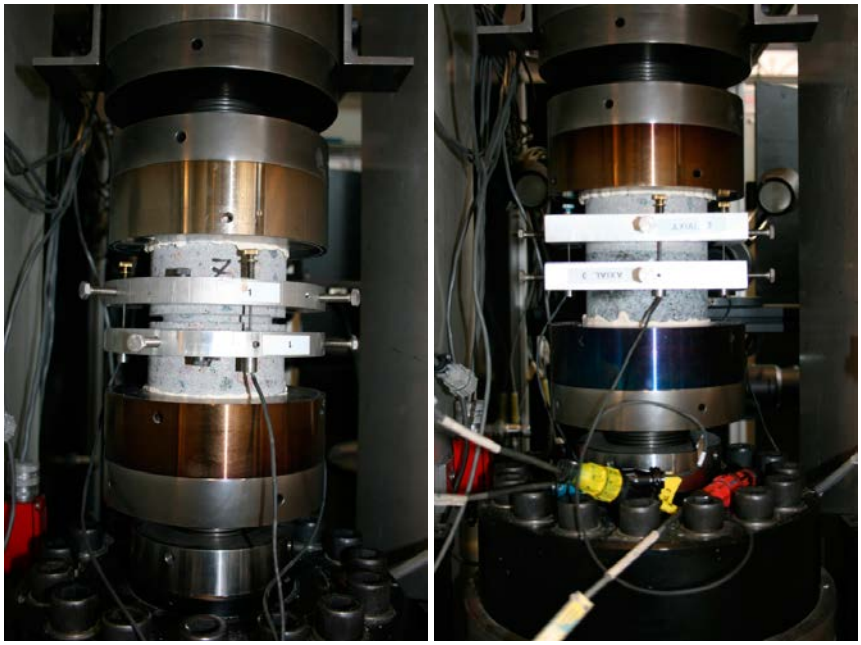

Figure 6-6. *Experimental test setup for the direct tensile tests on a) the concrete material and b) the rock-concrete interface.*

The crack opening w, in the post-peak regime, was evaluated according to RILEM (2007) by subtracting the elastic deformation δ_e from the measured displacement δ as:

$$w = \delta - \delta_e = \delta - \frac{\sigma}{E} l_g = \delta - \frac{\sigma}{K} \quad (6\text{-}1)$$

where σ is the tensile stress, E is the modulus of elasticity and l_g is the gauge length. Since the notches and the interface hamper the direct measurement of the modulus of elasticity in tension, the ratio E/l_g was replaced by the elastic stiffness K, which was evaluated directly from the tensile stress-displacement relations. The fracture energy, G_F, was calculated from the area under the stress-crack opening curve as:

$$G_F = \int \sigma(w) dw \quad (6\text{-}2)$$

A summary of the direct tensile test results can be found in Table 6-2 and detailed information in Flansbjer and Magnusson (2014b).

Table 6-2. Results from direct tensile tests on rock-concrete interface specimens, approximately 90 days after casting.

Specimen	Area [cm^2]	Age [days]	Failure mode	Peak tensile stress [MPa]	Tensile bond strength [MPa]	Fracture energy [N/m]
DTT-RCI-2	77.8	93	Interface	3.6	3.6	25.8
DTT-RCI-3	77.8	93	Interface	3.8	3.8	–
DTT-RCI-4	77.8	93	Interface	3.7	3.7	26.8
DTT-RCI-5	77.8	97	Concrete	4.1	–	–
DTT-RCI-6	77.9	97	Interface	3.9	3.9	–
DTT-RCI-7	77.8	97	Interface	4.0	4.0	–
			Mean μ	3.9	3.8	26.3
			Std. dev. σ	0.2	0.1	0.7

The failure occurred at the rock-concrete interface in all cases except in one case, where it occurred in the concrete outside the measuring range, close to the loading plate. In the former cases, the results from the optical full-field deformation measurements confirmed that the cracking was restricted to the interface without major cracking in the concrete, see Flansbjer and Magnusson (2014b). Comparing the results from the direct tensile tests with fixed end conditions, it can be seen that the tensile bond strength of the horizontal interface (Table 6-2) is at the same level as the tensile strength of the concrete (Table 3-12 in Section 3.2.2). The failure mode at the interface was very brittle and it was only possible to evaluate the stress-crack opening relation and fracture energy for two of the tests, see Figure 6-7 and Table 3-12. It can be noted that the fracture energy from the rock-concrete interface cracking is about 1/5 of the concrete fracture energy stated in Section 3.2.2. The main reason for this is the absence of coarse aggregates crossing the failure zone.

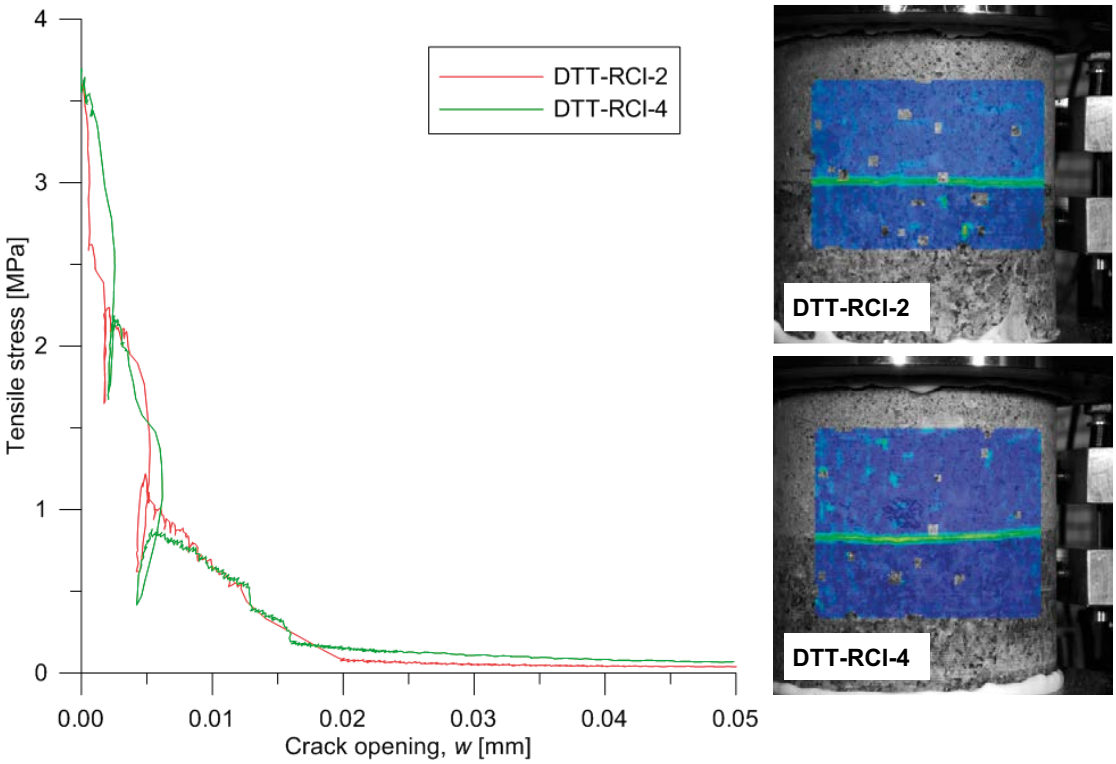

Figure 6-7. *Tensile stress vs. crack opening from direct tensile tests on rock-concrete interface specimens (DTT-RCI-2 and DTT-RCI-4).*

6.3 Shear tests

Shear-tests were also conducted on cylinders core-drilled from the rock-concrete block 2a, which was manufactured by casting concrete on top of a horizontal rock surface. The cores, of approximately 80 mm and 65 mm in diameter, were cut to a final length of 100 mm with the joint plane approximately located in the centre of the final specimen, see Figure 6-8. Each specimen was then fixated into one lower and one upper steel holder using fast setting cement, such that the joint plane was centred in the opening between the holders, see Figure 6-8.

The shear strength of the rock-concrete interface and the residual shear strength of the broken interface were determined by shear load tests on cylinders at different constant normal stress levels according to the test programme presented in Table 6-3. For specimens DST-RCI-7 and DST-RCI-8, seven successive shear cycles (*s1–s7*) were also conducted on the broken interface with various constant normal stress levels. The specimens, on which a normal stress was applied, had a diameter of 65 mm, whereas the specimens with no applied normal stress had a diameter of 80 mm. The tests were conducted at an age of approximately 90 days. A summary of test results can be found in Table 6-3 and more detailed information in Flansbjer and Magnusson (2014b).

Table 6-3. Test programme and summary of results for direct shear tests on rock-concrete interface specimens.

Specimen	Area [cm^2]	Age [days]	Shear seq. [1)]	Normal stress [MPa]	Peak shear stress [MPa]	Res. shear stress [MPa]	Res. shear stress/ Normal stress	Failure mode [2)]
DST-RCI-1	32.5	91	s	5	11.5	4.3	0.86	b
DST-RCI-2	32.5	91	s	3	11.0	2.4	0.80	b
DST-RCI-3	32.3	90	s	10	15.6	6.0	0.60	c
DST-RCI-4	32.6	90	s	10	15.7	7.1	0.71	c
DST-RCI-7	50.0	90	s	0	6.1	0	–	a
			s1	5	4.8	4.3	0.85	–
			s2	10	8.5	8.2	0.82	–
			s3	30	23.7	22.4	0.75	–
			s4	20	14.7	14.7	0.74	–
			s5	10	7.8	7.8	0.78	–
			s6	30	21.6	21.6	0.72	–
			s7	5	4.1	4.1	0.81	–
DST-RCI-8	50.6	90	s	0	6.2	0	–	a
			s1	5	3.9	3.5	0.70	–
			s2	10	7.2	7.0	0.70	–
			s3	20	14.1	14.0	0.70	–
			s4	30	20.9	20.8	0.69	–
			s5	20	14.3	14.3	0.72	–
			s6	10	7.4	7.4	0.74	–
			s7	5	3.8	3.8	0.76	–

[1)] Shear sequence: s = shear cycle on intact interface; s# = shear cycle on broken interface.

[2)] Failure mode: a = in interface; b = mainly in interface; c = inclined failure plane crossing interface.

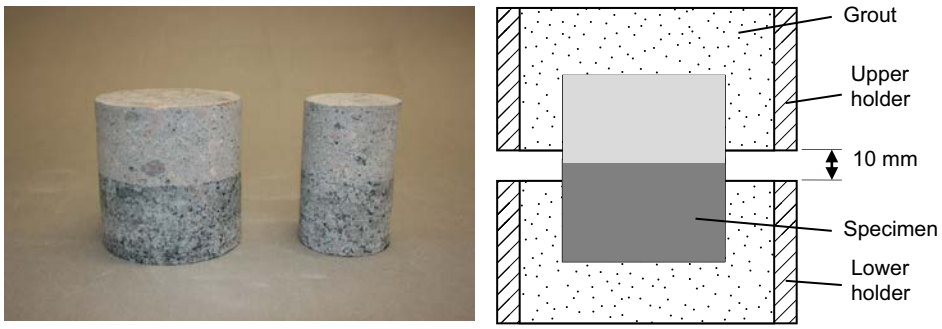

Figure 6-8. *Photo of shear test specimens (left) and illustration of specimen cast in the specimen holders (right).*

The shear stress vs. shear displacement is shown in Figure 6-9 for the tests on specimens with intact interface, and in Figure 6-10 and Figure 6-11 for the tests on broken interface of specimens DST-RCI-7 and DST-RCI-8 respectively.

The failure mode at the interface was very brittle, resulting in a shear stress drop. In the cases with an applied normal stress, the shear stress drop was followed by a new shear stress peak, after which the shear stress declined towards a residual shear stress level of the broken interface. In the tests (DST-RCI-3 and DST-RCI-4) with the highest normal stress level an inclined failure plane crossing the interface was observed, which indicates that the peak stress and the residual stress are not the exact values of the interface. The friction coefficient μ of the broken interface, determined for each test as the residual shear stress divided by the normal stress, was in the range of 0.60 and 0.86, see Table 6-3. In Figure 6-12, the peak shear stress of the intact interface and the residual shear stress of the broken interface are plotted against the corresponding normal stress.

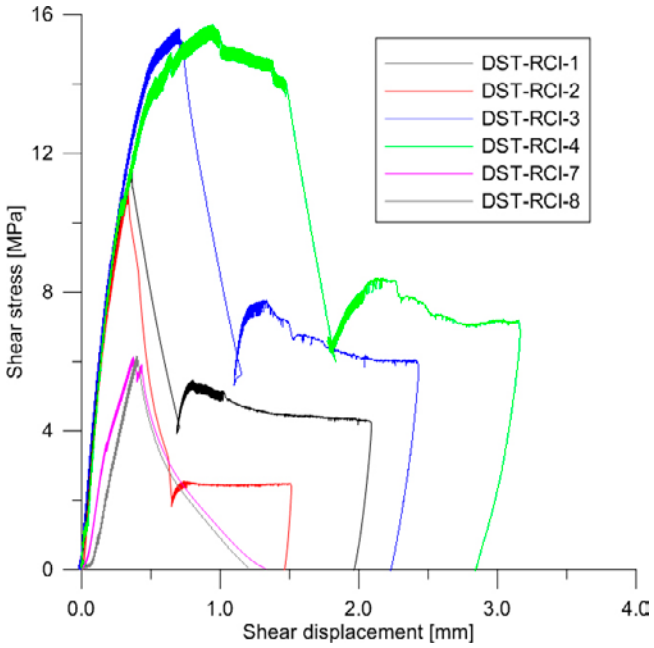

Figure 6-9. *Shear stress vs. shear displacement from direct shear tests on rock-concrete interface specimens (DST-RCI-#).*

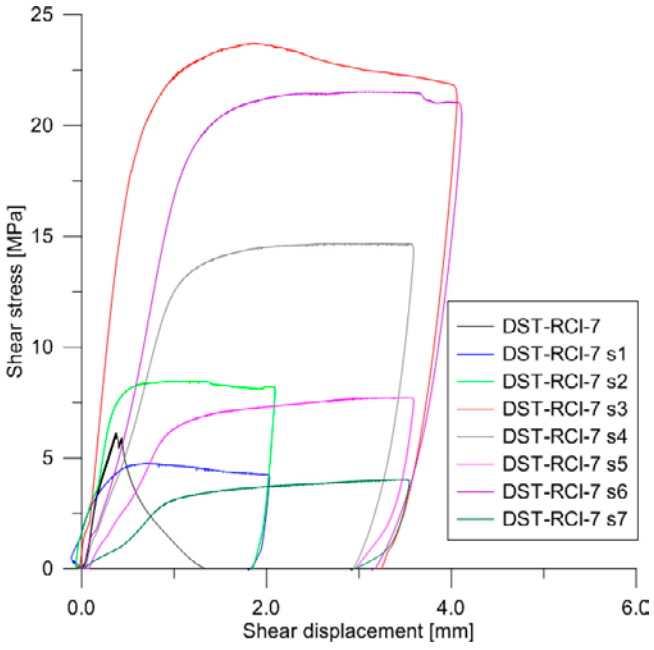

Figure 6-10. *Shear stress vs. shear displacement from direct shear tests on rock-concrete interface specimen DST-RCI-7.*

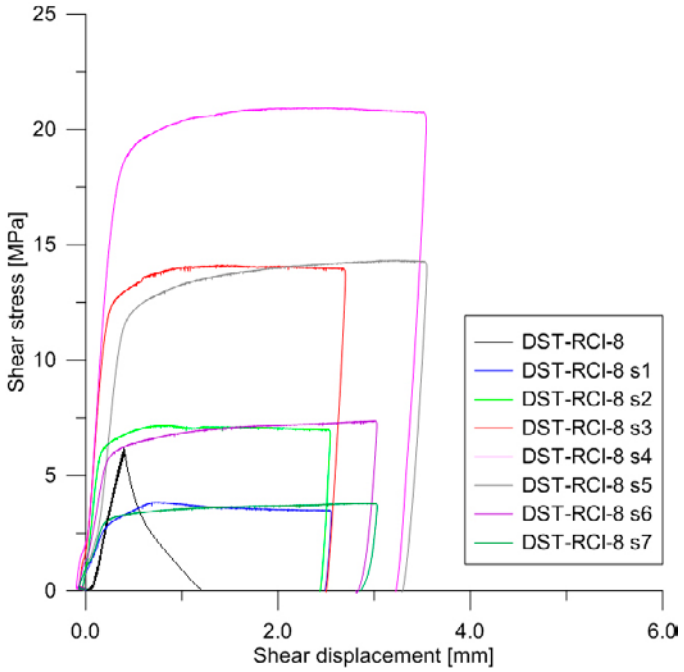

Figure 6-11. *Shear stress vs. shear displacement from direct shear tests on rock-concrete interface specimen DST-RCI-8.*

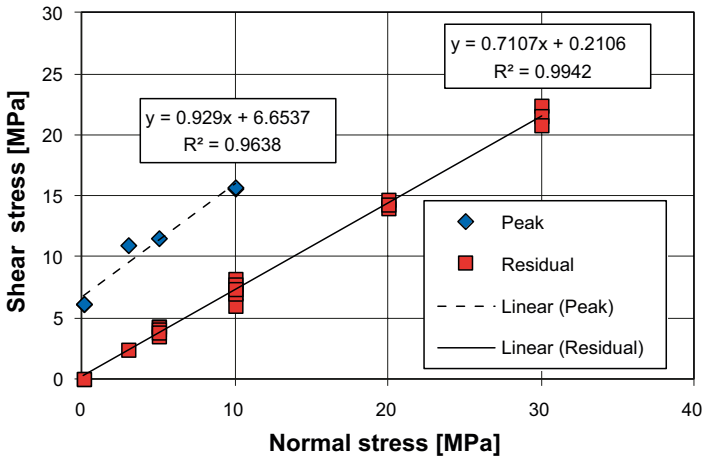

Figure 6-12. *Peak shear stress and residual shear stress vs. normal stress from direct shear tests on rock-concrete interface specimens.*

6.4 Discussion of the results

6.4.1 Tensile bond strength and fracture energy

The tensile bond strength was determined by pull-off tests on cylinders cored through the rock-concrete interface at different times after casting. A significant difference in bond strength between vertical interface and horizontal interface was observed. For the specimens taken from blocks with vertical interface the majority of the failures occurred at the interface, while for the specimens taken from blocks with horizontal interface the majority of the failures occurred instead in the concrete. The lower bond strength and the mode of failure at the interface suggest that the bond is weaker when the concrete is cast against a vertical rock surface.

The tensile bond strength, together with the tensile softening behaviour of the rock-concrete interface, was also evaluated 90 days after casting by direct tensile tests with fixed end conditions on rock-concrete cores drilled from a panel with horizontal interface.

The failure occurred at the interface in all cases except in one, where it occurred in the concrete outside the measuring range, close to the loading plate. In the former cases, the results from optical full-field deformation measurements confirmed that the cracking was restricted to the interface without major cracking in the concrete. The tensile bond strength of the horizontal interface was at the same level as the tensile strength of the concrete.

The failure of the interface was very brittle and it was only possible to evaluate the stress-crack opening relation and fracture energy for two of the tests. The mean fracture energy obtained was 26.3 N/m. It can be noted that the fracture energy from the rock-concrete interface cracking was about 1/5 of the concrete fracture energy.

6.4.2 Shear bond strength

The shear strength of the rock-concrete interface and the residual shear strength of the broken interface were determined by shear load tests at different constant normal stress levels on cylinders core-drilled from a rock-concrete block. The friction coefficient μ of the broken interface, determined for each test as the residual shear stress divided by the normal stress, was in the range of 0.60 and 0.86.

7 Concluding remarks

The main focus of the laboratory tests conducted in this project was to investigate further the mechanical properties of the low-pH concrete mix B200, especially from 90 days after casting onwards. The results summarized in the report can be divided into four categories: hardened concrete properties; shrinkage; creep; and interaction between concrete and rock. These results will contribute to improve numerical modelling of the structural behaviour of the concrete plug prior to and under loading, in order to analyse among others the effects of the pressure on deformations, cracking and water tightness of the concrete plug. The creep tests are still ongoing at the time of writing this report.

The results from direct tensile tests showed that the tensile bond strength between concrete and rock proved to be in the same order of magnitude as the tensile strength of the concrete. However, the failure mode at the interface between rock and concrete was much more brittle than that of the concrete. One of the design requirements for the dome plug is that it should be considered as stress free 90 days after casting. This means that the shrinkage during the first 90 days should be considered as free shrinkage, i.e. without restraint. Therefore the concrete plug has to undergo a sufficient shrinkage during this time so that release from the rock surface is achieved. In the full-scale test of the dome plug, the plug did not fully release from the rock surface. Reasons for this are most likely due to low early shrinkage and the strong bond between concrete and rock. The pull-off tests suggest that the probability of achieving a release is larger as early as possible after casting. For this reason, it would be beneficial to conduct further investigations on the early age shrinkage, using both dilatometer measurements and tests on sealed beams according to Vogt et al. (2009).

It is of importance that concrete mix B200 can be reproduced at other laboratories and especially at concrete plants. Therefore, results obtained in this study, within the KBP 1004 project, were compared to results reported in Vogt et al. (2009). A comparison made between compressive strength results at 90 days from tests on cubes cast at different laboratory showed a rather expected variation inside each test series; however, the results obtained in the different test series suggest a significant variation between the test series. A possible explanation could be that concrete mix B200 is sensitive to small variations in the mixing order or small variations in the mix composition. Therefore further investigations concerning the robustness of the concrete mix and mixing order are needed, not least in view of the observed variations in air content.

A comparison was also made between compressive strength results from tests on cubes cast at different large-scale castings obtained in this study, within the KBP 1004 project, and results reported in Vogt et al. (2009). The first two large-scale castings carried out in the KBP 1004 project should be considered as test castings before the full-scale casting of the dome plug. The results from the casting of the dome plug presented a much lower scatter than the results of the test castings. However, the compressive strength of the concrete was significantly lower than compared to Vogt et al. (2009); which can almost certainly be explained by the high air content. Furthermore, it is always difficult to adjust the conditions in a concrete plant for a single large- scale test of a rather unique concrete mix.

The comparison of results from large-scale castings and laboratory tests suggest that it is possible to use concrete mix B200; however, since the strength was lower than expected in the full-scale dome plug, there is a need for additional large-scale castings to ensure that the reference concrete strength can be reached. Furthermore, the mixer used was a drum mixer and if force mixing shall be used the mixing order may have to be adjusted. The influence of the type of fine aggregate should be studied, especially if crushed sand from the Forsmark area (the location of the Spent Fuel Repository) should be used instead of natural sand from the Kalmar area (where concrete for the large-scale tests was produced).

Finally, experiences from the B200-concrete test series show that further clarification is needed regarding quality control requirements and acceptance criteria of the young concrete properties, e.g. what are the appropriate criteria on the slump flow and when should it be tested. Standardization of the examinations and tests to be performed at any lab castings and full-scale castings is essential for reliable and successful construction of the KBS-3V concrete dome plugs.

References

SKB's publications can be found at www.skb.se/publications.

ASTM, 2010. ASTM C512: Standard test method for creep of concrete in compression. West Conshohocken, PA: ASTM International.

Bartlett F, MacGregor J G, 2003. Equivalent specified concrete strength from core test data. Concrete International 17, 52–58.

Dahlström L-O, Magnusson J, Gueorguiev G, Johansson M, 2009. Feasibility study of a concrete plug made of low pH concrete. SKB R-09-34, Svensk Kärnbränslehantering AB.

FIB, 2009. Structural concrete: textbook on behaviour, design and performance. Vol. 1 2nd ed. Lausanne: Fédération Internationale du Béton. (fib Bulletin 51)

Flansbjer M, Magnusson J, 2014a. System design of Dome plug. Creep properties at high stress levels of concrete for deposition tunnel plugs. SKB P-13-37, Svensk Kärnbränslehantering AB.

Flansbjer M, Magnusson J, 2014b. System design of Dome plug. Mechanical properties of rock–concrete interface. SKB P-13-38, Svensk Kärnbränslehantering AB.

Iravani S, MacGregor J G, 1994. High performance concrete under high sustained compressive stresses. Structural Engineering report No. 200, Department of Civil Engineering, University of Alberta, Canada.

ISO, 2009. ISO 1920-9:2009: Testing of concrete – Part 9: Determination of creep of concrete cylinders in compression. Geneva: International Organization for Standardization.

Ljungkrantz C, Möller G, Petersons N, 1997. Betonghandbok. Material. 2nd ed. Solna: Svensk byggtjänst. (In Swedish.)

Malm R, 2012. Low-pH concrete plug for sealing the KBS-3V deposition tunnels. SKB R-11-04, Svensk Kärnbränslehantering AB.

RILEM, 2001. Final recommendation of RILEM TC 162-TDF: Test and design methods for steel fibre reinforced concrete. Uni-axial tension test for steel fibre reinforced concrete. Materials and Structures 34, 3–6.

RILEM, 2007. Experimental determination of the stress-crack opening curve for concrete in tension. Final report of RILEM Technical Committee TC 187-SOC, RILEM.

SIS, 2000. SS 137215: Betongprovning – Hårdnad betong – Krympning (Concrete testing – Hardened concrete – Shrinkage). Stockholm: Swedish Standards Institute. (In Swedish.)

SIS, 2001. SS-EN 206-1: Betong - Del 1: Fordringar, egenskaper, tillverkning och överensstämmelse (Concrete – Part 1: Specification, performance, production and conformity). Stockholm: Swedish Standards Institute. (In Swedish.)

SIS, 2005a. SS 137231:2005: Betongprovning – Hårdnad betong – Draghållfasthet hos provkroppar. (Concrete testing – Hardened concrete – tensile strength of test specimens). Stockholm: Swedish Standards Institute. (In Swedish.)

SIS, 2005b. SS 137232:2005: Betongprovning – Hårdnad betong – Elasticitetsmodul vid tryckprovning. (Concrete testing – Hardened concrete – Modulus of elasticity in compression). Stockholm: Swedish Standards Institute. (In Swedish.)

SIS, 2005c. SS-EN 1992-1-1:2005: Eurocode 2: Design of concrete structures – Part 1-1: General rules and rules for buildings. Stockholm: Swedish Standards Institute.

SIS, 2007. SS-EN 13791:2007: Assessment of in-situ compressive strength in structures and precast concrete components. Stockholm: Swedish Standards Institute.

SIS, 2009a. SS-EN 12390-3:2009: Testing hardened concrete – Part 3: Compressive strength of test specimens. Stockholm: Swedish Standards Institute.

SIS, 2009b. SS-EN 12390-6:2009: Testing hardened concrete – Part 6: Tensile splitting strength of test specimens. Stockholm: Swedish Standards Institute.

SIS, 2009c. SS-EN 12504-1:2009: Testing concrete in structures – Part 1: Cored specimens – Taking, examination and testing in compression. Stockholm: Swedish Standards Institute.

SIS, 2009d. SS-EN 12390-2:2009: Testing hardened concrete – Part 2: Marking and curing specimens for strength tests. Stockholm: Swedish Standards Institute.

SIS, 2009e. SS-EN 12390-7:2009: Testing hardened concrete – Part 7: Density of hardened concrete. Stockholm: Swedish Standards Institute.

SKB, 2010. Design and production of the KBS-3 repository. SKB TR-10-12, Svensk Kärnbränslehantering AB,

True G, 2003. Core sampling and testing. In Newman J B, Choo B S (eds). Advanced concrete technology. Vol 1, Constituent materials. Oxford: Butterworth-Heinemann, Chapter 5.

Vogt C, Lagerblad B, Wallin K, Baldy F, Jonasson J-E, 2009. Low pH self compacting concrete for deposition tunnel plugs. SKB R-09-07, Svensk Kärnbränslehantering AB.

Appendix A

Collection of results from tests on strength and stiffness properties of concrete B200 conducted in KBP 1004

A1 Results obtained from large-scale castings

A1.1 Casting of the concrete specimen

Table A1-1. Results from compression strength tests at different ages of cubes cast at the concrete plant.

Lorry load	Batch	28 days $f_{c,cube}$ [MPa]	28 days Density [kg/m^3]	90 days $f_{c,cube}$ [MPa]	90 days Density [kg/m^3]
1	1-1	89.9	2,360	106.7	2,390
1	1-2	76.8	2,310	93.4	2,320
2	2-1	62.7	2,320	81.7	2,300
2	2-2	69.8	2,390	91.0	2,380
3	3-1	54.1	2,390	72.8	2,310
3	3-2	54.5	2,380	73.5	2,370
Mean μ		68.0	2,358	86.5	2,345
Std. dev. σ		13.9	35	13.1	39

Table A1-2. Results from compression strength tests of cubes cast on-site.

Lorry load	28 days $f_{c,cube}$ [MPa]	28 days Density [kg/m^3]
1	74.6	2,360
1	74.7	2,310
1	69.8	2,330
2	56.3	2,300
2	56.0	2,290
2	62.4	2,340
3	50.4	2,330
3	51.0	2,340
3	50.7	2,330
Mean μ	60.7	2,326
Std. dev. σ	10.1	22

Table A1-3. Results from tensile splitting strength tests at different ages of cubes cast at the concrete plant.

Lorry load	Batch	28 days $f_{t,sp,cube}$ [MPa]	28 days Density [kg/m^3]	90 days $f_{t,sp,cube}$ [MPa]	90 days Density [kg/m^3]
1	1-1	6.65	2,440	6.65	2,380
1	1-2	6.50	2,400	6.65	2,400
2	2-1	5.30	2,310	6.80	2,320
2	2-2	5.85	2,390	6.10	2,370
3	3-1	5.00	2,370	5.80	2,360
3	3-2	5.30	2,390	6.40	2,340
Mean μ		5.80	2,383	6.40	2,362
Std. dev. σ		0.7	43	0.4	29

A1.2 Casting of the concrete back-wall

Table A1-4. Results from compression strength tests at 28 days of cubes cast at the concrete plant.

Lorry load	$f_{c,cube}$ [MPa]	Density [kg/m^3]
1	33.2	2,380
2	49.7	2,300
3	38.5	2,360
Mean μ	40.5	2,347
Std. dev. σ	8.4	42

Table A1-5. Results from compression strength tests at 28 days of cubes cast on-site.

Lorry load	$f_{c,cube}$ [MPa]	Density [kg/m^3]
3	29.5	2,390

A1.3 Casting of the full-scale dome plug and of the concrete monolith

Table A1-6. Results from compression strength tests at different ages of cubes cast at the concrete plant.

Lorry load	At arrival on-site		7 days		28 days		90 days	
	Air[1] [%]	Density [kg/m^3]	$f_{c,cube}$ [MPa]	Density [kg/m^3]	$f_{c,cube}$ [MPa]	Density [kg/m^3]	$f_{c,cube}$ [MPa]	Density [kg/m^3]
1	8.5	n/a	19.5	2,150	42.5	2,160	53.8	2,160
3	7.8	2,210	16.0	2,150	38.4	2,170	56.5	2,190
5	9.0	2,180	18.0	2,160	40.9	2,130	54.9	2,170
7	6.6	2,210	18.3	2,160	43.1	2,160	59.9	2,170
9	7.8	2,210	16.4	2,170	38.6	2,130	51.5	2,180
11	7.2	2,180	16.7	2,200	38.3	2,200	55.3	2,180
13	7.1	2,240	18.8	2,190	40.0	2,200	59.3	2,210
Mean μ	7.7	2,205	17.7	2,169	40.3	2,164	55.9	2,180
Std. dev. σ	0.8	23	1.3	20	2.0	29	3.0	16

[1]Air content was also measured at the concrete plant for batches 5 and 7 and found to be 10.0% for both.

Table A1-7. Results from compression strength tests at different ages of cubes cast on-site.

Lorry load	At arrival on-site		7 days		28 days		90 days	
	Air [%]	Density [kg/m^3]	$f_{c,cube}$ [MPa]	Density [kg/m^3]	$f_{c,cube}$ [MPa]	Density [kg/m^3]	$f_{c,cube}$ [MPa]	Density [kg/m^3]
1	8.5	n/a	19.6	2,210	40.2	2,220	54.4	2,170
3	7.8	2,210	19.2	2,190	41.4	2,220	55.8	2,200
5	9.0	2,180	19.7	2,170	43.3	2,190	57.5	2,210
7	6.6	2,210	21.1	2,230	45.4	2,210	63.4	2,210
9	7.8	2,210	18.6	2,190	40.1	2,190	54.3	2,180
11	7.2	2,180	18.5	2,200	43.6	2,210	59.4	2,190
13	7.1	2,240	20.2	2,240	43.4	2,220	61.3	2,220
Mean μ	7.7	2,205	19.6	2,204	42.5	2,209	58.0	2,197
Std. dev. σ	0.8	23	0.9	24	2.0	13	3.5	18

Table A1-8. Results from tensile splitting strength tests at different ages of cubes cast at the concrete plant.

Lorry load	At arrival on-site		7 days		28 days		90 days	
	Air[1] [%]	Density [kg/m^3]	$f_{t,sp,cube}$ [MPa]	Density [kg/m^3]	$f_{t,sp,cube}$ [MPa]	Density [kg/m^3]	$f_{t,sp,cube}$ [MPa]	Density [kg/m^3]
1	8.5	n/a	2.35	2,170	4.05	2,120	4.70	2,160
3	7.8	2,210	2.15	2,180	4.05	2,210	5.00	2,150
5	9.0	2,180	2.25	2,150	4.35	2,150	5.05	2,160
7	6.6	2,210	2.15	2,150	4.25	2,180	5.60	2,180
9	7.8	2,210	2.05	2,160	4.00	2,170	5.10	2,150
11	7.2	2,180	2.00	2,200	4.05	2,190	5.05	2,180
13	7.1	2,240	2.10	2,190	4.15	2,210	5.15	2,200
Mean μ	7.7	2,205	2.15	2,171	4.13	2,176	5.09	2,169
Std. dev. σ	0.8	23	0.10	20	0.10	33	0.25	19

[1]Air content was also measured at the concrete plant for batches 5 and 7 and found to be 10.0% for both.

Table A1-9. Results from tensile splitting strength tests at different ages of cubes cast on-site.

Lorry load	At arrival on-site		7 days		28 days		90 days	
	Air [%]	Density [kg/m^3]	$f_{t,sp,cube}$ [MPa]	Density [kg/m^3]	$f_{t,sp,cube}$ [MPa]	Density [kg/m^3]	$f_{t,sp,cube}$ [MPa]	Density [kg/m^3]
1	8.5	n/a	2.20	2,150	4.40	2,150	5.40	2,200
3	7.8	2,210	2.30	2,210	4.05	2,170	5.45	2,200
5	9.0	2,180	2.30	2,170	4.30	2,170	5.60	2,190
7	6.6	2,210	2.30	2,240	4.40	2,220	5.90	2,230
9	7.8	2,210	2.10	2,180	4.25	2,190	5.35	2,200
11	7.2	2,180	2.20	2,210	4.30	2,200	5.70	2,210
13	7.1	2,240	2.40	2,220	4.60	2,230	5.55	2,210
Mean μ	7.7	2,205	2.26	2,197	4.33	2,190	5.56	2,206
Std. dev. σ	0.8	23	0.10	31	0.15	29	0.20	13

A1.4 Cores drilled from the concrete monolith

Table A1-10. Results from compressive strength tests at different ages on specimens of dimensions Ø100×100 mm from horizontal cores drilled from the concrete monolith. Measured density ρ (kg/m^3) is given in brackets.

Specimen position [mm]	$f_{c,core}$ [MPa]				
	28 days	90 days	135 days	182 days	377 days
150	38.7 (2,200)	60.5 (2,210)	64.5 (2,200)	66.1 (2,200)	73.2 (2,200)
450	40.3 (2,240)	63.5 (2,210)	66.8 (2,190)	71.4 (2,220)	74.8 (2,220)
750	41.5 (2,240)	63.9 (2,260)	60.6 (2,240)	69.2 (2,210)	73.5 (2,260)
Mean μ	40.2 (2,227)	62.6 (2,227)	64.0 (2,210)	68.9 (2,210)	73.8 (2,227)
Std. dev. σ	1.4 (23)	1.9 (29)	3.1 (26)	2.7 (10)	0.9 (31)

Table A1-11. Results from tensile splitting strength tests at different ages on specimens of dimensions Ø100×100 mm from horizontal cores drilled from the concrete monolith. Measured density ρ (kg/m^3) is given in brackets.

Specimen position [mm]	$f_{t,sp,core}$ [MPa]				
	28 days	90 days	135 days	182 days	377 days
150	4.05 (2,200)	5.30 (2,220)	5.20 (2,220)	6.00 (2,200)	6.25 (2,200)
450	4.35 (2,270)	5.10 (2,250)	5.10 (2,240)	5.80 (2,220)	6.40 (2,220)
750	4.20 (2,270)	5.30 (2,250)	5.40 (2,240)	6.10 (2,210)	6.20 (2,260)
Mean μ	4.20 (2,247)	5.23 (2,240)	5.23 (2,233)	5.97 (2,210)	6.28 (2,227)
Std. dev. σ	0.15 (40)	0.12 (17)	0.15 (12)	0.15 (10)	0.10 (31)

Table A1-12. Results from compressive strength tests at different ages on specimens of dimensions Ø100×200 mm from horizontal cores drilled from the concrete monolith. Measured density ρ (kg/m^3) is given in brackets.

Specimen position [mm]	$f_{c,core}$ [MPa] 28 days	90 days	377 days
150	36.3 (2,220)	54.0 (2,210)	60.3 (2,200)
450	40.8 (2,270)	59.8 (2,250)	70.6 (2,270)
750	42.2 (2,300)	62.3 (2,280)	71.1 (2,280)
Mean μ	39.8 (2,263)	58.7 (2,247)	67.3 (2,250)
Std. dev. σ	3.1 (40)	4.3 (35)	6.1 (44)

Table A1-13. Results from tests for the determination of the modulus of elasticity in compression at different ages on specimens of dimensions Ø100×200 mm from horizontal cores drilled from the concrete monolith.

Specimen position [mm]	90 days				377 days			
	$f_{c,core}$ [MPa]	Density [kg/m^3]	E_0 [GPa]	E_c [GPa]	$f_{c,core}$ [MPa]	Density [kg/m^3]	E_0 [GPa]	E_c [GPa]
150	53.3	2,220	26.9	27.6	61.4	2,200	27.8	28.6
450	58.3	2,260	28.8	29.5	69.2	2,240	30.7	31.3
750/870	59.3	2,310	31.5	32.3	67.9	2,260	32.0	32.6
Mean μ	57.0	2,263	29.1	29.8	66.2	2,233	30.2	30.8
Std. dev. σ	3.2	45	2.3	2.4	4.2	31	2.2	2.0

Table A1-14. Results from compressive strength tests at different ages on specimens of dimensions Ø100×100 mm from vertical cores drilled from the concrete monolith. Measured density ρ (kg/m^3) is given in brackets.

Specimen position [mm]	$f_{c,core}$ [MPa] 28 days	90 days	377 days
250	40.0 (2,230)	60.9 (2,210)	73.4 (2,190)
550	40.0 (2,250)	62.9 (2,250)	76.4 (2,240)
750–850	41.4 (2,270)	62.7 (2,270)	74.0 (2,250)
940	–	61.5 (2,270)	–
Mean μ	40.5 (2,250)	62.0 (2,250)	74.6 (2,227)
Std. dev. σ	0.8 (20)	1.0 (28)	1.6 (32)

Table A1-15. Results from compressive strength tests at different ages on specimens of dimensions Ø100×200 mm from vertical cores drilled from the concrete monolith. Measured density ρ (kg/m^3) is given in brackets.

Specimen position [mm]	$f_{c,core}$ [MPa] 28 days	90 days	377 days
150/250	40.2 (2,190)	60.3 (2,200)	70.1 (2,180)
450/550	42.5 (2,270)	62.5 (2,260)	75.5 (2,240)
750/810	42.3 (2,300)	63 (2,290)	74.1 (2,270)
Mean μ	41.7 (2,253)	61.9 (2,250)	73.2 (2,230)
Std. dev. σ	1.3 (57)	1.4 (46)	2.8 (46)

Table A1-16. Results from tests for the determination of the modulus of elasticity in compression at different ages on specimens of dimensions Ø100×200 mm from vertical cores drilled from the concrete monolith.

Specimen position [mm]	90 days				377 days			
	$f_{c,core}$ [MPa]	Density [kg/m^3]	E_0 [GPa]	E_c [GPa]	$f_{c,core}$ [MPa]	Density [kg/m^3]	E_0 [GPa]	E_c [GPa]
250/150	58.8	2,220	28.8	29.7	72.3	2,190	29.9	30.4
450/550	62.1	2,250	30.1	30.9	76.0	2,240	30.6	31.1
750/850	58.3	2,270	29.2	30.0	78.2	2,280	32.3	33.2
Mean μ	59.7	2,247	29.4	30.2	75.5	2,237	30.9	31.6
Std. dev. σ	2.1	25	0.7	0.6	3.0	45	1.2	1.5

A2 Results obtained in creep tests

A2.1 First test run

Table A2-1. Compressive strength – 150 mm cube. Measured density ρ (kg/m^3) is given in brackets.

Specimen #	$f_{c,cube}$ [MPa]				
	90 days	110 days	450 days	820 days	1,185 days
1	75.5 (2,380)	75.8 (2,380)	82.8 (2,360)	84.8 (2,350)	85.9 (2,380)
2	76.4 (2,370)	75.7 (2,370)	86.6 (2,360)	86.7 (2,360)	88.5 (2,400)
3	75.7 (2,350)	73.4 (2,360)	88.1 (2,360)	83.8 (2,350)	87.2 (2,390)
4	76.8 (2,350)	76.4 (2,360)	86.4 (2,380)	–	–
5	78.9 (2,350)	75.6 (2,360)	85.7 (2,330)	–	–
Mean μ	76.7 (2,360)	75.4 (2,366)	85.9 (2,358)	85.1 (2,353)	87.2 (2,390)
Std. dev. σ	1.4 (14.1)	1.1 (8.9)	2.0 (17.9)	1.5 (5.8)	1.3 (10.0)

Table A2-2. Compressive strength at 90 days – Ø150×300 mm cylinder.

Specimen #	$f_{c,cyl}$ [MPa]	Density, ρ [kg/m^3]
1	75.1	2,350
2	74.9	2,350
3	74.7	2,360
4	74.6	2,360
5	73.7	2,350
Mean μ	74.6	2,354
Std. dev. σ	0.5	5.5

Table A2-3. Elastic modulus at 90 days – Ø150×300 mm cylinder.

Prov #	E_0 [GPa]	E_c [GPa]	$f_{c,cyl}$ [MPa]	Density, ρ [kg/m^3]
1	34.0	34.5	73.6	2,390
2	33.0	33.5	74.7	2,360
3	32.5	33.0	75.3	2,360
4	33.0	33.0	74.5	2,370
5	33.5	33.5	76.5	2,360
Mean μ	33.2	33.5	75.3	2,368
Std. dev. σ	0.6	0.6	0.9	13.0

Table A2-4. Compressive strength at 90 days – Ø100×200 mm cylinder.

Specimen #	$f_{c,cyl}$ [MPa]	Density, ρ [kg/m^3]
1	75.5	2,320
2	75.3	2,330
3	75.1	2,330
4	75.3	2,320
5	75.5	2,330
Mean μ	75.3	2,326
Std. dev. σ	0.2	5.5

Table A2-5. Compressive strength at 90 days – Ø100×300 mm cylinder cast in plastic pipe.

Specimen #	$f_{c,cyl}$ [MPa]	Density, ρ [kg/m^3]
1	67.8	2,370
2	71.4	2,350
3	72.2	2,360
Mean μ	70.5	2,360
Std. dev. σ	2.3	10.0

Table A2-6. Compressive strength at 90 days – Ø100×200 mm cylinder cast in plastic pipe.

Specimen #	$f_{c,cyl}$ [MPa]	E_0 [GPa]	$E_0\varepsilon_c$ [MPa]			$E_0\varepsilon_c$ / $f_{c,cyl}$ [–]		
			η=0.01	η=0.02	η=0.05	η=0.01	η=0.02	η=0.05
1	74.6	33.7	35	43	54	0.47	0.58	0.73
2	75.3	33.1	45	49	58	0.60	0.65	0.77
3	75.7	34.1	41	46	56	0.54	0.61	0.74
4	74.4	32.4	56	58	63	0.75	0.77	0.84
5	74.8	34.1	33	38	52	0.45	0.51	0.68
Mean μ	75.0	33.5	42.0	46.7	56.3	0.56	0.62	0.75
Std. dev. σ	0.5	0.76	8.9	7.3	4.4	0.12	0.10	0.06

A2.2 Second test run

Table A2-7. Compressive strength – 150 mm cube. Measured density ρ (kg/m^3) is given in brackets.

Specimen #	$f_{c,cube}$ [MPa]		
	87 days	470 days	820 days
1	65.5 (2,370)	89.7 (2,380)	90.9 (2,370)
2	69.7 (2,370)	85.5 (2,370)	90.5 (2,380)
3	68.2 (2,370)	84.6 (2,380)	92.0 (2,360)
Mean μ	67.8 (2,370)	86.6 (2,377)	91.1 (2,370)
Std. dev. σ	2.1 (0.0)	2.7 (5.8)	0.8 (10)

Table A2-8. Compressive strength at 87 days – Ø150×300 mm cylinder.

Specimen #	$f_{c,cyl}$ [MPa]	Density, ρ [kg/m^3]
1	63.8	2,370
2	64.3	2,340
3	63.9	2,360
4	64.1	2,340
5	64.0	2,340
Mean μ	64.0	2,350
Std. dev. σ	0.2	14.1

Table A2-9. Compressive strength at 86 days – Ø90×180 mm cylinder cast in plastic pipe.

Specimen #	$f_{c,cyl}$ [MPa]	E_0 [GPa]	E_0^* [GPa]	$E_0\varepsilon_c$ [MPa] η=0.01	η=0.02	η=0.05	$E_0\varepsilon_c$ / $f_{c,cyl}$ [–] η=0.01	η=0.02	η=0.05
1	71.8	34.5	31.2	30	35	39	0.41	0.48	0.55
2	71.4	32.1	30.9	37	41	50	0.52	0.57	0.70
3	70.5	33.4	31.6	31	35	45	0.44	0.50	0.64
4	70.7	35.5	33.2	35	37	44	0.49	0.52	0.62
5	72.3	34.5	31.0	33	35	38	0.46	0.48	0.52
Mean μ	71.3	34.0	31.6	33.0	36.5	43.3	0.46	0.51	0.61
Std. dev. σ	0.8	1.3	0.9	2.9	2.7	4.8	0.04	0.04	0.07

E_0^* is evaluated from as the secant modulus between 0.5 MPa and $\sigma_{cm}(t_0)$ = 49.4 MPa, where $\sigma_{cm}(t_0)$ is the applied stress level of the creep tests in the in second test run.

Table A2-10. Compressive strength at 86 days – Ø90×270 mm cylinder cast in plastic pipe.

Specimen #	$f_{c,cyl}$ [MPa]	E_0 [GPa]	E_0^* [GPa]	$E_0\varepsilon_c$ [MPa] η=0.01	η=0.02	η=0.05	$E_0\varepsilon_c$ / $f_{c,cyl}$ [–] η=0.01	η=0.02	η=0.05
1	68.2	32.6	31.1	35	40	48	0.51	0.58	0.70
2	67.7	35.5	32.7	33	34	41	0.48	0.50	0.60
3	70.1	34.3	33.5	45	48	53	0.64	0.68	0.75
Mean μ	68.7	34.1	32.4	37.5	40.4	47.0	0.55	0.59	0.68
Std. dev. σ	1.3	1.5	1.3	6.6	6.8	6.1	0.09	0.09	0.08

E_0^* is evaluated from as the secant modulus between 0.5 MPa and $\sigma_{cm}(t_0)$ = 49.4 MPa, where $\sigma_{cm}(t_0)$ is the applied stress level of the creep tests in the in second test run.

A3 Results obtained in tests on bond between concrete and rock

Table A3-1. Compressive strength at 90 days – 150 mm cube.

Specimen #	$f_{c,cube}$ [MPa]	Density, ρ [kg/m^3]
1	81.6	2,370
2	84.4	2,370
3	82.7	2,380
4	82.2	2,370
5	78.5	2,380
Mean μ	81.9	2,374
Std. dev. σ	2.2	5.5

Table A3-2. Compressive strength at 90 days – Ø150×300 mm cylinder.

Specimen #	$f_{c,cyl}$ [MPa]	Density, ρ [kg/m^3]
1	79.0	2,350
2	78.0	2,350
3	77.4	2,330
4	77.6	2,340
5	78.0	2,340
Mean μ	78.0	2,342
Std. dev. σ	0.6	8.4

Table A3-3. Compressive strength – core specimens Ø100×100 mm.

Specimen #	12 days		29 days		90 days	
	$f_{c,core}$ [MPa]	ρ [kg/m^3]	$f_{c,core}$ [MPa]	ρ [kg/m^3]	$f_{c,core}$ [MPa]	ρ [kg/m^3]
1	33.3	2,310	56.4	2,320	82.0	2,320
2	34.6	2,320	54.5	2,330	81.1	2,330
3	33.4	2,310	55.3	2,330	83.9	2,340
4	33.4	2,300	54.0	2,320	81.0	2,330
5	33.6	2,310	55.2	2,330	82.9	2,340
Mean μ	33.7	2,310	55.1	2,326	82.2	2,332
Std. dev. σ	0.5	7.1	0.9	5.5	1.2	8.4

Table A3-4. Splitting tensile strength – core specimens Ø100×100 mm. Measured density ρ (kg/m^3) is given in brackets.

Specimen #	$f_{t,sp,core}$ [MPa]		
	12 days	29 days	90 days
1	3.2 (2,320)	4.4 (2,340)	5.2 (2,330)
2	3.1 (2,320)	4.5 (2,350)	5.3 (2,340)
3	3.5 (2,310)	3.9 (2,340)	6.0 (2,350)
4	3.4 (2,320)	4.0 (2,340)	5.3 (2,350)
5	3.4 (2,310)	4.7 (2,360)	5.9 (2,350)
Mean μ	3.3 (2,316)	4.3 (2,346)	5.5 (2,344)
Std. dev. σ	0.2 (5)	0.3 (9)	0.4 (9)

Table A3-5. Tensile strength at 90 days – core specimens Ø65×100 mm.

Specimen #	$f_{t,core}$ [MPa]
1	3.4
2	3.1
3	2.7
4	3.2
5	3.0
6	3.8
Mean μ	3.2
Std. dev. σ	0.4

Table A3-6. Tensile strength and fracture energy – notched core specimens Ø100×100 mm.

Specimen	Area [cm^2]	Age [days]	$f_{t,core}$ [MPa]	G_F [N/m]
DTT-C-2	50.9	89	3.8	109
DTT-C-3	49.4	89	3.6	111
DTT-C-4	49.6	90	3.6	127
DTT-C-5	49.9	90	3.6	146
DTT-C-6	49.5	90	3.9	106
DTT-C-7	49.5	90	3.3	129
Mean μ			3.6	121
Std. dev. σ			0.2	15

Appendix B

Results from tests on shrinkage properties of concrete B200

B1 Results obtained from tests conducted at CBI

Table B1-1. Shrinkage results for sealed specimens.

	Shrinkage – sealed						
Time [days]	Beam 1 [‰]	Beam 2 [‰]	Beam 3 [‰]	Beam 4 [‰]	Beam 5 [‰]	Mean μ [‰]	CV [%]
1	0.000	0.000	0.000	0.000	0.000	0.000	–
2	0.049	0.047	0.042	0.038	0.034	0.042	14.6
8	0.058	0.056	0.050	0.050	0.048	0.052	8.2
17	0.033	0.030	0.024	0.026	0.021	0.027	18.3
38	0.067	0.053	0.055	0.047	0.053	0.055	12.8
70	0.077	0.071	0.065	0.062	0.063	0.068	9.4
92	0.081	0.070	0.068	0.064	0.065	0.069	9.7
168	0.091	0.082	0.078	0.076	0.075	0.080	8.2
300	0.135	0.126	0.123	0.115	0.116	0.123	6.5
385	0.150	0.138	0.136	0.126	0.129	0.136	7.0
471	0.142	0.142	0.147	0.138	0.147	0.143	2.6
549	0.172	0.161	0.162	0.147	0.150	0.158	6.2
644	0.176	0.164	0.162	0.145	0.147	0.158	8.1
743	0.190	0.182	0.179	0.162	0.167	0.176	6.5
952	0.246	0.235	0.231	0.209	0.215	0.227	6.7
1,099	0.256	0.242	0.240	0.215	0.220	0.235	7.2

Table B1-2. Change of weight for sealed specimens.

	Shrinkage – sealed						
Time [days]	Beam 1 [%]	Beam 2 [%]	Beam 3 [%]	Beam 4 [%]	Beam 5 [%]	Mean μ [%]	CV [%]
1	0.000	0.000	0.000	0.000	0.000	0.000	–
2	0.032	0.043	0.042	0.021	0.032	0.034	25.9
8	0.193	0.213	0.190	0.171	0.203	0.194	8.2
17	0.310	0.298	0.286	0.277	0.309	0.296	4.9
38	0.471	0.458	0.434	0.416	0.469	0.449	5.3
70	0.631	0.607	0.582	0.565	0.629	0.603	4.8
92	0.685	0.671	0.656	0.629	0.704	0.669	4.3
168	0.952	0.937	0.931	0.863	0.970	0.931	4.4
300	1.294	1.246	1.269	1.162	1.290	1.252	4.3
385	1.508	1.459	1.502	1.353	1.504	1.465	4.5
471	1.733	1.672	1.714	1.556	1.696	1.674	4.2
549	1.915	1.853	1.904	1.716	1.845	1.846	4.3
644	1.915	2.055	2.126	1.886	2.069	2.010	5.2
743	2.343	2.279	2.359	2.089	2.293	2.272	4.8
952	2.760	2.715	2.782	2.483	2.698	2.688	4.4
1,099	3.070	3.024	3.121	2.781	2.997	2.999	4.3

Table B1-3. Shrinkage results for specimens stored in 50% RH and 20°C.

Time [days]	Shrinkage – 50% RH Beam 1 [‰]	Beam 2 [‰]	Beam 3 [‰]	Beam 4 [‰]	Beam 5 [‰]	Mean μ [‰]	CV [%]
1	0.000	0.000	0.000	0.000	0.000	0.000	–
2	0.058	0.060	0.055	0.066	0.057	0.059	6.9
8	0.129	0.130	0.127	0.135	0.123	0.129	3.4
17	0.182	0.184	0.178	0.187	0.173	0.181	3.1
38	0.249	0.254	0.245	0.259	0.239	0.249	3.1
70	0.308	0.313	0.306	0.317	0.296	0.308	2.6
92	0.306	0.311	0.300	0.311	0.292	0.304	2.7
168	0.371	0.379	0.374	0.381	0.364	0.374	1.8
300	0.425	0.428	0.421	0.431	0.412	0.423	1.7
385	0.439	0.443	0.437	0.446	0.426	0.438	1.7
471	0.471	0.475	0.468	0.482	0.456	0.470	2.0
549	0.472	0.477	0.474	0.488	0.461	0.474	2.0
644	0.472	0.483	0.482	0.491	0.462	0.478	2.3
743	0.474	0.497	0.486	0.496	0.475	0.485	2.3
952	0.516	0.527	0.517	0.537	0.507	0.521	2.2
1,099	0.516	0.522	0.515	0.534	0.507	0.519	1.9

Table B1-4. Change of weight for specimens stored in 50% RH and 20°C.

Time [days]	Weight change – 50% RH Beam 1 [%]	Beam 2 [%]	Beam 3 [%]	Beam 4 [%]	Beam 5 [%]	Mean μ [%]	CV [%]
1	0.000	0.000	0.000	0.000	0.000	0.000	–
2	20.792	21.654	24.969	25.220	25.040	23.535	9.1
8	39.088	39.401	40.292	40.766	39.837	39.877	1.7
17	42.028	42.366	43.220	43.730	42.687	42.806	1.6
38	44.090	44.441	45.254	45.760	44.690	44.847	1.5
70	45.063	45.500	46.255	46.639	45.612	45.814	1.4
92	44.788	45.257	45.988	46.325	45.323	45.536	1.3
168	45.349	45.881	46.595	46.835	45.880	46.108	1.3
300	45.306	45.903	46.617	46.737	45.858	46.084	1.3
385	45.433	46.061	46.776	46.867	45.998	46.227	1.3
471	45.751	46.347	47.053	47.160	46.287	46.520	1.3
549	46.004	46.633	47.298	47.410	46.533	46.776	1.2
644	46.353	46.972	47.639	47.758	46.887	47.122	1.2
743	46.470	47.131	47.777	47.844	46.994	47.243	1.2
952	46.332	46.983	47.575	47.649	46.790	47.066	1.2
1,099	46.279	46.919	47.596	47.562	46.715	47.014	1.2

Table B1-5. Shrinkage results for specimens stored in water.

	Shrinkage – water curing						
Time [days]	Beam 1 [‰]	Beam 2 [‰]	Beam 3 [‰]	Beam 4 [‰]	Beam 5 [‰]	Mean μ [‰]	CV [%]
1	0.000	0.000	0.000	0.000	0.000	0.000	–
2	–0.077	–0.071	–0.037	–0.077	–0.140	–0.066	–56.4
8	–0.109	–0.099	–0.078	–0.103	–0.237	–0.097	–65.1
17	–0.156	–0.152	–0.117	–0.152	–0.311	–0.144	–53.1
38	–0.147	–0.144	–0.105	–0.140	–0.325	–0.134	–65.0
70	–0.140	–0.136	–0.093	–0.130	–0.311	–0.125	–68.2
92	–0.150	–0.154	–0.109	–0.149	–0.324	–0.141	–59.7
168	–0.158	–0.159	–0.110	–0.139	–0.308	–0.142	–54.5
300	–0.156	–0.159	–0.086	–0.139	–0.302	–0.135	–59.5
385	–0.158	–0.164	–0.109	–0.147	–0.292	–0.145	–47.9
471	–0.162	–0.168	–0.090	–0.143	–0.270	–0.141	–46.6
549	–0.167	–0.158	–0.097	–0.138	–0.305	–0.140	–55.9
644	–	–	–	–	–0.319	–	–
743	–	–	–	–	–	–	–
952	–	–	–	–	–	–	–
1,099	–	–	–	–	–	–	–

Table B1-6. Change of weight for specimens stored in water.

	Weight change – water curing						
Time [days]	Beam 1 [%]	Beam 2 [%]	Beam 3 [%]	Beam 4 [%]	Beam 5 [%]	Mean μ [%]	CV [%]
1	0.000	0.000	0.000	0.000	0.000	0.000	–
2	–1.859	–1.781	–1.746	–2.108	–2.484	–1.874	–16.4
8	–3.188	–3.037	–2.950	–3.215	–3.559	–3.098	–7.5
17	–3.800	–3.821	–3.688	–3.985	–4.279	–3.823	–6.0
38	–4.278	–4.250	–4.089	–4.417	–4.874	–4.259	–7.0
70	–4.745	–4.668	–4.838	–5.124	–5.511	–4.844	–7.1
92	–4.953	–4.915	–5.131	–5.429	–5.876	–5.107	–7.8
168	–5.119	–5.055	–5.347	–5.587	–6.064	–5.277	–7.8
300	–5.503	–5.516	–5.640	–5.883	–6.419	–5.636	–6.8
385	–5.669	–5.645	–5.651	–5.914	–6.367	–5.720	–5.4
471	–5.815	–5.742	–5.619	–5.788	–6.294	–5.741	–4.5
549	–6.241	–6.106	–6.237	–6.262	–6.795	–6.212	–4.3
644	–6.303	–5.903	–6.096	–6.030	–6.617	–6.083	–4.6
743	–6.365	–6.074	–6.020	–6.199	–6.837	–6.165	–5.3
952	–	–	–	–	–	–	–
1,099	–	–	–	–	–	–	–

B2 Results obtained from tests conducted at C.lab

Table B2-1. Shrinkage results for sealed specimens.

	Shrinkage – sealed						
Time [days]	S1 [‰]	S2 [‰]	S3 [‰]	S4 [‰]	S5 [‰]	Mean μ [‰]	CV [%]
1	0.000	0.000	0.000	0.000	0.000	0.000	–
7	0.021	0.168	0.029	0.108	0.071	0.079	76.5
14	0.021	0.152	0.008	0.126	0.039	0.069	94.3
21	0.052	0.184	0.023	0.152	0.039	0.090	80.3
35	0.045	0.197	0.044	0.189	0.045	0.104	78.2
56	0.031	0.184	0.026	0.197	0.047	0.097	88.1
71	0.037	0.192	0.034	0.199	0.045	0.101	85.1
91	0.052	0.213	0.042	0.210	0.055	0.114	77.4
119	0.045	0.215	0.042	0.241	0.076	0.124	78.1
154	0.089	0.241	0.068	0.257	0.097	0.151	60.4
196	0.097	0.249	0.073	0.265	0.097	0.156	59.3
238	0.108	0.260	0.094	0.278	0.105	0.169	54.3
280	0.100	0.260	0.078	0.283	0.108	0.166	58.8
365	0.108	0.247	0.086	0.289	0.111	0.168	55.2
456	0.118	0.260	0.099	0.315	0.126	0.184	52.9
548	0.129	0.265	0.102	0.333	0.134	0.193	52.4
639	0.129	0.260	0.107	0.346	0.139	0.196	52.4
730	0.136	0.278	0.112	0.349	0.153	0.206	49.9
912	0.164	0.307	0.137	0.385	0.188	0.236	44.6
1,095	0.176	0.325	0.136	0.404	0.197	0.248	45.5

Table B2-2. Change of weight for sealed specimens.

	Weight change – sealed						
Time [days]	S1 [%]	S2 [%]	S3 [%]	S4 [%]	S5 [%]	Mean μ [%]	CV [%]
1	0.00	0.00	0.00	0.00	0.00	0.000	–
7	0.00	0.00	0.00	–0.01	–0.01	–0.004	–136.9
14	–0.01	–0.01	–0.01	0.00	–0.01	–0.008	–55.9
21	–0.01	–0.01	–0.01	–0.02	–0.02	–0.015	–41.2
35	–0.01	–0.01	–0.02	–0.02	–0.02	–0.017	–35.0
56	–0.04	–0.02	–0.02	–0.03	–0.02	–0.027	–34.7
71	–0.01	–0.02	–0.02	–0.03	–0.03	–0.023	–39.6
91	–0.03	–0.03	–0.03	–0.03	–0.03	–0.032	–2.1
119	–0.03	–0.03	–0.03	–0.04	–0.03	–0.034	–15.8
154	–0.03	–0.03	–0.03	–0.05	–0.04	–0.038	–27.0
196	–0.03	–0.03	–0.04	–0.05	–0.05	–0.042	–26.7
238	–0.04	–0.04	–0.04	–0.07	–0.05	–0.049	–21.6
280	–0.05	–0.05	–0.05	–0.07	–0.05	–0.055	–10.4
365	–0.05	–0.05	–0.05	–0.08	–0.06	–0.059	–18.1
456	–0.06	–0.06	–0.06	–0.09	–0.06	–0.068	–15.8
548	–0.06	–0.06	–0.07	–0.10	–0.08	–0.074	–19.3
639	–0.07	–0.07	–0.08	–0.10	–0.09	–0.082	–12.3
730	–0.08	–0.08	–0.08	–0.11	–0.10	–0.091	–12.5
912	–0.09	–0.09	–0.10	–0.13	–0.11	–0.106	–14.0
1,095	–0.09	–0.09	–0.10	–0.13	–0.11	–0.106	–14.0

Table B2-3. Shrinkage results for specimens stored in 50% RH and 20°C.

	Shrinkage – 50% RH						
Time [days]	D1 [‰]	D2 [‰]	D3 [‰]	D4 [‰]	D5 [‰]	Mean μ [‰]	CV [%]
1	0.000	0.000	0.000	0.000	0.000	0.000	–
7	0.118	0.118	0.147	0.147	0.134	0.133	10.9
14	0.155	0.162	0.191	0.197	0.189	0.179	10.7
21	0.171	0.209	0.243	0.245	0.239	0.222	14.4
35	0.247	0.259	0.288	0.297	0.284	0.275	7.7
56	0.302	0.301	0.343	0.353	0.334	0.327	7.3
71	0.307	0.312	0.356	0.376	0.355	0.341	8.9
91	0.370	0.366	0.406	0.416	0.395	0.391	5.6
119	0.362	0.369	0.411	0.445	0.429	0.403	9.0
154	0.415	0.419	0.458	0.476	0.461	0.446	6.1
196	0.420	0.429	0.471	0.484	0.471	0.455	6.3
238	0.444	0.455	0.500	0.503	0.492	0.479	5.7
280	0.433	0.442	0.479	0.508	0.497	0.472	7.0
365	0.441	0.442	0.490	0.505	0.495	0.475	6.4
456	0.446	0.448	0.495	0.521	0.516	0.485	7.5
548	0.465	0.466	0.518	0.547	0.537	0.507	7.7
639	0.465	0.469	0.518	0.553	0.542	0.509	8.0
730	0.470	0.469	0.518	0.550	0.542	0.510	7.6
912	0.516	0.509	0.552	0.591	0.582	0.550	6.8
1,095	0.517	0.510	0.558	0.600	0.587	0.554	7.3

Table B2-4. Change of weight for specimens stored in 50% RH and 20°C.

	Weight change – 50% RH						
Time [days]	D1 [%]	D2 [%]	D3 [%]	D4 [%]	D5 [%]	Mean μ [%]	CV [%]
1	0.00	0.00	0.00	0.00	0.00	0.00	–
7	–3.18	–3.12	–3.49	–3.51	–3.40	–3.34	–5.5
14	–3.44	–3.40	–3.78	–3.84	–3.72	–3.64	–5.5
21	–3.57	–3.53	–3.92	–4.19	–3.95	–3.83	–7.3
35	–3.72	–3.68	–4.07	–4.16	–4.04	–3.93	–5.5
56	–3.80	–3.80	–4.17	–4.27	–4.15	–4.04	–5.5
71	–3.87	–3.84	–4.21	–4.30	–4.18	–4.08	–5.2
91	–3.90	–3.87	–4.25	–4.31	–4.21	–4.11	–5.0
119	–3.93	–3.89	–4.26	–4.32	–4.22	–4.13	–4.9
154	–3.94	–3.92	–4.29	–4.33	–4.24	–4.14	–4.8
196	–3.94	–3.92	–4.29	–4.33	–4.26	–4.15	–4.9
238	–3.95	–3.93	–4.30	–4.33	–4.23	–4.15	–4.7
280	–3.95	–3.93	–4.30	–4.33	–4.23	–4.15	–4.7
365	–3.94	–3.92	–4.29	–4.32	–4.22	–4.14	–4.7
456	–3.94	–3.92	–4.28	–4.30	–4.20	–4.12	–4.5
548	–3.95	–3.93	–4.29	–4.30	–4.21	–4.13	–4.4
639	–3.96	–3.94	–4.29	–4.31	–4.21	–4.14	–4.3
730	–3.95	–3.94	–4.29	–4.31	–4.21	–4.14	–4.4
912	–3.93	–3.92	–4.26	–4.31	–4.21	–4.13	–4.6
1,095	–3.93	–3.92	–4.26	–4.24	–4.14	–4.10	–4.1

Table B2-5. Shrinkage results for specimens stored in water. Note that some corrosion on the gauge studs occurred (black rust) and this was removed at 730 days.

	Shrinkage – water curing						
Time [days]	W1 [‰]	W2 [‰]	W3 [‰]	W4 [‰]	W5 [‰]	Mean μ [‰]	CV [%]
1	0.000	0.000	0.000	0.000	0.000	0.000	–
7	–0.055	–0.060	–0.071	–0.097	–0.116	–0.080	–32.4
14	–0.102	–0.076	–0.118	–0.121	–0.137	–0.111	–20.8
21	–0.097	–0.089	–0.118	–0.137	–0.161	–0.120	–24.3
35	–0.105	–0.076	–0.113	–0.132	–0.153	–0.116	–24.9
56	–0.107	–0.081	–0.121	–0.153	–0.163	–0.125	–26.7
71	–0.123	–0.097	–0.139	–0.166	–0.176	–0.140	–22.9
91	–0.131	–0.113	–0.142	–0.176	–0.189	–0.150	–21.2
119	–0.212	–0.110	–0.160	–0.161	–0.179	–0.164	–22.4
154	–0.199	–0.102	–0.131	–0.182	–0.171	–0.157	–25.1
196	–0.157	–0.079	–0.142	–0.168	–0.176	–0.144	–27.0
238	–0.139	–0.037	–0.136	–0.200	–0.147	–0.132	–44.9
280	–0.152	–0.068	–0.150	–0.200	–0.142	–0.142	–33.2
365	–0.134	–0.063	–0.150	–0.221	–0.161	–0.146	–39.0
456	–0.123	–0.068	–0.147	–0.237	–0.166	–0.148	–41.6
548	–0.115	–0.068	–0.139	–0.234	–0.166	–0.145	–42.7
639	–0.128	–0.076	–0.129	–0.239	–0.171	–0.149	–41.0
730	–0.165	–0.094	–0.186	–0.258	–0.184	–0.178	–32.9
912	–0.178	–0.094	–0.197	–0.266	–0.208	–0.189	–32.9
1,095	–0.154	–0.087	–0.192	–0.258	–0.213	–0.181	–35.7

Table B2-6. Change of weight for specimens stored in water. Note that some corrosion on the gauge studs occurred (black rust) and this was removed at 730 days.

	Weight change – water curing						
Time [days]	W1 [%]	W2 [%]	W3 [%]	W4 [%]	W5 [%]	Mean μ [%]	CV [%]
1	0.00	0.00	0.00	0.00	0.00	0.00	–
7	0.32	0.41	0.43	0.70	0.66	0.50	33.5
14	0.39	0.49	0.50	0.76	0.73	0.57	28.2
21	0.38	0.47	0.49	0.66	0.60	0.52	21.2
35	0.43	0.54	0.55	0.86	0.82	0.64	29.4
56	0.44	0.53	0.53	0.89	0.87	0.65	32.3
71	0.50	0.60	0.62	0.92	0.89	0.71	26.4
91	0.46	0.57	0.58	0.94	0.92	0.70	31.7
119	0.56	0.66	0.67	0.99	0.98	0.77	25.9
154	0.57	0.69	0.69	1.00	0.98	0.78	24.6
196	0.58	0.71	0.72	0.99	0.95	0.79	22.1
238	0.58	0.70	0.70	1.03	1.00	0.80	25.2
280	0.60	0.72	0.73	1.03	1.01	0.82	23.5
365	0.61	0.73	0.74	1.04	1.02	0.83	23.2
456	0.62	0.74	0.76	1.07	1.03	0.84	23.2
548	0.62	0.74	0.77	1.08	1.05	0.85	23.9
639	0.62	0.74	0.76	1.08	1.05	0.85	24.0
730	0.62	0.75	0.77	1.09	1.05	0.86	23.9
912	0.63	0.74	0.76	1.09	1.06	0.86	24.2
1,095	0.64	0.76	0.78	1.10	1.09	0.87	23.8